Effects of Gut-Derived Inflammation and Oxidative Stress on Vascular Dysfunction and Arterial Hypertension in Experimental Celiac Disease

Dissertation

Zur Erlangung des Grades

Doktor der Naturwissenschaften

(Dr. rer. nat.)

Am Fachbereich Biologie

der Johannes Gutenberg-Universität Mainz

Karin Keppeler

Geb. am 15. Oktober 1993 in Ravensburg

Mainz, Juni 2025

Die vorliegende Arbeit wurde von Januar 2020 bis Juli 2024 im Labor für Molekulare Kardiologie durchgeführt, welches Teil des Zentrums für Kardiologie I der Universitätsmedizin Mainz ist.

1. Betreuer: xx

2. Betreuer: xx

Dekan: Univ.-Prof. Dr. Eckhard Thines

1. Berichterstatter: xx
2. Berichterstatter: xx

Tag der mündlichen Prüfung: 09.12.2025

Für alle, die mich unterstützt haben

I. Zusammenfassung

Zöliakie (CeD) wird zunehmend mit einem erhöhten kardiovaskulären Risiko in Verbindung gebracht. Klinische Studien weisen auf höhere Mortalitätsraten und eine Zunahme kardiovaskulärer Ereignisse bei Zöliakie-Patienten hin. Ziel dieser Arbeit war es, mithilfe des NOD-DQ8-Mausmodells die Auswirkungen aktiver und nicht-aktiver Zöliakie auf das Herz-Kreislauf-System zu untersuchen. Ein besonderer Fokus lag auf den zugrundeliegenden Mechanismen und beteiligten zellulären sowie molekularen Komponenten.

Die Ergebnisse zeigten eine erfolgreiche Induktion der Zöliakie im Mausmodell, gekennzeichnet durch eine Infiltration von Immunzellen und Kryptenhyperplasie im Dünndarm, was zu einem reduzierten Verhältnis aus Zottenhöhe und Kryptentiefe führte. Systemische Analysen ergaben signifikante gliadininduzierte Veränderungen, darunter ein erhöhter Blutdruck und gesteigerte Serumcholesterinwerte. Trotz nachweislich erhöhter Entzündungswerte und oxidativem Stress im Herzen konnten keine funktionellen Einschränkungen der Herzleistung festgestellt werden. Hingegen wurde im Aortengewebe eine deutliche Gefäßdysfunktion beobachtet, bedingt durch oxidativen und nitro-oxidativen Stress sowie eine vermehrte Infiltration myeloider Immunzellen. Die Analyse des Fettgewebes zeigte unterschiedliche Reaktionen: Das perivaskuläre Fettgewebe (PVAT) wies eine stärkere proinflammatorische Beteiligung auf als das epididymale Fettgewebe (EWAT). Im Gehirn konnte eine erhöhte Expression entzündungsrelevanter Gene nachgewiesen werden, was auf weitreichende systemische Entzündungsreaktionen hinweist. Ein Wechsel zu einer glutenfreien Diät führte innerhalb von zwei Wochen zu einer Normalisierung des Blutdrucks, der Gefäßfunktion und der oxidativen Stresswerte. Dies unterstreicht das Potenzial der diätetischen Intervention zur Umkehrung entzündungsbedingter Schäden. Die Analyse mittels Olink-Plasma-Proteomik identifizierte Interleukin-17A (IL-17A) als möglichen Schlüsselmediator, der intestinale Entzündungsprozesse mit systemischen und vaskulären Effekten verbindet. Diese Ergebnisse tragen zum Verständnis der Beziehung zwischen Zöliakie, systemischen Entzündungen und kardiovaskulären Komplikationen bei und verdeutlichen die Bedeutung einer frühzeitigen Diagnose sowie geeigneter diätetischer Maßnahmen zur Prävention solcher Folgeerkrankungen.

II. Summary

Celiac disease (CeD) has been recognized as a condition associated with an elevated cardiovascular risk. Clinical studies report higher mortality rates and a greater incidence of cardiovascular events in CeD patients. This study aimed to investigate the cardiovascular effects of active and non-active CeD using the NOD-DQ8 mouse model, with a particular focus on the underlying mechanisms and the involved cellular and molecular components.

The results demonstrated successful induction of CeD in the mouse model, characterised by immune cell infiltration and crypt hyperplasia in the small intestine, leading to a reduced villous height-to-crypt depth ratio. Systemic analyses revealed significant gliadin-induced changes, including elevated blood pressure and increased serum cholesterol levels. Despite increased inflammatory markers and oxidative stress in the heart, no functional impairments in cardiac performance were observed. In contrast, pronounced vascular dysfunction was detected in aortic tissue, driven by oxidative and nitro-oxidative stress, along with increased infiltration of myeloid immune cells.

Adipose tissue analysis revealed differential responses: perivascular adipose tissue (PVAT) exhibited stronger pro-inflammatory involvement than epididymal white adipose tissue (EWAT). Brain tissue analysis showed elevated expression of inflammation-related genes, indicating widespread systemic inflammatory responses.

A switch to a gluten-free diet led to a normalization of blood pressure, vascular function, and oxidative stress levels within two weeks, underscoring the potential of dietary interventions to reverse inflammation-related damage.

Olink plasma proteomics identified interleukin-17A (IL-17A) as a potential key mediator linking intestinal inflammation to systemic and vascular effects. These findings enhance the understanding of the relationship between CeD, systemic inflammation, and cardiovascular complications, highlighting the importance of early diagnosis and appropriate dietary measures to prevent such complications.

III. Table of Contents

IV. List of Figures

V. List of Tables

VI. List of Abbreviations

3-NT	3-Nitrotyrosine
4-HNE	4-Hydroxynonenal
ACh	Acetylcholine
AHA	American Heart Association
AID	Autoimmune disease
ANA	Antinuclear antibodies
APC	Antigen-presenting cell
AW	Anterior wall
BP	Blood pressure
BSA	Bovine serum albumin
BW	Body weight
CAD	Coronary artery disease
CBC	Complete blood count
cDNA	Complementary deoxyribonucleic acid
cGMP	Cyclic guanosine monophosphate
CHOD-PAP	Cholesterol oxidase-peroxidase aminophenazone
CI	Confidence interval
CO	Cardiac output
CrD	Crypt depth
CTL	Cytotoxic T lymphocyte
CTX	Cholera toxin
CVD	Cardiovascular disease
Cybb	Murine gene for NADPH oxidase 2
DC	Dendritic cells
DD	Distal duodenum
DGK	German Cardiac Society
EDHF	Endothelium-derived hyperpolarizing factor
EF	Ejection fraction
ELISA	Enzyme-linked immunosorbent assay
EMPA	Empagliflozin
ESC	European Society of Cardiology
FMD	Flow-mediated dilation
FMT	Faecal microbiota transplantation
GCD	Gluten-containing diet
GFD	Gluten-free diet
GLP-1	Glucagon-like peptide-1
GTN	Nitroglycerine
HCl	Hydrochloric acid
HCT	Haematocrit
HGB	Haemoglobin
HLA	Human leukocyte antigen
HR	Hazard ratio
IBS	Inflammatory bowel disease
IEC	Intestinal epithelial cells
IEL	Intraepithelial lymphocyte
Ifng	Murine gene for interferon-gamma
IFN-γ	Interferon-gamma

IHC ..... Immunohistochemical
IHD ..... Ischemic heart disease
IL-1 ..... Interleukin-1
Il17a ..... Murine gene for interleukin-17A
Il6 ..... Murine gene for interleukin-6
IMT ..... Intima-media thickness
IVC ..... Individually ventilated cage
KCl ..... Potassium chloride
LMIC ..... Low- and middle-income countries
LV ..... Left ventricular
LVEDD ..... Left ventricular end-diastolic diameter
LVESD ..... Left ventricular end-systolic diameter
MC ..... Metabolic cage
MCH ..... Mean corpuscular haemoglobin
MCHC ..... Mean corpuscular haemoglobin concentration
MCV ..... Mean corpuscular volume
ME ..... Metabolizable energy
MI ..... Myocardial infarction
NCD ..... Noncommunicable diseases
NfE ..... Nitrogen free extract
NIBP ..... Non-invasive blood pressure
NK ..... Natural killer
NO_2^- ..... Nitrite
NO_3^- ..... Nitrate
NOD ..... Non-Obese Diabetic
NOS ..... Nitric oxide synthase
Nos1 ..... Murine gene for nNOS (neuronal)
Nos2 ..... Murine Gene for iNOS (inducible)
Nox2 ..... NADPH oxidase 2
NPX ..... Normalized protein expression
NRCeD ..... Non-responsive Celiac Disease
PEA ..... Proximity extension assay
PGI2 ..... Prostacyclin
PLAX ..... Parasternal long axis
PLT ..... Platelets
PT ..... Pepsin and trypsin
PVAT ..... Perivascular adipose tissue
PW ..... Posterior wall
QoL ..... Quality of life
qRT-PCR ..... Quantitative real-time, reverse transcription PCR
RA ..... Rheumatoid arthritis
RBC ..... Red blood cells
RONS ..... Reactive oxygen and nitrogen species
ROS ..... Reactive oxygen species
RT-qPCR ..... *See* qRT-PCR
SDG ..... Sustainable Development Goal
SGLT2 ..... Sodium/glucose cotransporter 2
SLE ..... Systemic lupus erythematosus
SV ..... Stroke volume
T1D ..... Type 1 diabetes mellitus
TBP ..... TATA-box binding protein

TG2 ..... Tissue transglutaminase
TLCK ..... Tosyl-lysine-chloromethyl-ketone
Tnfa ..... Murine gene for tumor necrosis factor alpha
Tnfα ..... Tumor necrosis factor-alpha
Tregs ..... Regulatory T cells
TTE ..... Transthoracic echocardiography
UN ..... United Nations
Vcam1 ..... Vascular cell adhesion molecule 1
VH ..... Villous height
VH:CrD ..... Villous height to crypt depth ratio
VPR ..... Volume-Pressure Recording
WBC ..... White blood cells
WHO ..... World Health Organization
XIST ..... X-inactive specific transcript

1. Introduction

1.1. Cardiovascular Diseases

1.1.1. Definition and Overview

Cardiovascular diseases (CVDs) represent a group of disorders affecting the heart and vasculature, constituting a significant global health concern due to their high prevalence and severe health outcomes, including mortality. Comprehending the fundamentals of CVDs, their various forms, and common characteristics is essential for understanding the complexity of these conditions and their impact on public health, thereby informing effective prevention and therapeutic strategies [1]. CVDs interfere with the heart's capacity to sustain adequate circulation, leading to downstream effects on tissue oxygenation and nutrient supply. These conditions, categorised as noncommunicable diseases (NCD), involve disruptions in cardiac function or vascular integrity, leading to a wide range of cardiovascular disorders, as illustrated in **Figure 1-1** [2].

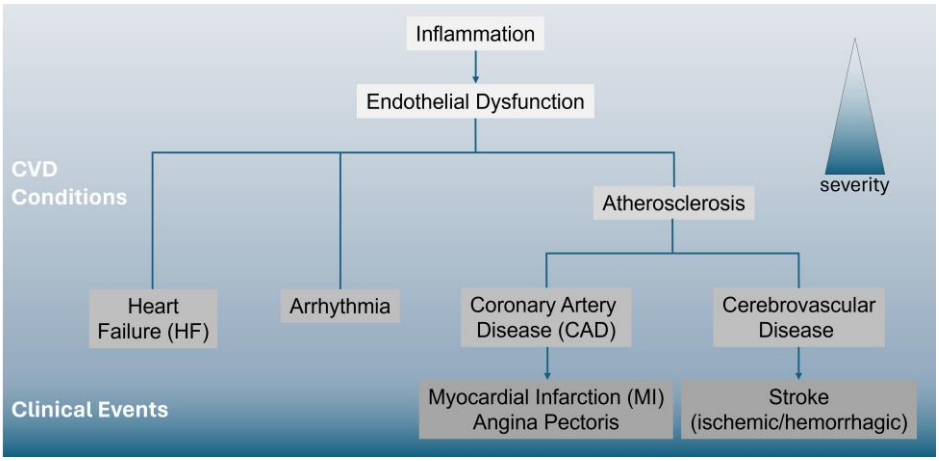

Figure 1-1: Key types of CVD. This diagram highlights the increasing severity of cardiovascular conditions potentially leading to clinical events. Initially, inflammation may trigger endothelial dysfunction, setting the stage for the onset of atherosclerosis. Adapted from [3, 4].

Key types include coronary artery disease (CAD), also known as ischemic heart disease (IHD), which is primarily caused by atherosclerosis. This condition leads to development of atherosclerotic plaque formation and narrowing of coronary arteries, potentially resulting in myocardial infarction (MI). Similarly, cerebrovascular diseases, which affect the blood vessels supplying the brain, can lead to a stroke following a disruption in cerebral blood flow. This interruption can result from either

a blockage (ischemic stroke) or a rupture (haemorrhagic stroke) of brain blood vessels. The heart's diminished pumping efficiency characterises heart failure (HF) due to conditions like CAD or hypertension. Additionally, arrhythmia, which involves irregular heart rhythms or rates, can significantly affect cardiovascular health and is often associated with underlying heart diseases or systemic imbalances [5, 6].

1.1.2. Prevalence and Global Impact

CVDs remain a leading health concern on a global scale. According to the World Health Organization (WHO), CVDs are the foremost cause of death globally, with an estimated 17.9 million deaths in 2019, representing 32% of all global deaths. **Figure 1-2** illustrates a substantial rise in absolute numbers of CVD-related mortality and prevalence over the past few decades, underlining the increasing global health burden [7, 8].

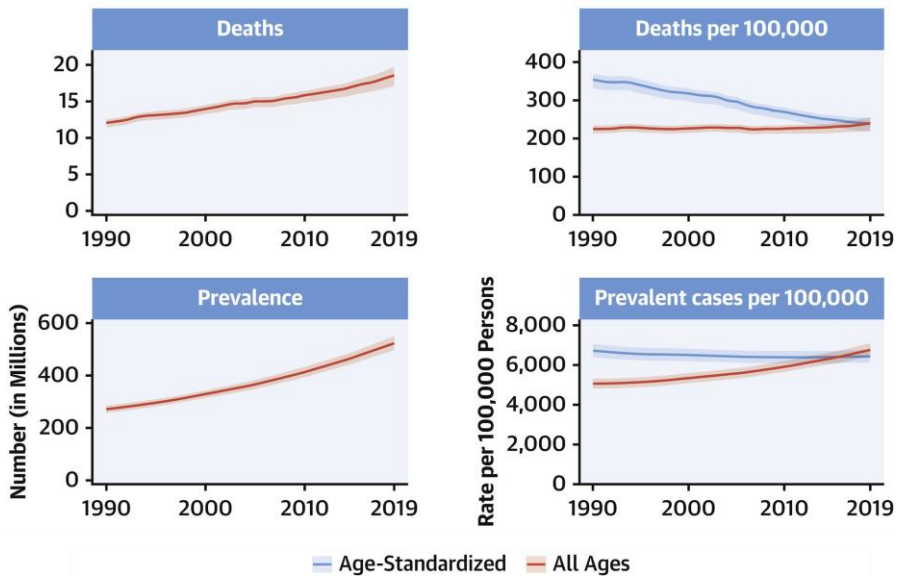

Figure 1-2: Global data on CVD mortality and prevalence in absolute numbers and rates with and without age-standardization from 1990 to 2019. Adapted from [9].

Predominantly, CAD and stroke are the most prevalent and lethal, responsible for over 85% of these deaths. Notably, the burden of these diseases disproportionately impacts low- and middle-income countries (LMIC), accounting for more than three-quarters of CVD deaths worldwide [10, 11]. The burden of CVDs extends beyond their impact on mortality. They are a leading cause of morbidity worldwide, significantly contributing to disability and reducing the quality of life (QoL). For

instance, HF currently affects an estimated 64.3 million people globally, leading to hospitalisation and long-term disability [12, 13].

The economic implications of CVDs are enormous. According to a study published by the World Economic Forum and the Harvard School of Public Health, CVDs will cause more than 1 trillion USD (~ 930 billion EUR[1]) in lost economic output in 2030, a substantial increase from about 863 billion USD (~ 800 billion EUR) in 2010. These costs include direct costs, such as healthcare expenditures for hospital stays, medications, and other treatments, and indirect costs, such as lost productivity due to disability and premature death [14, 15].

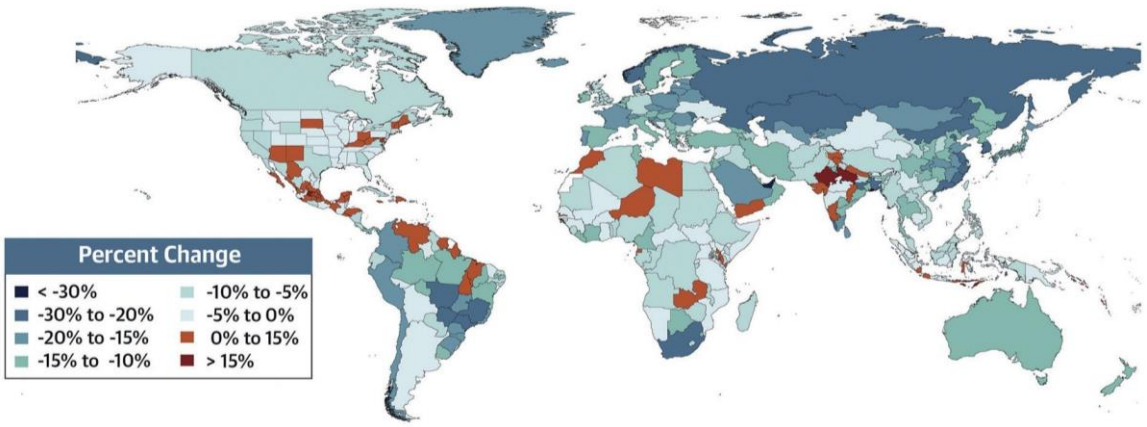

Figure 1-3: Change in % of age-standardized CVD death rate from 2010-2019. Adapted from [9] with permission.

While the global burden of CVD remains a pivotal health concern, recent analyses present a nuanced picture of global trends in CVD incidence and mortality. Although there has been an increase in the absolute number of CVD cases and deaths, a reflection of changes in population age, a significant decrease in age-standardized incidence and mortality rates has been observed in most countries (**s. Figure 1-2** and **Figure 1-3**). This pattern suggests strides toward achieving the WHO's goal of a 25% reduction in premature mortality from NCDs by 2025, and the Sustainable Development Goal (SDG) target 3.4 set by the United Nations (UN), which aims for a one-third reduction by 2030. Nevertheless, this progress is not uniform across the globe. Particularly in LMIC, there are alarming increases in both CVD incidence and mortality, underscoring persistent disparities. Moreover, the current pace of progress is insufficient to meet the ambitious international health goals. This indicates an

[1] with the current exchange rate of 1 USD = 0.93 EUR (06.03.2025)

urgent need for accelerated efforts and targeted strategies, especially in under-resourced areas, to not only address the immediate challenges posed by CVD but also to ensure that the advancement towards WHO and SDG targets is both equitable and expedited [16-18].

1.1.3. Pathophysiology

CVDs encompass a diverse set of disorders, each with their unique pathophysiology, yet sharing common pathophysiological features such as endothelial dysfunction, inflammation, atherosclerosis, and thrombosis. These elements are pivotal in the onset and progression of most CVD as illustrated in **Figure 1-4** .

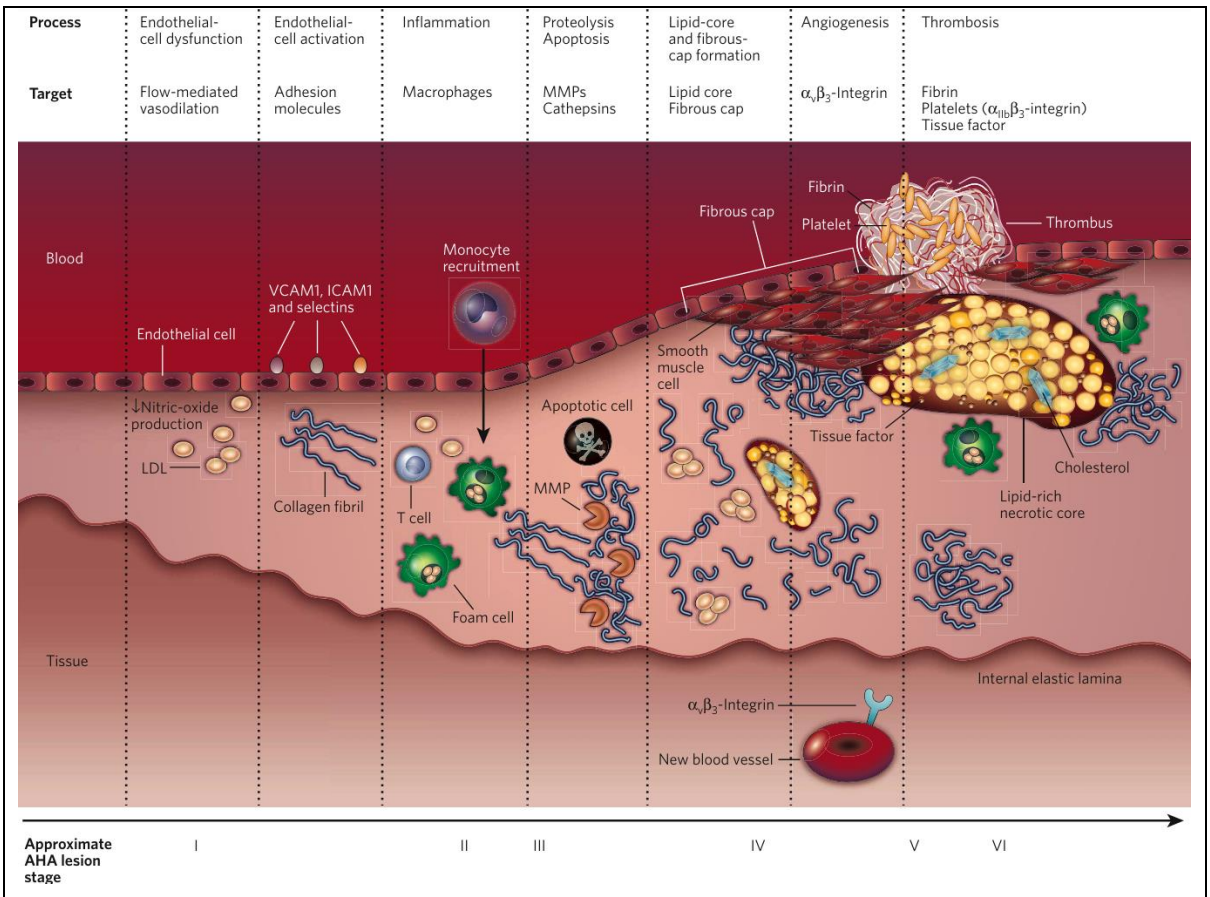

Figure 1-4: Atherogenesis, the Progression of Atherosclerosis. This illustration depicts the development of an atherosclerotic lesion from a healthy blood vessel (left) to one with advanced atherosclerosis featuring a thrombus (right). The classification of atherosclerotic lesions according to the American Heart Association (AHA, [19]) delineates key changes around the vessel, including endothelial dysfunction, inflammation, and plaque accumulation, which can also act as potential clinical molecular targets for diagnosis. Reproduced from [20] with permission from Springer Nature.
Abbreviations: ICAM1 - intercellular adhesion molecule 1, LDL - low-density lipoprotein, MMP - matrix metalloproteinase; VCAM1 - vascular cell adhesion molecule 1.

Atherosclerosis is a key pathophysiological process involved in the development of many CVDs, especially CAD. It involves the accumulation of plaques composed of calcium deposits, necrotic lipid cores, macrophages, and smooth muscle cells (SMC), leading to their hardening and narrowing, and subsequently impairing blood flow to the heart and other organs. Plaque rupture in arteries can initiate thrombosis, potentially leading to acute cardiovascular events such as MI or strokes. This clot formation is a physiological mechanism that typically occurs as a natural response to vascular injury, obstructing blood flow and escalating the risk of severe outcomes [21, 22]. Inflammation is crucial in the development and progression of CVDs, driving both plaque formation and instability. Chronic inflammation, which leads to persistent oxidative stress, intensifies atherosclerosis and other pathological changes, often triggered by classical risk factors such as high cholesterol levels and hypertension. This inflammation can contribute significantly to endothelial dysfunction, which is instrumental in furthering cardiovascular impairment and disease progression [23].

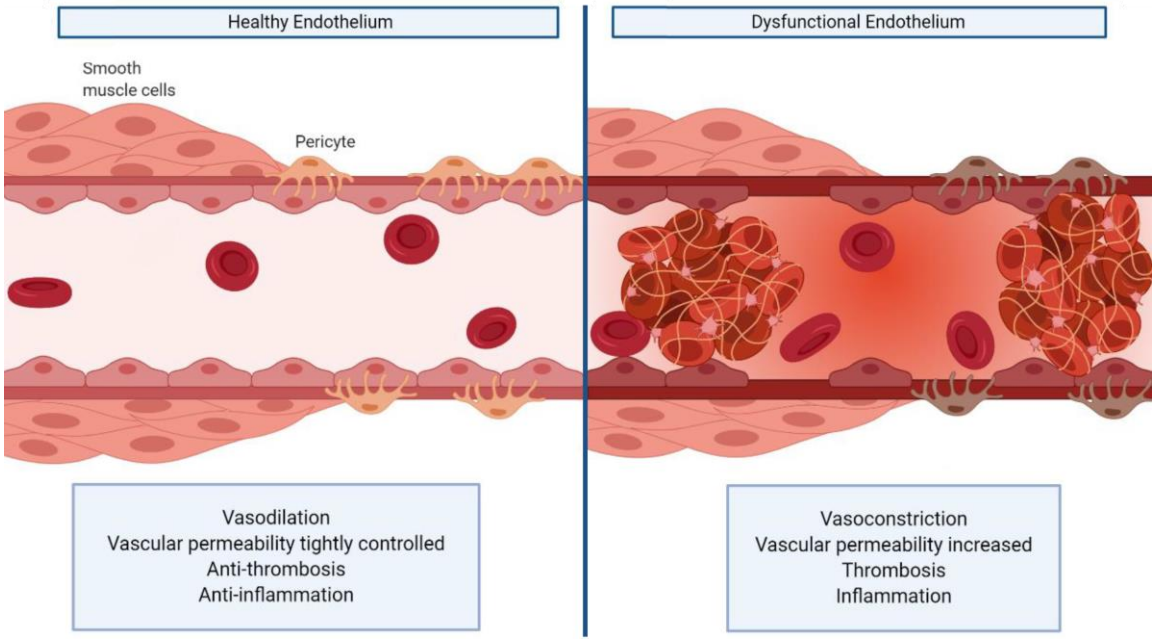

Figure 1-5: Comparison of Healthy and Dysfunctional Endothelium. This illustrates the architecture of a healthy vascular endothelium (left), showing endothelial cells, SMCs, and pericytes maintaining vascular integrity and function. It contrasts with the dysfunctional endothelium (right), where disrupted endothelial barrier and cell function lead to vasoconstriction, increased permeability, thrombosis, and inflammation, marking the onset of vascular diseases. Adapted from [24] with permission.

The endothelium, the inner lining of blood vessels, is a crucial player in the pathogenesis of CVD. In a healthy state (s. **Figure 1-5**), the endothelium maintains

vascular tone and permeability, prevents clot formation, and suppresses inflammatory responses. However, endothelial dysfunction, often caused by again hypertension (and vice versa) and high cholesterol levels, fosters atherosclerosis and CVD progression. Flow-mediated dilation (FMD) has emerged as an early, non-invasive marker of endothelial dysfunction and subclinical atherosclerosis. Impaired FMD has also been observed in patients with already-established hypertension and HF [25-28]. Moreover, conditions such as hypertension can cause structural and functional heart changes, contributing to HF and arrhythmias, leading to increased morbidity and mortality in CVDs [24, 29].

At the cellular and molecular levels, the development of CVDs involves alterations in gene expression, cell signalling, metabolism, and apoptosis. These changes affect various cell types, including endothelial, smooth muscle, and immune cells. Understanding these alterations is crucial for unravelling the complex mechanisms underlying CVDs and for identifying more effective early detection strategies using appropriate surrogate biomarkers in clinic and preclinical settings [30, 31].

1.1.3.1. Nitro-Oxidative and Oxidative Stress

To comprehend the development and progression of CVDs, it is essential to delve deeper into the molecular changes driven by inflammation and oxidative stress within the vascular system. This understanding is fundamental for the early detection and observation of atherogenesis. While the following section covers only a fraction of the impacted physiological processes, it highlights critical concepts in an emerging and evolving field. Endothelial dysfunction is now recognized as an early indicator of clinically silent atherosclerosis at the tissue functionality level. To fully appreciate the changes occurring on a cellular and molecular level, it is helpful to first understand the respective physiological processes in a healthy state [32-34].

The vascular endothelium regulates vascular tone by releasing vasodilatory and vasoconstrictive mediators. Key vasodilators include nitric oxide (NO), prostacyclin (PGI2), and endothelium-derived hyperpolarizing factor (EDHF). As shown in **Figure 1-6** basically NO, produced by eNOS (endothelial NO-Synthase), increases intracellular cyclic guanosine monophosphate (cGMP), leading to smooth muscle relaxation and vasodilation [35].

Vasoconstrictive substances produced by the endothelium include endothelin-1 (ET-1), angiotensin II (ATII), and thromboxane (TXA2). These mediators regulate vascular tone under various physiological conditions by promoting smooth muscle contraction. This physiological regulation of vasodilation and vasoconstriction ensures proper peripheral resistance, which, together with cardiac output, regulates blood pressure and maintains cardiovascular homeostasis [35, 36].

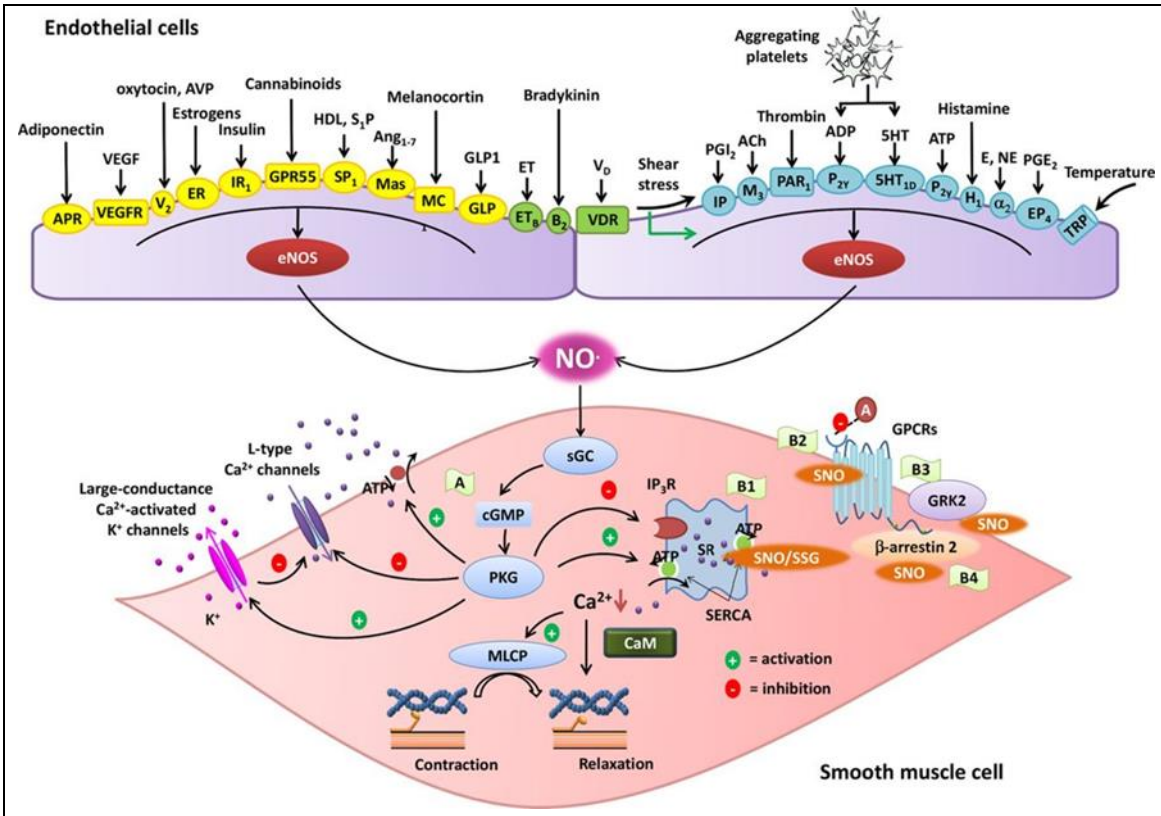

Figure 1-6: Endothelium-dependent vascular regulation via NO. Top: Physical factors (shear stress, temperature) and neurohumoral mediators (though receptor activation) increase NO release by eNOS. Numerous activation signals are dependent on Ca^{2+} (blue), post-translational modifications (yellow), or both (green). Bottom: Vascular SMC contraction is driven by increased intracellular Ca^{2+}. NO modulates this process through multiple pathways, including activation of soluble guanylyl cyclase (sGC) producing cGMP, which activates protein kinase G (PKG), inhibiting Ca^{2+}-influx and promoting Ca^{2+}-efflux and reuptake. NO also induces S-nitrosylation (SNO) and S-glutathionylation (SSG) of proteins, regulating various cellular functions. Reproduced from [35] with permission from Wolters Kluwer Health, Inc.

Abbreviations: α - α-adrenergic receptor; 5HT - serotonin (5-hydroxytryptamine); 5HT1d - serotoninergic (5 hydroxytryptamine) receptor 1D subtypes; Ang1–7 - angiotensin1–7; AdipoR - adiponectin receptor; AVP - arginine vasopressin; B - kinin receptor; E - epinephrine; EP4 - prostaglandin E2-receptor 4; ER - nongenomic estrogen receptor; ET(-1) - endothelin-1; ETb - endothelin-receptor B subtypes; GLP - glucagon-like peptide-1, glucagon-like peptide receptor; GPR55 - G-protein–coupled receptor 55; H - histaminergic receptor; HDL - high-density lipoproteins; IP - prostacyclin receptor; IR1 - insulin receptor; M - muscarinic receptor; Mas - Mas receptor; MC - melanocortin receptor; NE - norepinephrine; P - purinergic receptor; PAR - protease activated receptor; PGE2 - prostaglandin E2; SERCA -sarco/endoplasmic reticulum calcium-ATPase; SP1 - sphingosine 1-phosphate; TRP - transient potential receptor V4; V - vasopressin receptor; VEGF - vascular endothelial growth factor; VEGFR - VEGF-receptor; VD - vitamin D; and VDR - vitamin D receptor. Credit: Paul M. Vanhoutte. Circulation Research. Thirty Years of Saying NO, Volume: 119, Issue: 2, Pages: 375-396, DOI: 10.1161/CIRCRESAHA.116.306531.

However, this delicate equilibrium can be disrupted by oxidative stress, which arises from an imbalance between the generation of reactive oxygen and nitrogen species (RONS, both ROS and RNS) and the body's antioxidant defences. Major RONS sources in the vascular system include NADPH oxidases, NO-synthases, mitochondria, xanthine oxidase, and cytochrome P450 enzymes [37, 38].

NADPH oxidases are a family of various human isoforms (NOX1-NOX5) that generate reactive oxygen species (ROS). The ROS generated by NADPH oxidases plays crucial roles in various physiological processes, including innate immunity and the modulation of redox-dependent signalling cascades. When activated, NOX2 (formerly known as $gp91^{phox}$) produces superoxide anions, which are critical in causing endothelial dysfunction and promoting atherogenesis. This process is particularly relevant during the oxidative burst of immune cells such as neutrophils and macrophages, where NOX2 generates large amounts of superoxide in response to immune challenges. NOX2-derived superoxide can react with NO, decreasing its bioavailability and forming peroxynitrite, a potent oxidant that further damages vascular cells and contributes to the pathogenesis of atherosclerosis [39, 40].

The family of NO-synthases (NOS), including neuronal NOS (nNOS), inducible NOS (iNOS), and endothelial NOS (eNOS), also contribute to oxidative stress. While nNOS and eNOS are constitutively expressed, iNOS is typically expressed during inflammatory responses, leading to the overproduction of NO and subsequent nitro-oxidative stress. Under such conditions, eNOS can become uncoupled, producing superoxide instead of NO. This again exacerbates vascular damage by weakening the endothelial cell layer, increasing permeability, and allowing inflammatory cell infiltration [41-43].

Markers such as 3-nitrotyrosine (3-NT) and 4-hydroxynonenal (4-HNE) indicate nitro-oxidative stress in tissues. Elevated plasma levels of nitrite and nitrate reflect increased NOS activity and oxidative stress.

1.1.3.2. (Chronic) Inflammation

Inflammation is a crucial physiological response to tissue injury and infection, serving as a protective mechanism that facilitates tissue healing and defence

against pathogenic stimuli, involving both innate and adaptive immune responses. However, when inflammation becomes chronic, it can lose its beneficial effects and instead contribute to the development and progression of various diseases, including CVD. The interplay between oxidative stress and chronic inflammation is critical in the development and progression of CVDs. These two processes are almost inseparable, as they go hand in hand in perpetuating vascular damage [44, 45]. Chronic inflammation significantly contributes to CVDs by facilitating plaque formation and instability. Various cytokines and adhesion molecules are key players in this inflammatory process, creating a feedback loop that perpetuates both oxidative stress and inflammation. This mutual reinforcement exacerbates vascular damage and promotes atherosclerosis, highlighting the interdependent nature of these pathological processes [46]. Inflammation can occur anywhere in the body, and cytokines and other inflammatory mediators enter the bloodstream, travelling to sites of inflammation, affecting blood vessels, and contributing to vascular inflammation. In the following section, some relevant candidates involved in this process are introduced.

Cytokines, particularly TNF-α, interleukin-1 (IL-1), and IL-6, are central to the inflammatory response in CVDs. TNF-α, released by activated macrophages, induces the expression of other inflammatory cytokines and adhesion molecules on endothelial cells, critical in early atherosclerosis [47, 48].

Vascular cell adhesion molecule 1 (VCAM1) and its intercellular adhesion molecule 1 (ICAM1) are expressed on endothelial cells in response to such inflammatory stimuli (s. Stage I, **Figure 1-4**). Both mediate the adhesion of leukocytes to the endothelium and their subsequent transmigration, which is essential for the initiation of atherosclerosis [49, 50].

Interferon-gamma (IFN-γ) plays a significant role in the development and progression of CVD by inducing oxidative stress, promoting foam cell accumulation, and stimulating smooth muscle cell proliferation and migration (s. Stage II-IV, **Figure 1-4**). Cytokines such as IL-6 and IL-17 are involved in the acute phase response and chronic inflammation, with elevated levels linked to increased cardiovascular risk. Additionally, IL-17 induces the expression of VCAM1 through the NF-κB signalling pathway, further promoting inflammation and atherosclerosis. However,

the role of IL-17A in atherosclerosis is complex, with studies reporting contradictory effects on plaque size and stability [51-55].

$CD11b^+$ cells, a subset of monocytes, play a crucial role in atherosclerosis by promoting monocyte recruitment and atherosclerosis development (s. Stage II, **Figure 1-4**). Flow cytometric analysis provides insights into immune cell infiltration and activation in vascular tissues. Gene expression levels of these inflammatory markers in various tissues offer a comprehensive view of the inflammatory status [56, 57]. In cardiovascular pathophysiology, the roles of inflammation and oxidative stress are complex and not fully elucidated. The molecular mechanisms associated with the physiological responses to inflammation and oxidative stress in CVD are complex and require further investigation [44, 58]. Their interplay contributes to the initiation, progression, and complications of atherosclerotic plaque formation and represents potential therapeutic targets in CVD management.

1.1.4. (Non-Traditional) Risk Factors for CVD

Traditional risk factors, which can be divided into social, behavioural, and metabolic categories or modifiable and non-modifiable, and include factors such as ageing, smoking, hypertension, dyslipidaemia, and diabetes mellitus, are widely recognized for their substantial contribution to the incidence of CVD [1].

In recent years, an array of non-traditional cardiovascular risk factors has been identified, shedding new light on the multifaceted nature of cardiovascular health and disease. These factors, often under-recognized in conventional risk assessments, encompass autoimmune and inflammatory diseases, psychosocial stressors not traditionally included in risk assessments, genetic predispositions, and the broader concept of the exposome [59-62].

Numerous autoimmune diseases (AIDs), such as systemic lupus erythematosus (SLE), rheumatoid arthritis (RA), and possibly celiac disease (CeD), have been associated with a higher risk of CVD (for more details refer to section 1.3). The mechanistic link between autoimmunity and CVD involves chronic inflammation, both topics are covered in more detail in the sections 1.1.3.2 and 1.3.

In the post-COVID world, psychosocial stress has gained significant relevance and is poised to become increasingly critical in the future. The fast-paced nature of contemporary life further amplifies the importance of addressing psychosocial stressors. These stressors, including chronic stress, depression, noise pollution, and social isolation, have been linked to an elevated risk of developing CVD. They impact cardiovascular health through mechanisms such as activation of the stress-response system (hypothalamic-pituitary-adrenal axis and sympathetic nervous system), promotion of unhealthy behaviours like poor diet and physical inactivity, and exacerbation of inflammation and metabolic changes. Understanding and mitigating these stressors is essential for improving cardiovascular health outcomes in the years to come [63-67].

The exposome concept, first introduced by Christopher Wild in 2005, was developed to complement the genome by emphasizing the critical role of environmental exposures in disease development [68]. It encompasses all the above-mentioned contributors and additional environmental factors, as it represents the totality of environmental exposures an individual encounters throughout their lifetime. This includes lifestyle factors, psychosocial stressors, physical activity, and chemical exposures such as soil, water, and air pollution (s. **Figure 1-7**). Understanding the exposome is essential for a holistic approach to health, not just CVD, as it encompasses the complex interplay of various factors that impact an individual's overall well-being and disease risk [69, 70].

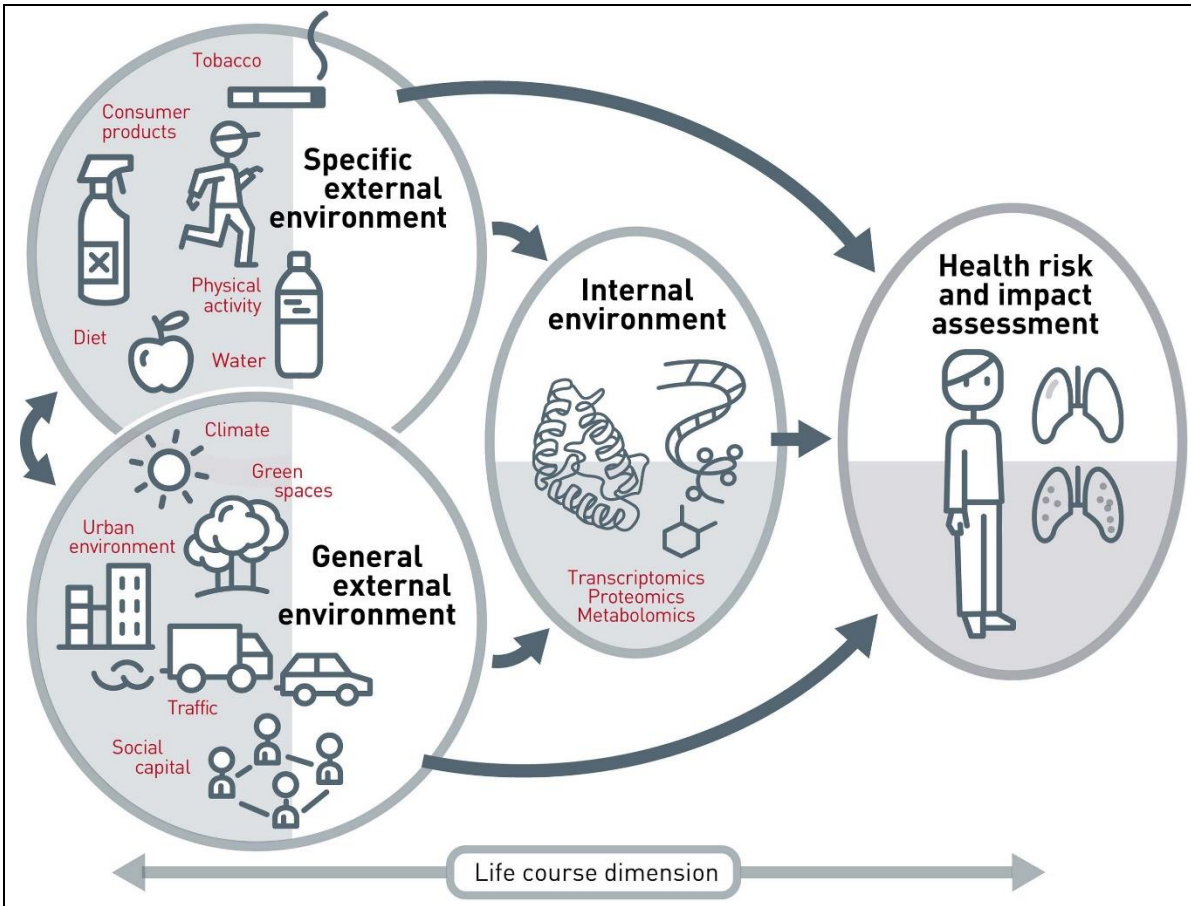

Figure 1-7: Conceptualization of the exposome concept. This framework, adapted from Vrijheid and the ISGlobal, illustrates the exposome as comprising three interconnected domains: the general external environment (e.g., climate, traffic, social capital), the specific external environment (e.g., diet, tobacco, water), and the internal environment, which includes biological responses such as transcriptomics, proteomics, and metabolomics. These components interact dynamically across the life course and collectively influence health risk and impact, particularly in chronic diseases such as cardiovascular and respiratory disorders.
Abbreviation: ISGlobal - Barcelona Institute for Global Health/Instituto de Salud Global de Barcelona.
Reproduced from [71] with permission from BMJ Publishing Group Ltd.

Recognizing and understanding these non-traditional cardiovascular risk factors is essential. They enhance our comprehension of the complex aetiology and pathophysiology of CVD, improve risk stratification methods, and create opportunities for novel preventive and therapeutic approaches. With ongoing advancements in medical research and technology, the list of non-traditional risk factors is expected to grow, providing deeper insights into cardiovascular health and better management options for this global health issue [72, 73].

1.1.5. Current Treatment and Prevention Strategies

The management of CVD involves a comprehensive range of treatments and prevention strategies aimed at mitigating symptoms, slowing disease progression, and improving overall QoL. This chapter explores the critical components of CVD management, including pharmacological treatments, surgical interventions, lifestyle modifications, public health initiatives, and emerging therapeutic approaches such as targeting the gut microbiome.

Medications are pivotal in managing CVD by controlling symptoms, managing risk factors, and preventing complications. Key classes of medications include antihypertensive drugs, such as ACE inhibitors, calcium channel blockers, and diuretics, which are crucial in controlling high blood pressure, a significant risk factor for CVDs. Statins are the gold standard for lowering cholesterol levels, aiming to reduce LDL levels to less than 70 mg/dL for high-risk and diabetic patients. These medications reduce the risk of heart attacks and strokes. Additionally, antiplatelet and anticoagulant medications, including aspirin and warfarin, help prevent blood clots, a common problem in various CVDs. However, these medications can have side effects such as dizziness, fatigue, and gastrointestinal issues, and their long-term use may lead to other health concerns, such as kidney damage [74-77].

Emerging therapies like glucagon-like peptide-1 (GLP-1) analogues and sodium/glucose cotransporter 2 (SGLT2) inhibitors are also becoming important in the management of CVDs, especially for patients with comorbid conditions like diabetes. GLP-1 analogues, originally developed for diabetes management, have shown cardiovascular benefits, including weight loss, improved glycaemic control, and reduced risk of major adverse cardiovascular events. The LEADER trial (Liraglutide Effect and Action in Diabetes: Evaluation of Cardiovascular Outcome Results) demonstrated a 13% reduction in major adverse cardiovascular events in patients treated with liraglutide compared to placebo (hazard ratio (HR), 0.87; 95% confidence interval (CI), 0.78 to 0.97; p-value=0.01) [78, 79]. SGLT2 inhibitors, another class of diabetes medication, have demonstrated significant benefits in reducing heart failure hospitalizations and cardiovascular mortality. The EMPA-REG OUTCOME trial (Empagliflozin Cardiovascular Outcome Event Trial in Type 2 Diabetes Mellitus Patients) showed a 38% (3.7%, vs. 5.9%) relative risk reduction in cardiovascular death and a 35% relative risk reduction (2.7% and 4.1%) in heart

failure hospitalizations in patients treated with empagliflozin compared to placebo [80-82].

Novel promising therapeutic approaches include traditional anti-inflammatory drugs, specific immunomodulation, and vaccination against atherosclerotic disease. Other emerging therapies aim to reduce lipoprotein(a) levels, a variant of LDL, and directly target inflammation [83, 84].

Notably, the CANTOS trial demonstrated that anti-inflammatory therapy with canakinumab, a monoclonal antibody that targets IL-1β, improved cardiovascular outcomes. canakinumab at a dose of 150 mg every 3 months led to a 15% relative reduction in the risk of the primary endpoint for patients compared to the placebo group (HR, 0.85; 95% CI, 0.74 to 0.98; p-value=0.021). [85].

Similarly, the LoDoCo2 trial showed that low-dose colchicine reduced the risk of cardiovascular events in patients with chronic coronary disease. Traditionally used to treat gout, colchicine has anti-inflammatory properties that have been repurposed for CVD. Its mechanism involves the inhibition of microtubule polymerization, which reduces leukocyte activation and migration. 0.5 mg of colchicine once daily reduced the risk of the primary composite endpoint (cardiovascular death, MI, ischemic stroke, or ischemia-driven coronary revascularization) by 31% compared to the placebo group (HR, 0.69; 95% CI, 0.57 to 0.83; p-value<0.001). These findings underscore the importance of addressing inflammation in CVD management and open new opportunities for treatment strategies that could benefit patients with both cardiovascular and AIDs [86].

For severe or advanced CVD cases, surgical procedures might be necessary. These include minimally invasive procedures like angioplasty and stenting, which widen narrowed or blocked arteries, and more invasive surgeries such as coronary artery bypass grafting and heart valve repair/replacement. These procedures can significantly improve cardiovascular function and QoL, but they come with inherent risks such as infection, bleeding, and adverse reactions to anaesthesia [87].

To prevent the need for surgical interventions, early preventive measures such as lifestyle modifications are crucial. Essential modifications include adopting a healthy diet low in saturated fats, cholesterol, and sodium, engaging in regular physical activity, quitting smoking, and implementing stress management techniques to

mitigate the adverse effects of stress on heart health, essentially reducing modifiable cardiovascular risk factors. Regular health check-ups to monitor blood pressure, cholesterol levels, and blood sugar can help detect potential issues early. However, these changes require significant commitment and discipline, and individuals may face barriers such as lack of time, resources, and social support [1, 88, 89].

Recognizing that lifestyle modifications can be challenging on an individual level; public health initiatives aim to facilitate these changes on a societal level. By implementing policies and creating environments that promote healthy behaviours, these initiatives help make it easier for individuals to adopt and maintain heart-healthy lifestyles. These initiatives include education and awareness campaigns designed to inform the public about CVD risk factors and prevention strategies, regulations such as restrictions on tobacco advertising and sales, and the promotion of environments conducive to physical activity and healthy food choices. Promoting healthy food choices can have a profound impact on cardiovascular health, partly by influencing the gut microbiome [74, 90].

The gut microbiome can influence lipid metabolism, inflammation, and atherosclerosis development. Strategies targeting the microbiome include dietary modifications, probiotics, prebiotics, and faecal microbiota transplantation (FMT). Further research is needed to fully understand the mechanisms and develop effective and safe microbiome-targeted therapies for CVDs [91].

There are extensive guidelines available from leading cardiovascular societies that provide evidence-based recommendations for the management of CVDs. These guidelines help standardize care and ensure that patients receive the most effective treatments. The most important guidelines are provided by:

- American Heart Association (AHA): More than 100 guidelines cover a wide range of topics, including management of cardiovascular patients, hypertension, risk assessment and prevention [88, 92-94].
- European Society of Cardiology (ESC): Comprehensive recommendations on the management of prevention, diagnosis, and treatment of CVD and (pre)diabetes [76, 95, 96].

- German Cardiac Society (DGK): These guidelines focus on the specific needs and practices on a national level but are also influential in shaping broader European standards [97].

These guidelines are regularly updated to incorporate the latest research findings and clinical practices, ensuring that healthcare providers can offer the most current and effective care to their patients.

The management of CVDs necessitates a multifaceted approach that combines medical interventions, lifestyle modifications, and supportive public health policies. The effectiveness of this approach depends on individual commitment, healthcare provider guidance, and a supportive public health environment. The emerging understanding of the role of inflammation and the microbiome in CVDs further enriches future strategies, potentially bridging treatment paradigms with those used for AIDs. This comprehensive approach not only aims to treat CVDs but also to prevent their occurrence and progression, ultimately improving patients' QoL and reducing the global burden of CVDs [9].

1.2. Celiac Disease and Autoimmunity

1.2.1. Definition and Overview

Autoimmune diseases (AIDs) represent a significant challenge in modern medicine due to their complex nature, difficulties in diagnosis, and treatment challenges. AIDs result from a breakdown in immune tolerance to self-antigens, leading to chronic inflammation and tissue destruction. The heterogeneity and unpredictable course of the more than 80 known AIDs, coupled with the absence of specific causative factors, highlight the complexity of their management [98-100].

AIDs affect approximately 10 in 100 individuals worldwide, with females accounting for 8 of these 10 cases [101, 102].

The mechanisms underlying this pronounced sex disparity remain a significant area of ongoing research. Recent studies suggest that approximately 23% of X-linked genes escape the necessary epigenetic X-inactivation by XIST (X-inactive specific transcript), leading to these genes being expressed at higher levels in female immune cells. This overexpression may contribute to an overactive immune

response, potentially explaining part of the sex bias observed in AIDs. This phenomenon represents just one of many factors under investigation, as researchers continue to explore the complex interplay between genetic, hormonal, and environmental influences on AID susceptibility [102-105].

AIDs often co-occur within individuals and families, suggesting shared aetiological pathways. The most common co-existing AIDs include multiple sclerosis (MS), autoimmune thyroid disease, type 1 diabetes mellitus (T1D), inflammatory bowel disease (IBS), and RA [101, 106]. The pathogenesis of AIDs involves a multifactorial interplay between genetic predispositions, environmental triggers, and immune system dysregulation. Genetic polymorphisms, particularly in genes related to the immune system, play a critical role in susceptibility to AIDs. Specific human leukocyte antigen (HLA) haplotypes are strongly associated with many autoimmune conditions, including MS, RA, and CeD. Despite these associations, the presence of risk alleles alone is insufficient for disease development, indicating the significant role of environmental factors and immune activation pathways. Immune system dysregulation in AIDs includes defects in central and peripheral tolerance mechanisms. Central tolerance occurs in the thymus, where autoreactive T cells are eliminated, while peripheral tolerance involves regulatory T cells (Tregs) and other mechanisms that suppress autoreactive immune responses. Failures in these tolerance mechanisms can lead to the survival and activation of autoreactive lymphocytes, which target self-tissues [98].

The role of the gut microbiome has also been increasingly recognized in the pathogenesis of AIDs. The interactions between the gut microbiota and the immune system are crucial in maintaining immune homeostasis. Dysbiosis, an imbalance in the microbial community, has been implicated in several AIDs. This suggests that the microbiome may influence disease onset and progression, making it highly relevant for future preventive and therapeutic approaches [98, 107].

CeD exemplifies an AID triggered by an environmental factor - in this case, gluten, a protein found in wheat, barley, and rye. In genetically predisposed individuals, gluten ingestion leads to an inappropriate immune response, resulting in inflammation and damage to the small intestine. CeD illustrates the complexity of autoimmune responses, demonstrating how genetic susceptibility, environmental triggers, and immune dysregulation converge to cause disease. The clinical

presentation of CeD is highly variable, ranging from gastrointestinal symptoms such as diarrhoea and abdominal pain to extra-intestinal manifestations like anaemia, osteoporosis, and neurological disorders. This variability underscores the necessity for comprehensive diagnostic approaches [108, 109].

The upcoming section will further explore the prevalence and incidence of CeD, providing insights into its epidemiology. Additionally, the detailed pathophysiology of CeD will be explored in the section 1.2.3, with an in-depth look at the immune mechanisms. Finally, we will discuss treatment and prevention strategies in section 1.2.4, emphasizing current management approaches and potential future therapies.

1.2.2. Prevalence and Incidence

As already mentioned, AIDs collectively impact approximately 10 in 100 individuals, with females accounting for 8 of these 10 cases [102, 103].

Over the last few decades, there has been a notable increase in the incidence of AIDs, particularly in westernized societies. This rise is attributed not only to genetic factors but also to environmental influences. For instance, the prevalence of antinuclear antibodies (ANAs), a common biomarker of autoimmunity, has increased, especially among young people. Although the reasons for this increase are not fully understood, they may be related to changes in the microbiota, chronic viral infections, and dietary habits [110-112].

The prevalence of CeD varies geographically, with significant differences reported between regions and populations. Globally, the prevalence of CeD is estimated to be approximately 1%, though this figure can fluctuate based on specific population studies and diagnostic criteria [113, 114]. In Western countries, particularly in Europe and North America, the prevalence of CeD is well-documented. In the United States, for instance, it is estimated that about 1 in 133 individuals (approx. 0.75%) have CeD. In Europe, the prevalence is slightly higher, with studies indicating that about 1 in 100 individuals are affected. These prevalence rates partially reflect both diagnosed and undiagnosed cases, emphasising the significant number of individuals who may remain asymptomatic or misdiagnosed [114-116].

The incidence of CeD has also seen a notable increase over the past few decades. This rise can be attributed to heightened awareness, improved diagnostic methods, and changes in environmental factors. The introduction of more sensitive and specific serological tests, such as the tissue transglutaminase (TG2) antibody test, has facilitated the detection of both symptomatic and asymptomatic cases [117].

Despite the high prevalence and rising incidence in many Western countries, the global burden of CeD remains unevenly distributed. In regions such as sub-Saharan Africa and East Asia, the reported prevalence is significantly lower. This discrepancy can be partially explained by genetic differences, dietary habits, and potentially underdiagnosis due to lack of awareness and limited access to diagnostic resources [114, 118].

The genetic predisposition to CeD is strongly associated with the HLA-DQ2 and HLA-DQ8 haplotypes. These genetic markers are present in approximately 30-40% of the general population, yet only a small fraction of these individuals develop CeD [119]. Several epidemiological studies have highlighted the importance of early life factors in the development of CeD. For instance, the timing and quantity of gluten introduction in infants' diets, as well as infections during early childhood, are discussed to influence the risk of developing CeD [120, 121].

1.2.3. Pathophysiology

CeD is a multifactorial autoimmune disorder, with its pathogenesis hinging on an intricate interplay between genetic, immunological, and environmental factors. Almost every individual with CeD carries at least one HLA-DQ2 or HLA-DQ8 gene (s. **Figure 1-8**). These alleles code for certain HLA-DQ dimeric receptors on the surface of antigen-presenting cells (APCs), which contribute to disease susceptibility based on the haplotype present. Additionally, other non-HLA genes are believed to contribute to disease susceptibility [122].

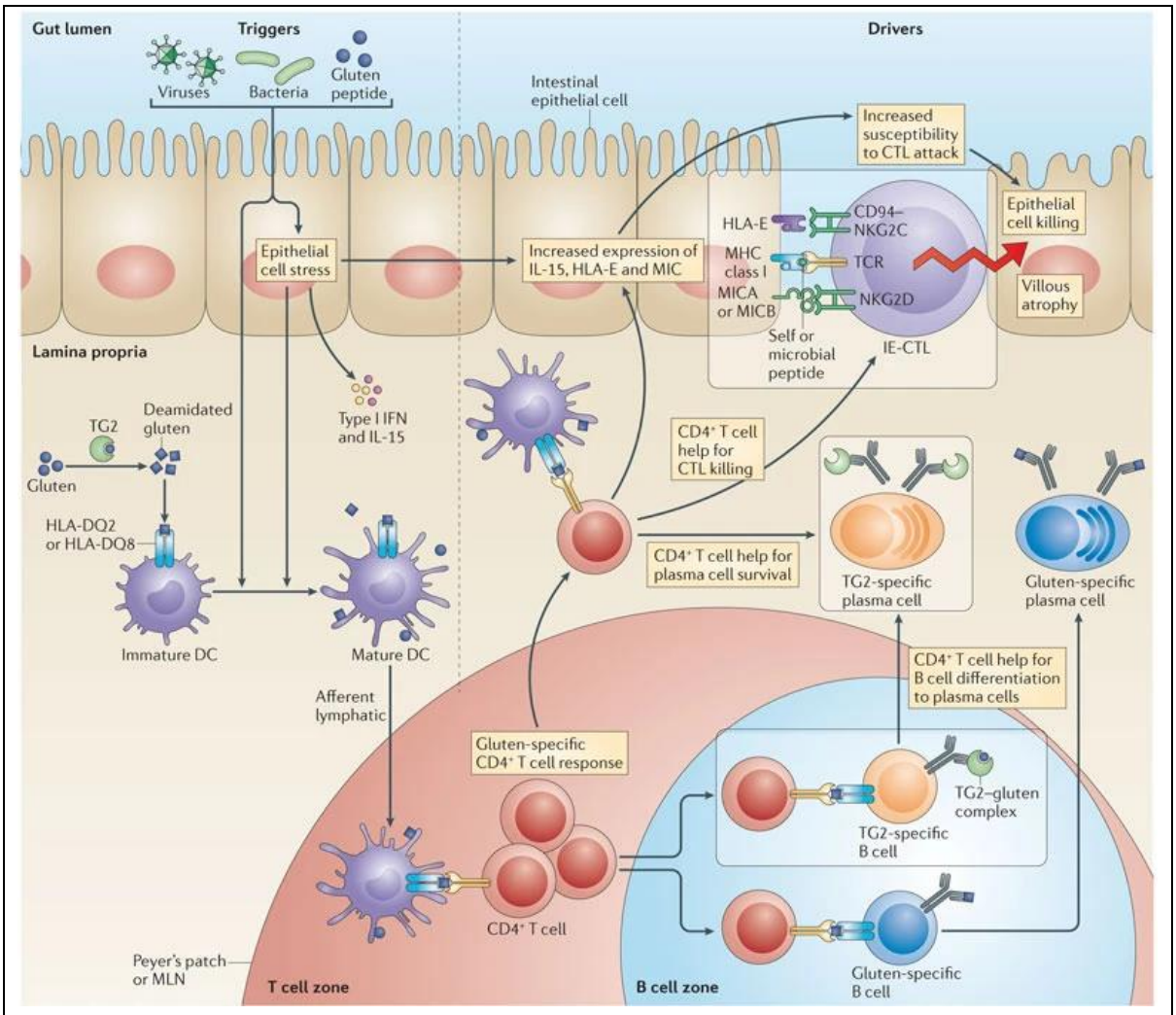

Figure 1-8: Immune Activation and Pathogenesis in CeD: Triggers activate APCs, like dendritic cells (DCs). Stressed intestinal epithelial cells (IECs) produce IL-15 and type I interferon (IFN), which mature DCs. Mature DCs present TG2-deamidated gluten to $CD4^+$ T cells in Peyer's patches or mesenteric lymph nodes (MLN), activating gluten-specific HLA-DQ2/DQ8-restricted $CD4^+$ T cells. TG2-gluten complexes are internalized by TG2-specific B cells, presenting gluten peptides to $CD4^+$ T cells, which aid in B cell differentiation into plasma cells producing autoantibodies. Activated $CD4^+$ T cells induce epithelial IL-15 and non-classical MHC class I expression, enhancing intraepithelial cytotoxic T lymphocyte (IE-CTL) activity, leading to epithelial damage and villous atrophy. Reproduced from [122] with permission from Springer Nature.

Upon ingestion, gluten is partially digested in the gastrointestinal tract, producing immunogenic peptides such as gliadin. These peptides traverse the epithelial barrier of the small intestine, facilitated by increased intestinal permeability. This increased permeability, often referred to as "leaky gut", may be influenced by both genetic and environmental factors [123]. In individuals with CeD, these gliadin peptides undergo deamidation by the enzyme TG2, which increases their immunogenicity. The deamidated gliadin peptides bind with high affinity to HLA-DQ2 or HLA-DQ8 molecules on APCs, such as dendritic cells (DCs) [124].

This interaction between gliadin peptides and $CD4^+$ T cells triggers a robust Th1-type adaptive immune response characterised by the production of pro-inflammatory cytokines, notably IFN-γ. This cytokine milieu promotes the activation and proliferation of cytotoxic T lymphocytes (CTLs) and B cells, the latter of which produce autoantibodies against TG2, endomysium, and gliadin, serving as critical diagnostic markers for CeD [125, 126]. The inflammatory cascade results in the activation of intraepithelial lymphocytes (IELs), which are pivotal in CeD pathogenesis. IELs exhibit increased cytotoxicity and secrete pro-inflammatory cytokines, including IFN-γ and TNF-α, leading to epithelial cell apoptosis and villous atrophy. This mucosal damage is characterised by the hallmark histological features of CeD: villous atrophy, crypt hyperplasia, and increased IELs. The resultant malabsorption leads to diverse clinical symptoms, from gastrointestinal issues to systemic complications such as anaemia and osteoporosis [127].

The innate immune system also plays a critical role in the early stages of CeD pathogenesis. Gliadin peptides can directly stimulate innate immune responses, independent of HLA-DQ2/DQ8 presentation, mediated through receptors like the chemokine receptor CXCR3. This interaction leads to the release of zonulin and increased intestinal permeability. Furthermore, innate immune cells such as natural killer (NK) cells contribute to the inflammatory milieu, exacerbating mucosal damage [128].

The gut microbiome is increasingly recognized as a crucial modulator of immune responses in CeD. Dysbiosis, characterised by an imbalance in the microbial community, has been consistently observed in CeD patients influencing disease onset and progression. Although early life factors such as gluten exposure and breastfeeding practices have been investigated, current evidence suggests they do not significantly influence immune tolerance or the onset of CeD [129-131].

In conclusion, the pathophysiology of CeD involves a multifaceted interplay between genetic predisposition, immune dysregulation, and environmental triggers. Despite considerable advances in understanding these mechanisms, they remain incompletely elucidated. Further research is necessary to unravel disease pathogenesis to support the development of targeted therapeutic and preventive strategies, which will be discussed in the subsequent section.

1.2.4. Current and Future Treatment Strategies

CeD currently lacks a definitive cure, with the only effective treatment being a strict, lifelong gluten-free diet (GFD). Currently, the primary treatment for CeD involves the complete elimination of gluten from the diet, which can be difficult to maintain, significantly impacts the QoL, and often leads to inadvertent gluten exposure. Cross-contamination, limited availability of gluten-free products, and social and economic constraints further complicate adherence to a GFD [132].

Research is actively exploring alternative and adjunctive therapies to the GFD, aiming to improve the QoL for individuals with CeD and reduce the burden of dietary management. A promising example are enzymatic dietary supplements, which involve the use of proteases to degrade gluten peptides in the gastrointestinal tract, thus reducing their immunogenicity. However, the effectiveness of these supplements is under debate. Despite the challenges that such supplements must overcome, especially the delivery and activity to and under gastrointestinal conditions, they could become a great addition to support a GFD [133-136].

Several therapeutic approaches in ongoing clinical trials are being developed and tested to modify the immune response in CeD and address gluten-induced inflammation more effectively using immunotherapy and small molecule inhibitors [137].

- ZED1227/TAK227 (Zedira, Dr. Falk, and Takeda): ZED1227 is a selective transglutaminase 2 (TG2) inhibitor that prevents the modification of gluten peptides, thereby reducing their immunogenicity. In a Phase 2a clinical trial, ZED1227 demonstrated a significant reduction in gluten-induced mucosal damage. Patients receiving the highest dose (100 mg) showed a recovery of VH:CrD ratios compared to placebo (mean difference: 0.48; 95% CI: 0.20-0.77; p-value<0.001). Additionally, IEL counts were significantly lower in the treatment group (mean difference: -9.6 cells/100 IECs; 95% CI: -14.4 to -4.8; p-value<0.001) [138].
- TPM502 (Topas Therapeutics): TPM502 is an innovative nanoparticle-based therapy designed to induce immune tolerance to gluten. The nanoparticles encapsulate gluten peptides and are administered orally, promoting a tolerogenic immune response in the gut-associated lymphoid tissue. Phase

1 studies have shown that TPM502 is safe and well-tolerated, with preliminary efficacy data indicating a reduction in gluten-specific T cell activation. Ongoing Phase 2 trials aim to further evaluate the efficacy and optimal dosing of TPM502 [139].

- KAN-101 (Anokion): This approach involves targeting gluten antigens to the liver, where they are presented in a tolerogenic context, thereby reprogramming the immune system to tolerate gluten. Phase 1 trial data suggest that KAN-101 is well-tolerated. Currently recruiting for phase 1b/2 and 2a clinical trials, which will evaluate the safety and efficacy, including biomarker responses with a gluten challenge [140-142].
- DONQ52 (Chugai Pharmaceutical Co.): DONQ52 is a bispecific antibody blocking HLA-DQ2.5-restricted T cell responses currently in Phase 1. Results from a proof-of-concept study with HLA-DQ2.5^{+} CeD patients indicate reduced T cell responses to wheat epitopes by a median of 87% (IQR 72–92) but did not affect T-cell responses to non-gluten antigens. [143, 144].

In addition to therapies targeting standard CeD, certain candidates are being evaluated for the treatment of non-responsive or refractory CeD (NRCeD), a condition where patients do not exhibit an adequate response to a GFD.

- PRV-015 (formerly AMG 714) (Amgen/Provention Bio): PRV-015 is an anti-IL-15 monoclonal antibody, which was tested in patients with classical CeD and NRCeD. In both Phase 2a clinical trials, PRV-015 demonstrated no significant efficacy in the respective primary endpoints (aberrant IEL reduction or VH:CrD ratio recovery). Positive effects on symptoms, like diarrhoea indicate the potential of PRV-015 as a therapeutic option for NRCeD [145, 146].

The future of CeD treatment lies in the development of therapies that go beyond the limitations of a gluten-free diet. Immunotherapy, small molecule inhibitors, and novel biological agents represent promising strategies that target different aspects of CeD pathogenesis. Ongoing research and clinical trials will be crucial in determining the safety, efficacy, and feasibility of these innovative approaches, to improve the QoL for individuals with CeD and potentially achieve long-term remission of the disease.

1.3. Celiac Disease and Cardiovascular Risk

Several AIDs are already well-known to increase the risk of cardiovascular events. RA, SLE, T1D, and psoriasis are particularly notable. Patients with these conditions have a higher incidence of MI, stroke, and other cardiovascular complications compared to the general population. A 2022 published population-based study in the UK, which included 22 million individuals, investigated the association between 19 AIDs and 12 CVDs. The study found that cardiovascular risk increased progressively with the number of AIDs present; one AID (HR 1.41; 95% CI: 1.37-1.45), two AIDs (HR 2.63; 95% CI: 2.49-2.78), three or more AIDs (HR 3.79; 95% CI: 3.36-4.27). This study also includes data from nearly 25,000 CeD patients, which also showed a significantly increased cardiovascular risk (HR 1.50; 95%CI: 1.33-1.69). Although this increased risk is much lower compared to SLE (HR 2.82; 95% CI: 2.38-3.33) and T1D (HR 2.36; 95% CI: 2.21-2.52), it is comparable to the risk levels observed for RA (HR 1.83; 95% CI: 1.74-1.92) and psoriasis (HR 1.47; 95% CI: 1.41-1.53) [130-134].

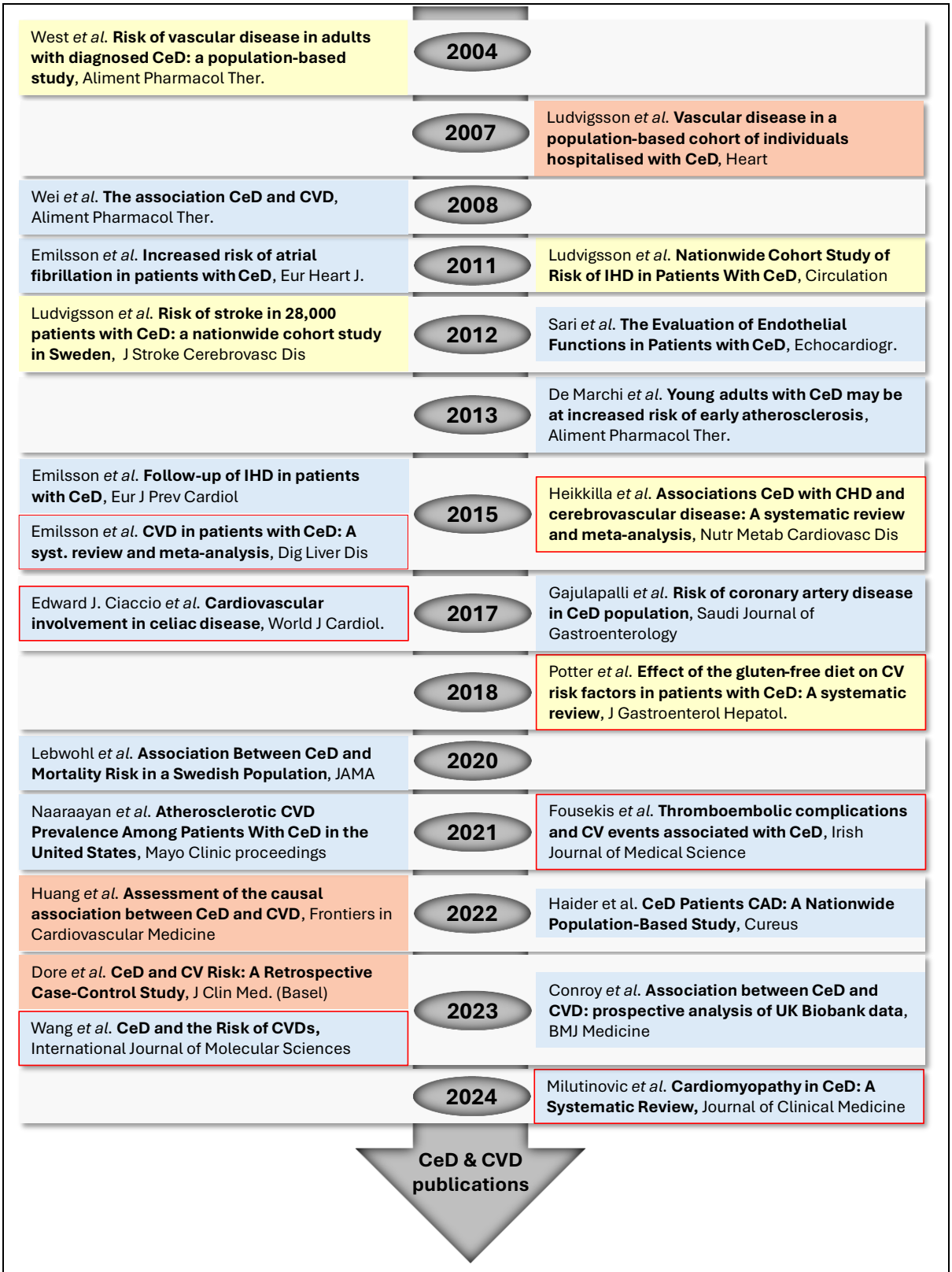

Figure 1-9: CeD and CVD Publications Timeline: Selection of 23 publications on the relationship between CeD and CVDs in adults: 7 reviews/meta-analyses (red frame) and 16 clinical studies. Blue boxes indicate publications, in general, supporting the hypothesis that untreated CeD increases cardiovascular risk. Orange boxes represent publications that do not support this hypothesis, while yellow boxes indicate mixed results/conclusions. The figure illustrates the evolving scientific interest and discussion regarding the impact of CeD on cardiovascular health [147-168].

As illustrated in **Figure 1-9**, research into the association between CeD and CVD began in the early 21st century following reports of increased mortality rates among CeD patients. Early investigations primarily focused on malignancies, with cardiovascular outcomes receiving less attention initially. This focus shifted when in 2004 West *et al.* aimed to evaluate the hypothesis that the typically lower classical cardiovascular risk profile observed in CeD patients would correspond to a reduced actual cardiovascular risk. Their study produced mixed results, failing to confirm the hypothesis conclusively. Instead, it highlighted the necessity for further research into the relationship between CeD and cardiovascular risk, thereby initiating a series of subsequent investigations in this field [147, 169-171].

Twenty years and more than twenty clinical studies later, it has become increasingly clear that there is an association between CeD and CVDs. Investigating this relationship is challenging due to several factors, including the relatively small cohort sizes available for study, the short duration of follow-up periods, and the limited number of observed cardiovascular events. Despite these challenges, most recent clinical studies suggest that individuals with CeD may be at an increased risk of developing cardiovascular complications.

The link between CeD and cardiovascular risk has been investigated in numerous clinical studies. However, the exact magnitude of this risk and the mechanisms driving it remain incompletely understood. Key questions include whether cardiovascular impairments associated with CeD are reversible, which molecular mediators are involved in the systemic inflammatory response, and how early diagnosis and dietary interventions can mitigate potential complications. Addressing these questions requires a robust experimental model to study the systemic effects of CeD and their impact on vascular health.

1.4. Aim

As outlined in the previous chapter, numerous clinical studies have investigated the relationship between CeD and cardiovascular risk. Recent findings have demonstrated not only increased mortality but also a higher incidence of cardiovascular events in CeD patients. While CeD is primarily considered an organ-specific AID, systemic inflammation has emerged as a critical contributor to atherogenesis. Although the observed increase of cardiovascular risk is less pronounced than in other AIDs, it underscores the importance of elucidating the underlying pathophysiological mechanisms. Preclinical studies play a vital role in this endeavor, emphasizing the necessity for an experimental animal model that comprehensively replicates the systemic effects of CeD to ensure translatable results.

This thesis aimed to characterize the NOD-DQ8 CeD mouse model to explore the cardiovascular implications of both "active" and "non-active" CeD conditions in male mice. The experimental design sought to mimic the clinical trajectory of male CeD patients, focusing on the symptomatic phase under a gluten-containing diet (GCD) and the subsequent remission phase following the transition to a gluten-free diet (GFD).

The study's primary objective was to assess whether the NOD-DQ8 model exhibits measurable cardiovascular impairments. Additionally, it aimed to investigate the molecular and cellular mechanisms driving these effects. Specifically, *in vivo* measurements of blood pressure were combined with *ex vivo* assessments of vascular function, including vasorelaxation and vasoconstriction. Additional parameters, such as glucose levels and cardiac function, were monitored to evaluate the potential development of T1D or spontaneous myocarditis, given the genetic predisposition of this mouse strain.

Recognizing that vascular inflammation and nitro-oxidative stress are critical factors in early atherogenesis, the study also examined their role in CeD-induced cardiovascular dysfunction through detailed mechanistic analyses. Gene expression studies and immunological assays were employed to quantify inflammatory markers and gain deeper insights into the systemic impact of CeD.

The findings from this work aim to bridge the gap between clinical observations and experimental models, providing new perspectives on the interplay between CeD and cardiovascular health.

2. Material

2.1. Antibodies

Antibodies were applied for immunohistochemical (IHC) staining (s. 3.3.2.4), flow cytometric analyses (s. 3.3.2.5) as well as Dot Blots (s. 3.3.5.1), dilutions are marked in brackets.

2.1.1. Primary Antibodies

Table 2-1: List of all used primary antibodies.

Product	Manufacturer	Product ID
Monoclonal anti-mouse CD16/CD32 (rat, 1:100≈5 ng/ml), Mouse BD Fc Block™	Pharmingen™, BD Biosciences	553141
Polyclonal anti-Nitrotyrosine (3-NT, rabbit, IHC 1:200≈5 µg/ml, DB 1:1000≈1 µg/ml)	Sigma-Aldrich/Merck	06-284
Polyclonal anti-4-Hydroxynonenal (4-HNE, goat, 1:1000≈1 µg/ml)	Chemicon®, Sigma-Aldrich/Merck	AB5605
Polyclonal anti-CD3 epsilon (rabbit, 1:1600≈0.13 ng/ml)	abcam	ab5690
Monoclonal anti-CD4 (rabbit, 1:400≈1.74 ng/ml)	abcam	ab183685
Monoclonal anti-CD68 (E3O7V, rabbit, 1:4000≈25 ng/ml,	Cell Signaling Technology	97778
Monoclonal anti-Ki67 (rabbit, 1:200≈0.15 ng/ml)	abcam	ab16667

2.1.2. Fluorescent/dye-labelled Antibodies

Table 2-2: List of all used fluorescent/dye-labelled antibodies.

Product	Manufacturer	Product ID
Monoclonal anti-CD11b (rat, 1:100), PE conjugated	Pharmingen™, BD Biosciences	553311
Monoclonal anti-CD45 (30-F11, rat, 1:100), APC-eFluor™ 780 conjugated	eBioscience, Invitrogen	47-0451-82
Monoclonal anti-NK1.1 (PK136, mouse, 1:100), PE-Cy(anine)7 conjugated	eBioscience, Invitrogen	25-5941-82
Monoclonal anti-TCR β Chain (hamster, 1:100), V450 conjugated	BD Biosciences	560706

2.1.3. Secondary Antibodies

Table 2-3: List of all used secondary antibodies.

Product	Manufacturer	Product ID
Goat anti-rabbit IgG (H+L), biotinylated (1:1000)	Invitrogen	B-2770
Goat anti-rabbit IgG (H+L), peroxidase-labelled (1:10,000)	Vector Laboratories	PI-1000-1
Goat anti-rat IgG, peroxidase-labelled (1:10000)	Santa Cruz	sc-2006
Horse anti-goat IgG (H+L), peroxidase-labelled (1:1000)	Vector Laboratories	PI-9500-1
Goat anti-rabbit IgG (H+L), biotinylated (1:500)	Vector Laboratories	BA-1000-1.5

2.2. Chemicals

Table 2-4: List of all chemicals.

Product	Manufacturer	Product ID
2-Mercaptoethanol (β-ME)	Sigma-Aldrich/Merck	M6250
Acetic acid (glacial) 100%	AppliChem	A2354
Acetylcholine chloride	Sigma-Aldrich/Merck	A6625
Agarose	Invitrogen	16500-100
Albumin Fraction V (BSA)	Roth	8076.3
Ammonium bicarbonate	Sigma-Aldrich/Merck	11213
Ammonium chloride (NH_4Cl)	Sigma-Aldrich/Merck	A9434
Antibody Diluent, Ready-to-use diluent, 125 mL	Agilent	S080983-2
Aprotinin	Sigma-Aldrich/Merck	A6279
Aqua-Phenol	Roth	A980.4
Braunol	B.Braun	3864065
Calcium chloride dihydrate ($CaCl_2 \cdot 2\ H_2O$)	Roth	T885.1
Chloroform - isoamyl alcohol mixture, 49:1	Sigma-Aldrich/Merck	25668
Cholera toxin (CTX)	Sigma-Aldrich/Merck	C8052
D(+)-Glucose monohydrate	Roth	6780.1
DEPC (diethylpyrocarbonate)-treated water, nuclease-free and autoclaved	Roth	T143.3
Dihydroethidium 95% (DHE)	Sigma-Aldrich/Merck	37291
Dithiothreitol (DTT)	Sigma-Aldrich/Merck	D0632
Di-Potassium hydrogen phosphate (K_2HPO_4)	Roth	P749.1
EDTA-free Protease Inhibitor Cocktail, cOmplete™	Roche	11873580001
Ethanol, absolute	Sigma-Aldrich/Merck	32205

Table 2-5: List of all chemicals (continued).

Product	Manufacturer	Product ID
Ethylenediaminetetraacetic acid (EDTA)	Sigma-Aldrich/Merck	E9884
Ethylene glycol-bis(2-aminoethylether)-N,N,N′,N′-tetraacetic acid (EGTA)	Sigma-Aldrich/Merck	E4378
Ethylenediaminetetraacetic acid tripotassium salt dihydrate (K_3EDTA • 2 H_2O)	Sigma-Aldrich/Merck	03664
Fetal calf serum (FCS)	Thermo Scientific	10270106
Gliadin	Sigma-Aldrich/Merck	G3375
Guanidine thiocyanate	AppliChem	A1107
HBSS (1x), Hanks' Balanced Salt Solution with calcium and magnesium	Sigma-Aldrich/Merck	55037C
Hematoxylin	Dako	S3309
Heparin-Natrium-25000	Ratiopharm	
HEPES sodium salt hydrate	Sigma-Aldrich/Merck	H2393
Indomethacin	Sigma-Aldrich/Merck	I7378
Isoflurane	Abbott	B506
Isopropanol	AppliChem	A3465
Ketamine hydrochloride/xylazine hydrochloride solution	Sigma-Aldrich/Merck	K113
L-012 (8-amino-5-chloro-7-phenylpyridol[3,4-d]pyridazine-1,4-(2H,3H)dione sodium salt	WAKO Chemicals	120-04891
Leupeptin hydrochloride	Sigma-Aldrich/Merck	L0649
L-Glutamine	Sigma-Aldrich/Merck	G3126
Magnesium sulphate heptahydrate ($MgSO_4$ • 7 H_2O)	Roth	8283.2
Methanol, 99.8 %	Sigma-Aldrich/Merck	322415
Midori Green Advance	NIPPON Genetics	MG04
Milk powder	Roth	T145.2
Nitroglycerin/glyceryl trinitrate (GTN), 1 mg/ml	Carinopharm	14269987
N-lauryl sarcosine sodium salt	Merck	814715
Normal Goat Serum Blocking Solution	Vector Laboratories	S-1000-20
Normal Horse Serum Blocking Solution, 2.5%	Vector Laboratories	S-2012-50
OCT (Optimal Cutting Temperature)-resin Tissue-Tek®	Sakura	4583
Paraffin wax, pellets, white	Sigma-Aldrich/Merck	76242
PBS (1x), Dulbecco's Phosphate Buffered Saline without calcium and magnesium	Sigma-Aldrich/Merck	D8537
Pepstatin A	Sigma-Aldrich/Merck	P5318
Phenylmethanesulfonyl fluoride (PMSF)	Sigma-Aldrich/Merck	P7626
Phosphatase Inhibitor Cocktail	Sigma-Aldrich/Merck	P2850
Ponceau S solution	Sigma-Aldrich/Merck	P7170

Table 2-6: List of all chemicals (continued).

Product	Manufacturer	Product ID
Potassium bicarbonate ($KHCO_3$)	Sigma-Aldrich/Merck	60339
Potassium chloride (KCl)	AppliChem	131494
Prostaglandin F2α	Cayman Chemicals	16010
Protease Inhibitor Cocktail	Sigma-Aldrich/Merck	P8340
RNase AWAY™	Thermo Scientific	7002
Roti Histofix 4 %	Roth	P087.1
Roti®-Quant	Roth	K015.1
Silicone grease Rotisilon C/D	Roth	8537.1
Sirius Red	Sigma-Aldrich/Merck	43665
Sodium azide (NaN_3)	Sigma-Aldrich/Merck	S2002
Sodium chloride (NaCl)	Roth	9265.1
Sodium citrate dihydrate	Sigma-Aldrich/Merck	W302600
Sodium DETC (diethyldithiocarbamate) trihydrate	Sigma-Aldrich/Merck	D3506
Sodium dodecyl sulfate (SDS)	Sigma-Aldrich/Merck	822050
Sodium hydrogen carbonate ($NaHCO_3$)	CELLPURE®, Roth	HN01.2
Sodium hydroxide, pellets (anhydrous) (NaOH)	Sigma-Aldrich/Merck	S8045
Sucrose	Sigma-Aldrich/Merck	S9378
Tosyl-lysine-chloromethyl-ketone (TLCK)	Sigma-Aldrich/Merck	T7254
Tris(hydroxymethyl)-aminomethane (Tris-base)	Sigma-Aldrich/Merck	252859
Tris-hydrochlorid (Tris-HCl)	Roth	9090.2
TritonX-100	Sigma-Aldrich/Merck	93420
Tween 20	Sigma-Aldrich/Merck	P2287
Wash buffer (IHC), 10x	Dako	S3006
Zein	Sigma-Aldrich/Merck	Z3625
Zymosan A from *S. cerevisiae*	Sigma-Aldrich/Merck	Z4250

2.3. Consumables/Disposables

Table 2-7: List of all consumables.

Product	Manufacturer	Product ID
Amersham™ Protran® Western blotting membranes, nitrocellulose, pore size 0.45 µm	Cytiva™	GE10600002
BD® Micro-Fine+ 0.3 ml Insulin Syringe U-100	Becton Dickinson	BEC 324826
Biotech CE Dialysis Tubing (500-1000 D, 16 mm)	Repligen	131090
Blood glucose test strips	Roche	6114963
C-Chip Disposable Hemocytometer, Neubauer Improved	NanoEnTek	DHC-N01
Cell Strainer 100 µm	Falcon®, Corning	352360
Cell Strainer 40 µm	Falcon®, Corning	352340
Cell Strainer 70 µm	Falcon®, Corning	352350
Centrifuge tube, 15 mL	Greiner	188271
Centrifuge tube, 50 mL	Greiner	227261

Table 2-8: List of all consumables (continued).

Product	Manufacturer	Product ID
Cover slips, microscope cover glass, "Diagonal", rectangular, 24 x 50 mm	Knittel Glas	LD2450
Cover slips, microscope cover glass, rectangular, 24 x 60 mm, thickness 0.13 - 0.16 mm	VWR®	631-1575
Eppendorf® Safe-Lock microcentrifuge tubes volume 0.5 mL	Eppendorf	0030121023
Eppendorf® Safe-Lock microcentrifuge tubes volume 1.5 mL	Eppendorf	0030120086
Eppendorf® Safe-Lock microcentrifuge tubes volume 2.0 mL	Eppendorf	0030120094
Eppendorf® Safe-Lock microcentrifuge tubes volume 5.0 mL	Eppendorf	0030119460
ep Dualfilter T.I.P.S.®, sterile, for volumes up to 2, 10, 20, 100, 200 and 1000 µl	Eppendorf	several
epT.I.P.S.® Standard, for volumes up to 2, 10, 20, 100, 200 and 1000 µl	Eppendorf	several
FACS tubes	Falcon®, Corning	352052
Glass petri dish	Duran	237554805
Microlance™ 3 24G cannula	Becton Dickinson	304100
Microlance™ 3 26G cannula, brown	Becton Dickinson	303800
Microlance™ 3 30G cannula, yellow	Becton Dickinson	304000
Microplate, 24 well, F-bottom, transparent	Greiner	662160
Microplate, 96 well, F-bottom, transparent	Greiner	655101
Microplate, 96 well, U-bottom, transparent	Greiner	650101
Microscope slides, *Menzel-Gläser*, SuperFrost® plus, 25 x 75 x 1.0 mm	Thermo Scientific, Menzel GmbH & Co KG	J1800AMNZ
Microscope slides, white Tab, SuperFrost® Adhesion, 25 x 75 x 1.0 mm	Epredia™	J1800AMNZ
NO-PAK column, 4.6 x 50 mm, reverse-phase/polystyrene	Eicom	
NO-RED column, copper-plated cadmium filings	Eicom	
PCR tubes, 0.2 mL	Kisker Biotech	G003-A
Petri dish, sterile	Greiner	632181
TipOne® Filter Tip, sterile, for volumes up to 2, 10, 20, 100, 200 and 1000 µl	Starlab	several

2.4. Enzymes and Standards

Table 2-9: List of used enzymes and standards.

Product	Manufacturer	Product ID
BD™ Cytometric Bead Array (CBA) Mouse IL-17A Standard	BD Biosciences	561669
Bovine Serum Albumin (BSA) Standard, 2 mg/ml	Pierce™, Thermo Scientific™	23209
Collagenase Type A	Worthington	LS004154
Liberase™ (Thermolysin Medium)	Roche	5401127001
Pepsin from porcine gastric mucosa	Sigma-Aldrich/Merck	P7000
Trypsin from bovine pancreas	Sigma-Aldrich/Merck	T9201
Transglutaminase from guinea pig liver (TG2)	Sigma-Aldrich/Merck	T5398

2.5. Experimental Diets

Table 2-10: List of used experimental diets from ssniff *Spezialdiäten*.

Product	Product ID
EF M, Gluten free	S8251-E030
EF M, 25 % CP from wheat Gluten (6.9 %)	S8251-E032

2.6. Media and Buffer

Table 2-11: List of used media and buffer.

Buffer/Media	Composition
ACK (Ammonium-Chloride-Potassium) lysis buffer	150 mM NH_4Cl, 10 mM $KHCO_3$, 0.1 mM EDTA, pH 7.2
FACS buffer	PBS, 2% (v/v) FBS, 1 mM EDTA
GIT (guanidinium thiocyanate) buffer	4 M guanidinium thiocyanate, 25 mM sodium citrate (pH 7.0), 0.5 % (w/v) N-laurosylsarcosine, 0.1 M 2-mercaptoethanol
Homogenization buffer	20 mM Tris-HCl, 250 mM sucrose, 3 mM EGTA, 20 mM EDTA, 0.5 mM PMSF, 1 % (v/v) protease inhibitor cocktail, 1 % (v/v) phosphatase inhibitor cocktail, 1 % (v/v) TritonX-100
KH (Krebs-Hepes) buffer	99 mM NaCl, 4.7 mM KCl, 2.5 mM $CaCl_2$, 1.2 mM $MgSO_4$, 25 mM $NaHCO_3$, 1 mM K_2HPO_4, 20 mM Na-HEPES, 11.1 mM D-glucose, pH 7.35
Organ bath buffer	99 mM NaCl, 4.7 mM KCl, 2.5 mM $CaCl_2$, 1.2 mM $MgSO_4$, 25 mM $NaHCO_3$, 1 mM K_2HPO_4, 0.01 mM Indomethacin, 11.1 mM D-glucose, 1 pellet NaOH, pH 7.35
PBS, 10x	1.37 M NaCl, 100 mM Na_2HPO_4, 27 mM KCl, 17.6 mM KH_2PO_4, pH 7.4
PBS/T, 1x	1x PBS, 0.1 % (v/v) Tween®-20
Protease Inhibitor Buffer (based on KH buffer)	fresh KH buffer, 1 % (v/v) aprotinin, 5 µg/ml leupeptin, 8 µg/ml pepstatin A
TAE (Tris-Acetate-EDTA) buffer, 50x	2 M Tris-base, 1 M acetic acid (glacial), 50 mM EDTA, pH 8.5
TBS, 10x	200 mM Tris-base, 1.5 M NaCl, pH 7.6
TBS/T, 1x	1x TBS, 0.1 % (v/v) Tween®-20
Tris DTT buffer	Tris Mem, 2 mM DTT
Tris Mem buffer	50 mM Tris-HCl, 2 tablets EDTA-free Protease Inhibitor Cocktail/per 100 ml, pH 7.4

2.7. qRT PCR Primer

Table 2-12: List of used TaqMan Gene Expression assays probe-and-primer sets from Applied Biosystems.

Gene Symbol	Gene Name	Assay ID
Cybb	Cytochrome b-245, beta polypeptide (Nox2)	Mm00432775_m1
Ifnγ	Interferon gamma	Mm01168134_m1
Il17a	Interleukin-17A	Mm00439619_m1
Il6	Interleukin-6	Mm00446190_m1
Itgam	Integrin α-M (CD11 antigen-like family member B)	Mm00434471_g1
Lep	Leptin	Mm00434759_m1
Nos1	Neuronal nitric oxide synthase (nNOS)	Mm01208059_m1
Nos2	Inducible nitric oxide synthase 2 (iNOS)	Mm00440485_m1
Tbp	TATA box binding protein	Mm00446973_m1
Tnfa	Tumor necrosis factor alpha	Mm00443259_g1
Vcam1	Vascular cell adhesion molecule 1	Mm00449197_m1

2.8. Reagents and Kits

Table 2-13: List of all used kits.

Product	Manufacturer	Product ID
ABC-HPR kit VECTASTAIN® Elite®	Vector Laboratories	PK-6100
BD OptEIA™ TMB Substrate Reagent Set	BD Biosciences	555214
BD™ Cytometric Bead Array (CBA) Mouse IL-17A Flex Set	BD Biosciences	560283
DAB substrate	Vector Laboratories	SK-4105
dNTP Mix	Thermo Scientific	R0242
Fixable Viability Dye (1:1000), eFluor™ 506	eBioscience™, BD Biosciences	65-0866
Gel Loading Buffer	Sigma-Aldrich/Merck	G2526
Olink® Target 96 Mouse Exploratory Panel (v.3801)	Olink®	95380
Pierce™ ECL Western Blotting Substrate	Thermo Scientific	32106
QuantiTect® Probe RT-PCR Kit	Qiagen	204445
SuperSignal™ West Femto Maximum Sensitivity Substrate	Thermo Scientific	34095

2.9. Software

Table 2-14: List of all used software.

Product	Company/Developer
Axiovision Rel 4.3	Zeiss
cellSens Imaging Software	Olympus
Clarity Lite Chromatographie Station	DataApex TECHLAB
Claude 3	Anthropic
CODA data acquisition	Kent Scientific Corporation
EndNote X9.3.3	Clarivate
Elicit	Elicit Research
FlowJo™ v10.8	Becton Dickinson
Gel-Pro Analyzer 6.0	Media Cybernetics
Grammarly v1.2.166.1677	Grammarly Inc.
GraphPad Prism 10	GraphPad Software, Inc.
Image J	National Institutes of Health
Insights Stat Analysis application	Olink®
LabChart Pro v8.1.24	ADInstruments
Microsoft 365 MSO Version 2502 Build 16.0.	Microsoft
NO Analyzer Noa-Wibn32.V1.4g	Sievers Instruments
Organbad Chart 5	ADInstruments GmbH
Revelation	Dynex Technologies
StepOne Software v2.3	Applied Biosystems
Vevo LAB Software	FUJIFILM VisualSonics

2.10. Surgical instruments

Table 2-15: List of all used surgical instruments.

Product	Manufacturer	Product ID
Dumont #5SF Forceps, straight, 11 cm	Fine Science Tools	11252-00
Dumont #7 - Fine Forceps	Fine Science Tools	11274-20
Extra Fine Bonn Scissors, straight, 8.5 cm	Fine Science Tools	14084-08
Extra Fine Graefe Forceps, curved, 10 cm	Fine Science Tools	11152-10
Graefe Forceps, straight, 10 cm	Fine Science Tools	11050-10
Noyes Spring Scissors, curved, 12 cm	Fine Science Tools	15011-12
Scissors curved, blunt-blunt, 12 cm	Fine Science Tools	14003-12
Strabismus Scissors Tungsten Carbide, curved, 9 cm	Fine Science Tools	14575-09
Vannas Spring Scissors - 2mm Cutting Edge, straight, 8 cm	Fine Science Tools	15000-03
Vannas Spring Scissors - 3mm Cutting Edge, straight, 8 cm	Fine Science Tools	15000-00

2.11. Technical Devices

Table 2-16: List of all used technical devices.

Product	Manufacturer
Alinity c system	Abbott
Analytical Balance LE225D	Sartorius
Benchtop centrifuge ROTOFIX 32	Hettich
BioPhotometer	Eppendorf
Bridge Amplifier, PowerLab 16/35	ADInstruments
Chemiluminescence plate reader Mithras^2 LB 943	Berthold Technologies
ChemiLux Imager (CsX-1400 M)	Intas
CODA® Animal holder, medium-sized, mice 25-50 g, black nose cones	Kent Scientific
CODA® High Throughput System (2-4 Channels) for Noninvasive Blood Pressure System (NIBP)	Kent Scientific
Cold light lamp KL1500 LCD	Schott
Cold light lamp KL1600 LED	Schott
Cryostat CM3050 S	Leica Biosystems
Eppendorf Research® plus, 1-channel, volumes up to 2, 10, 20, 100, 200 and 1000 µl	Eppendorf
Eppendorf Research® plus, 8-channel, volumes up to 100 and 200 µl	Eppendorf
ETH-255 Bridge/Bio Amplifier	CB Sciences
FACSCanto II Flow Cytometer with FACSDiva Software	BD Biosciences
Fluorescence microscope Axiovert 40CFL with Axiocam MRm	Zeiss
Force transducer	Kent Scientific / Pan Lab
Glucometer Accu-Chek® Aviva	Roche
Heating and magnetic stirrer MR Hei-Standard	Heidolph Instruments
Hematology analyzer KX-21N	Sysmex
Heraeus Megafuge 16R	Thermo Fisher
HPLC, ENO-20 NOx Analyzer	Eicom
Magnetic stirrer MR Hei-mix L	Heidolph Instruments
Metabolic cage for single mice	Tecniplast, Italy
Microscope IX71 with ColorView II camera	Olympus
Minifold® I vacuum dot-blot system, 96 dots	Whatman® Schleicher & Schuell
MiniSpin® Centrifuge	Eppendorf
MRX II microplate reader	Dynex Technologies
Octal Bridge Amp(lifier)	ADInstruments
Organ bath chambers	Radnoti
Paraffin dispenser EG 1120	Leica Biosystems
pH 211 Microprocessor pH Meter	Hanna Instruments
PowerPac™ Basic power supply	Bio-Rad
Precision Balance KB	KERN
Refrigerated benchtop centrifuge Mikro 22R	Hettich
Rotary microtome RM2145	Leica Biosystems

Table 2-17: List of all used technical devices (continued).

Product	Manufacturer
SimpliAmp™ Thermal Cycler	Thermo Fisher
StepOnePlus™ Real-Time PCR Systems	Applied Biosystems
Stereomicroscope MSZ 5000	Krüss
Stereomicroscope MSZ 5400	Krüss
Thermomixer comfort	Eppendorf
Tilt/roller mixer RS-TR05	Phoenix Instrument
Tissue Processor TP 1020	Leica Biosystems
TissueLyser LT	Qiagen
UV transilluminators iX	Intas
Vevo 3100 high-resolution imaging system	FUJIFILM VisualSonics
Vortex-Genie™ 2	Scientific Industries

3. Methods

The materials used in the methods described below are detailed in the previous section along with the manufacturer and product ID, including the applied dilution and concentration if applicable (s. Chapter 2).

3.1. Celiac Disease Murine Model

3.1.1. NOD-DQ8 Mice

All procedures involving animals were conducted in accordance with the German Animal Welfare Act [172]. The study received approval from the Federal Institutional Animal Care and Use Committee (*Landesuntersuchungsamt,* LUA) of Rhineland-Palatinate, Koblenz, Germany, under the permit number: 23 177-07/G 20-1-061. All animals were housed in a conventional colony within the institutional animal facility (TARC) and were maintained in filter-top cabinets or individually ventilated cages (IVC), each accommodating one to five mice. They had constant access to environmental enrichment, nesting material, a gluten-free diet (GFD), and water, under a 12-hour light/dark cycle.

The studies were performed with male transgenic NOD-DQ8 mice at the age of 8-12 weeks, which were bred in-house. This albino inbred strain, liberally provided by Prof. E. Verdu from McMaster University, Canada, expresses the human leukocyte antigen HLA-DQ8 (HLA-DQA1*0301; DQB1*0302) and lacks endogenous mouse class II genes ($A\beta^{0/0}$) [173, 174].

3.1.2. Pepsin and Trypsin Digest of Gliadin and Zein

Gliadins, a major fraction of gluten proteins, are known for containing immunogenic epitopes that trigger CeD in individuals with a genetic predisposition (for details s. section 1.2.3) [175]. These gliadin peptides, generated through digestion by gastrointestinal proteases like pepsin and trypsin (PT), become more potent in eliciting a gluten-specific T cell response following mostly deamidation and crosslinking by tissue transglutaminase (TG2, s. section 3.1.3), the primary CeD autoantigen in the intestinal lamina propria [124, 126].

The preparation of PT-digested and TG2-reacted gliadin (PT-TG2-gliadin, s. section 3.1.3), follows the gastrointestinal enzymatic process, slightly modified from previously established methods [173, 176, 177]. To begin, 4 g of gliadin or zein - the latter being the prolamin protein of maize [178] - are dissolved in 40 ml of 0.1 M hydrochloric acid (HCl). Following the dissolution, the mixture undergoes a first round of enzymatic digestion with 40 mg of pepsin. Pepsin, a gastric protease, acts on gliadin or zein in the acidic solution over 2 hours at 37°C and mixing at 300 rpm. After pepsin digestion, the pH was adjusted to 7.8, and 40 mg of trypsin was added. The solution was then incubated for another 2 hours at 37°C under mixing, replicating the duodenal protein digestion phase. To cease trypsin activity, the pH of the mixture was adjusted to 4.5, followed by the addition of 40 mg of tosyl-lysine-chloromethyl-ketone (TLCK). The solution then underwent a dialysis process against 0.01 M ammonium bicarbonate using Biotech CE Dialysis Tubing. This step is crucial for removing small molecules and enzymes, further purifying the protein fragments. Post-dialysis, the solution was freeze-dried and lyophilized, a process that removes water and stabilizes the peptides, making them suitable for long-term storage at −80°C.

The protein digestion was performed in co-operation with Manuel Alejandro Encalada Ventura, phD (TIM, University Medical Center Mainz), where the protocol was developed.

3.1.3. Deamidation and Crosslinking by Tissue Transglutaminase (TG2)

As previously mentioned in section 3.1.2, enhancing the gluten-specific T cell response involves further treating the digested gliadin. This process mimics *in vivo* gliadin peptide modification by TG2 in the intestinal mucosa, resulting in glutamine-deamidated gliadin. However, the crosslinking reaction that occurs during this treatment, though inevitable, is not desirable for this purpose [124, 126, 179].

Reaction conditions were adopted as previously published, the protocol was particularly adapted from Manuel Alejandro Encalada Ventura, phD (TIM, University Medical Center Mainz) and further optimized for optimal deamidation conditions [124, 180].

In brief, 40 mg of the lyophilized PT-gliadin or PT-zein underwent incubation with 5 units of Ca^{2+}-dependent TG2 from guinea pig liver. A unit of TG2 is defined as the amount that will catalyse the formation of 1 µmole of hydroxamate per minute from γ-glutamyl donor substrate (Nα-Z-Gln-Gly) and hydroxylamine at pH 6 at 37°C [181, 182]. This incubation was conducted at 37°C in 14 ml of 200 mM HEPES buffer containing 8 mM calcium chloride ($CaCl_2$) at a pH of 6.8 overnight. After incubation, the solution was divided into aliquots and stored at -80°C or -20°C for future use. Each 175 µl aliquot contained 0.5 mg of either PT-TG2-gliadin or PT-TG2-zein lyophilizate.

3.1.4. ON- and OFF-Study Treatment

The CeD model used in this study resembles other protocols and methods that have already been published [173, 183]. The treatment described here is largely derived from the protocol developed by Prof. D. Schuppan in collaboration with Aline Pesi, Susann Kahl, and Manuel Alejandro Encalada Ventura, phD (TIM, University Medical Center Mainz). Implementation included small adjustments to align with the objectives and parameters of the cardiovascular outcome.

For ON-study treatments (**s. Figure 3-1**), NOD-DQ8 mice were randomly divided into two groups: a gluten-free control group receiving zein from maize, and a gluten group exposed to gluten and gliadin from wheat. Each group underwent a series of three oral gavages administered at one-week intervals (on day 0, 7 and 14), each containing 0.5 mg of PT-TG2-gliadin or PT-TG2-zein lyophilizate (s. previous sections) combined with 25 µg of cholera toxin (CTX) in 0.2 ml DPBS. The addition of CTX is crucial as it facilitates intestinal permeabilization, thereby facilitating better entry into the lamina propria. Simultaneously with the initial gavage, the mice in the gluten group were switched to a gluten-containing diet (GCD), while the control group, sensitized with zein, continued a gluten-free diet (GFD).

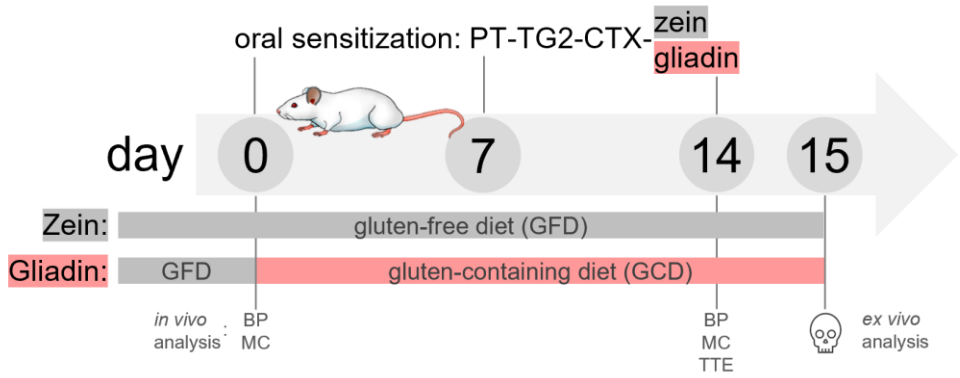

Figure 3-1: ON-study treatment scheme. Mice were divided into two groups: one receiving GFD with zein and the other GCD with gliadin oral sensitization over two weeks. Abbreviations: BP – blood pressure, CTX – cholera toxin, MC – metabolic cage, PT – pepsin-trypsin, TG2 – tissue transglutaminase 2, TTE – transthoracic echocardiography. Adapted from Keppeler *et al*., 2024 [184].

For the OFF-study treatments (s. **Figure 3-2**), the protocol initiated with the ON-study treatment. Following this, both groups underwent an additional 14-day period on GFD without any oral gavage. This phase was designed to assess whether the cardiovascular implications observed would be reversible following a recovery period on GFD.

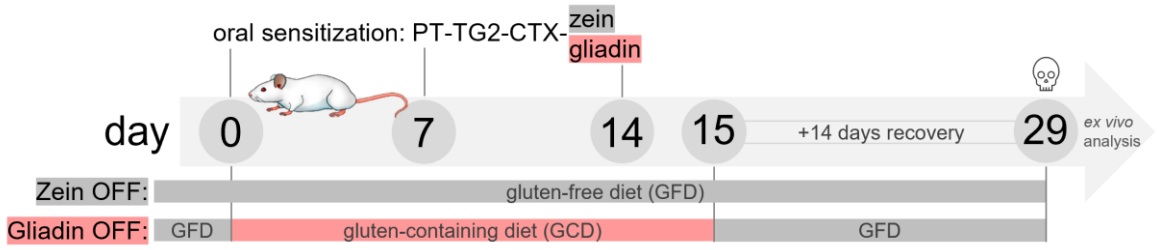

Figure 3-2: OFF-study treatment scheme. Following the ON-study treatment, both groups underwent an additional 14-day period on GFD without oral gavage to assess the recovery. Abbreviations: CTX – cholera toxin, PT – pepsin-trypsin, TG2 – tissue transglutaminase 2. Adapted from Keppeler *et al*., 2024 [184].

Both diets, the GFD and the GCD, were designed to be as comparable to each other as possible (besides the gluten fraction, s. **Table 3-1** and **Figure 3-3**) and were adapted from Prof. D. Schuppan's group (TIM, University Medical Center Mainz).

Table 3-1: Diet compositions of GFD and GCD (NfE; Nitrogen free Extract; soluble carbohydrate). Adapted from Keppeler *et al.*, 2024 [184].

Proximate Contents [%]	**GFD**	**GCD**
Crude protein	22.0	22.0
└CP Gluten (wheat)	-	5.5
Crude fat	4.8	4.9
Crude fiber	4.7	4.4
Crude ash	5.7	5.3
NfE	57.3	56.8
Metabolizable energy (Atwater) - MJ/kg	15.1	15.3
Protein [KJ%]	24	24
Fat [KJ%]	12	12
Carbohydrate [KJ%]	64	64

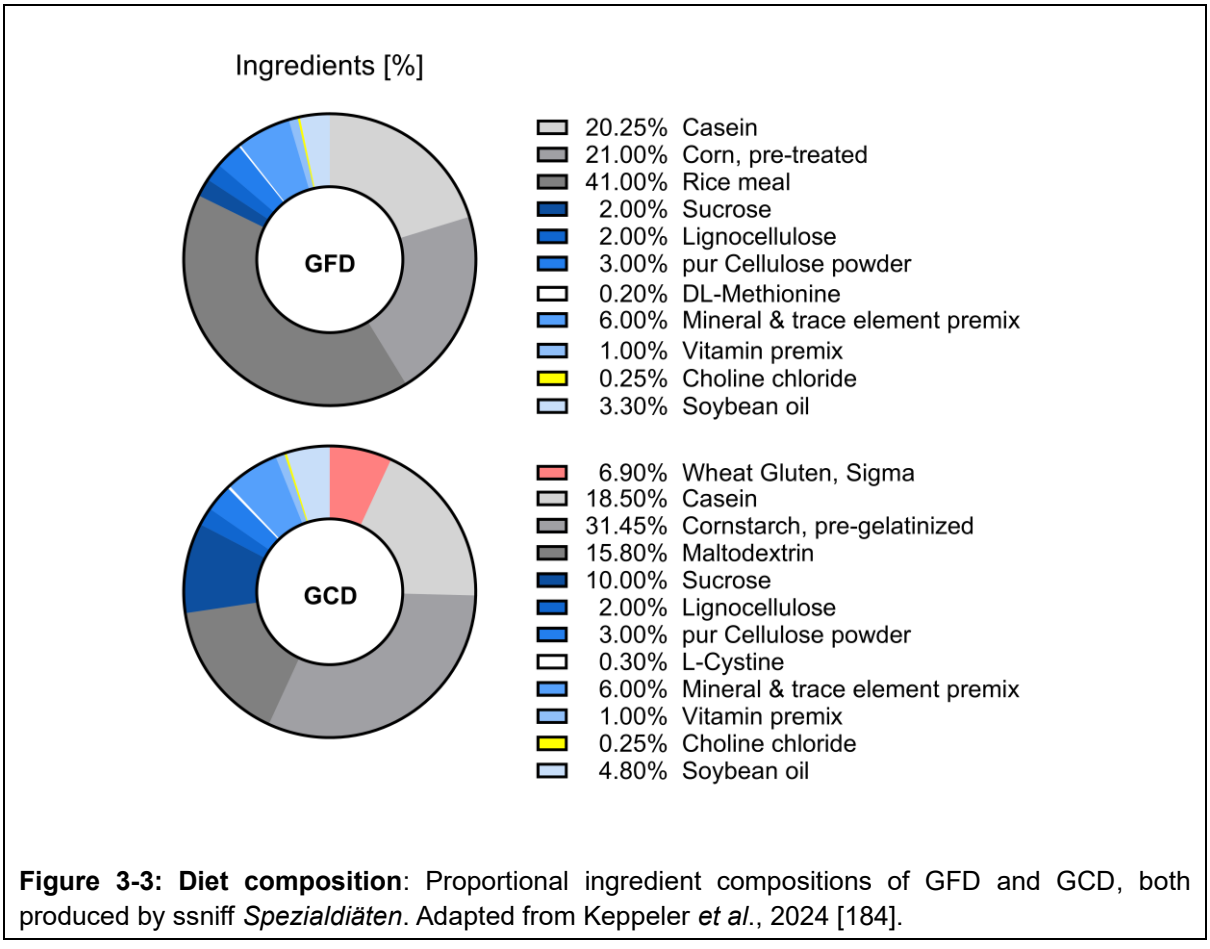

Figure 3-3: Diet composition: Proportional ingredient compositions of GFD and GCD, both produced by ssniff *Spezialdiäten*. Adapted from Keppeler *et al.*, 2024 [184].

Animal treatments were conducted with the technical assistance of Alexandra Rosenberger (Laboratory of Molecular Cardiology, University Medical Center Mainz).

3.2. *In vivo* Studies

3.2.1. Non-Invasive Blood Pressure (NIBP) Recordings

Non-invasive blood pressure (NIBP) measurements in mice were conducted using tail-cuff plethysmography, a method validated against radiotelemetry monitoring [185]. This technique relies on Volume-Pressure Recordings (VPR) to determine the tail blood volume changes indicative of blood pressure (CODA High Throughput System, Kent Scientific, CT, USA).

For the NIBP recordings, mice were restrained within a medium-sized mouse holder (Clear holders with black nose cones) on a warming pad to maintain body temperature. The tail was threaded through an occlusion tail cuff and a specific VPR sensor cuff. The occlusion cuff is alternately inflated and deflated to regulate blood flow in the tail, while the VPR cuff sensor measures tail blood volume changes corresponding to systolic and diastolic blood pressure (BP) [186].

Before the actual measurements, two to three training runs were conducted to acclimatize the mice to the procedure and minimize stress reactions. The baseline BP was determined before the first gavage (day -1) to ensure uniform levels. Experimental BP was then recorded on day 14 and day 28 in the case of an OFF-study. Each mouse underwent 15 to 20 NIBP cycles. The first five readings were discarded as acclimation cycles, and the average of at least five readings was used for BP calculations.

NIBP measurements were conducted with the technical assistance of Alexandra Rosenberger (Laboratory of Molecular Cardiology, University Medical Center Mainz).

3.2.2. Metabolic Cages (MC)

In the experimental setup, one mouse from each experimental group was randomly selected and placed in an individual metabolic cage, provided by Tecniplast, for a continuous period of 24 hours. This specific procedure was carried out twice: firstly, in the last 24 hours leading up to the commencement of treatment or oral gavage (spanning from day -1 to day 0) and, secondly, during the concluding 24 hours of the treatment phase (spanning from day 13 to day 14). The primary aim of this arrangement was to document any fluctuations in the consumption of food and water

that could be attributed to the various dietary regimens administered. Throughout these designated intervals, meticulous records were kept of urine and faeces excretion, alongside the quantities of food and water consumed, adapted from [187], with modifications.

To mitigate any variations in data that could arise from the natural circadian rhythms of the subjects, the initiation of measurements for each mouse was carefully scheduled to begin around the same time—precisely at noon. It is noteworthy to mention that, although the mice were granted unlimited access to food and water, the arrangement of the food source was such that it posed an additional challenge for the mice to access their sustenance, thereby introducing an element of difficulty in food procurement. This aspect of the experimental design is particularly significant, as the induced stress from this constrained accessibility is often linked to a noticeable reduction in body weight among the subjects. Consequently, there was a conscientious effort to monitor the body weight of the mice both before their entry into the metabolic cages and after their exit, to accurately assess the impact of this stress factor on their physical well-being.

These experiments were conducted with the technical assistance of Alexandra Rosenberger from the Laboratory of Molecular Cardiology at the University Medical Center Mainz.).

3.2.3. Transthoracic Echocardiography (TTE)

On day 14 of treatment, following the final oral gavage, mice were anaesthetized with 1.0–1.5 vol% isoflurane and positioned on a handling platform for cardiac function assessment. Before the procedure, chest fur was fully removed using commercial hair removal cream to ensure clear imaging. During the procedure, vital parameters such as electrocardiogram, breathing rate, and body temperature, which was maintained at 37°C with a heating system and infrared warming lamp, were closely monitored.

Transthoracic echocardiography images were acquired at a frame rate above 200 frames per second using the Vevo 3100 high-resolution imaging system (FUJIFILM VisualSonics, Canada) in combination with a 38 MHz linear array transducer (model MX 400). B-mode (brightness) and M-mode (motion) loops of the parasternal long axis (PLAX) were captured. Post-acquisition, left ventricular (LV) cardiac function,

including ejection fraction (EF) and cardiac output (CO), were quantified based on M-mode PLAX loops using Vevo LAB Software. Additionally, strain analysis was performed to evaluate intrinsic myocardial contractility, with global longitudinal strain quantified from standardized B-mode PLAX video loops for all left ventricular segments [188].

The echocardiography preparations and measurements were executed in collaboration with Dr. Stefanie Finger (CTH, University Medical Center Mainz), and with technical assistance from Alexandra Rosenberger (Laboratory of Molecular Cardiology, University Medical Center Mainz).

3.3. *Ex vivo* Studies

3.3.1. Tissue Sampling and Anaesthesia of Mice

Animals in the ON-study were sacrificed on day 15, a day after the third oral sensitization, and those in the OFF-study on day 29. This was conducted under deep anaesthesia induced by intraperitoneal injection of 120 mg/kg body weight ketamine and 16 mg/kg body weight xylazine, confirmed by the loss of the inter-toe reflex. After initially opening the abdominal region to collect urine from the bladder, the chest was subsequently opened. The blood extraction aimed to collect as much blood as possible, typically ranging from 400-800 µl for (EDTA-/citrate-) plasma and serum used for further analysis (s. section 3.3.3). Following a heparin injection, the heart, spleen, gastrointestinal tract (stomach to rectum), kidneys, adrenal gland, liver (any lobe), epididymal white adipose tissue (EWAT), aorta (from root to abdominal), and brain (frontal lobe) and were removed. Duodenum samples were dissected 3 mm directly after the stomach, in total 2.5 cm. As part of the heart-to-body weight ratio analysis (refer to section 3.3.2.1) hearts were first weighed following transection, after which only the left ventricle was collected for further processing. Collected organs or parts of it were processed in one of three ways: they were either snap-frozen in liquid nitrogen (s. section 3.3.4.1 and 3.3.5.1), fixed in ROTI Histofix formalin (s. section 3.3.2.4), or directly processed for subsequent tissue or cell-based experimental procedures (s. section 3.3.2.1, 3.3.2.2, 3.3.2.3 and 3.3.2.5).

Intestinal dissection was conducted in cooperation with Aline Pesi and Susann Kahl (TIM, University Medical Center Mainz).

3.3.2. Murine Tissue-Based

3.3.2.1. Heart/Body-Weight Ratios

To measure body weight changes and calculate the heart-to-body weight ratio as an indicator of cardiac hypertrophy, mice were weighed once every other day during treatment (s. 3.1.4) and isolated hearts were weighed post-transection (s. 3.3.1).

3.3.2.2. Isometric Tension Recordings

Segments of murine thoracic aorta, each 3-4 mm in length, were carefully cleaned to remove perivascular adipose tissue (PVAT) and other surrounding tissue, which was then set aside for further analysis. These prepared segments were subsequently mounted on force transducers within an organ bath for experimental studies. For vascular relaxation studies, these aortic rings were pre-constricted with prostaglandin $F_{2\alpha}$ (2 µM) to achieve at least 80% of the maximal tone induced by the potassium chloride (KCl) boluses before. The response to vasodilators was assessed by recording concentration-relaxation curves with endothelium-dependent acetylcholine (ACh, 1 nM to 3.3 µM) and endothelium-independent nitroglycerine (GTN, 1 nM to 32 µM), as previously described [63]. Additionally, concentration-contraction curves were obtained in response to KCl depolarization (5 mM to 80 mM). A stable temperature of 37 °C and a continuous flow of carbogen gas were maintained throughout the measurements.

Organ bath chamber data was created with the technical assistance of Jörg Schreiner and Alexandra Rosenberger (Laboratory of Molecular Cardiology, University Medical Center Mainz). Additionally, the cleaning of the aortas was a collaborative effort within our group, involving Dr. Lea Stohm, Henning Ubbens, Leonie Küster, Simon Lange, Dominika Mihaliková, phD, Marin Kuntić, phD and Ivana Kuntić, phD.

3.3.2.3. Dihydroethidium (DHE)-Dependent Fluorescence Microtopography

After tissue sampling (s. section 3.3.1), isolated murine cardiac left ventricles and thoracic aortic ring segments, the latter with PVAT still attached and 4 mm in length, were initially preserved in fresh protease inhibitor buffer (s. section 0) and incubated at 37°C for 10 min. Following incubation, they were embedded in Tissue-Tek O.C.T.

compound-resin, with the resulting resin cylinders carefully frozen on liquid nitrogen and subsequently stored in tubes at -80°C until cutting. Both, cardiac and aortic cross-sections were cut at the cryostat (8 µm thick), mounted on microscope glass slides and stored at -80°C until staining. For DHE staining the cryosections were incubated with dihydroethidium (DHE; 1 µM freshly diluted in DPBS) for 30 min at 37°C in darkness and protected with a cover slip for immediate fluorescence microtopography [189]. Fluorescence was detected with a Zeiss Axiovert 40 CFL microscope using specific filters (rhodamine filter (excitation at 510–560 nm; emission at ≥ 590 nm, red DHE oxidation-derived fluorescence) and a DAPI filter (excitation at 365 nm; emission at ≥ 420 nm, green autofluorescence of the aortic elastic lamina [190])), and the red ROS-derived fluorescence were quantified for integrated optical density (IOD) of the region of interest (mean pixel intensity of endothelium and media only in case of aortic samples and whole image for cardiac samples) using ImageJ software.

DHE-dependent fluorescence microtopography analysis was conducted with the technical assistance of Alexandra Rosenberger and Jörg Schreiner (Laboratory of Molecular Cardiology, University Medical Center Mainz).

3.3.2.4. Immunohistochemical (IHC) Staining and Densitometric Analysis

Aortic ring segments, each measuring 3-4 mm and retaining intact adventitia and perivascular fat, were preserved in 4% formaldehyde, and subsequently embedded in paraffin (FFPE), before being sectioned into 5 µm slices. After the removal of paraffin, the samples were prepared with a 2.5% normal horse serum blocking solution and then subjected to staining with primary antibodies specifically targeting 3-NT. The staining process utilized a biotinylated secondary goat anti-rabbit antibody at a 1:1000 dilution [63]. For the visualization of antigen-antibody complexes, the ABC reagent followed by the DAB (3,3'-diaminobenzidine) peroxidase substrate was employed, facilitating the chromogenic detection. Visualization of the stained sections was achieved using an Olympus IX71 microscope at a 20x objective magnification, with images captured by an Olympus ColorView II camera. Densitometric analysis for the quantification of 3-NT positive proteins within the aortic tissue utilized Image J software, enhanced with the IHC Toolbox and custom macros, as outlined in VIII. Appendix [191]. Results were

expressed as a percentage of the stained area within the aortic tissue, adhering to methodologies established in prior studies [192].

Aortic histological analyses were performed with the technical assistance of Angelica Karpi and Nicole Glas (Laboratory of Molecular Cardiology, University Medical Center Mainz).

Duodenal samples, cleaned and prepared via FFPE, measuring 1.5 cm, were sectioned twice independently to produce two 5 µm thick slices. Following blocking with a 5% normal goat serum solution, sections were stained with primary antibodies targeting CD3, CD4, CD68, and Ki67 (s. section 2.1 for dilution details), and then incubated with a biotinylated goat anti-rabbit at a 1:500 dilution. Colour development again utilized the ABC reagent and DAB peroxidase substrate. Stained sections were visualized using a Leica DMi8 microscope, with intraepithelial lymphocyte (IEL) counts conducted on a minimum of 10 randomly selected duodenal villi, normalized against epithelial nuclear cell counts using Image J software. Similarly, CD4 and CD68 positive T cells and macrophages, respectively, were counted in the lamina propria and normalized against epithelial cell counts. Analysis of villous height (VH) and crypt depth (CrD) was performed on at least 10 well-oriented villi, following previously described methodologies [173, 183].

Duodenal histological analyses were performed with the cooperation of Aline Pesi (TIM, University Medical Center Mainz).

3.3.2.5. Flow Cytometry

Flow cytometry is a critical tool for quantifying cell populations based on their physical and biochemical properties using laser-induced scatter and fluorescence signals [193]. Here, this technique was specifically utilized for the quantification of aortic immune cell infiltration, providing precise insights into the cellular dynamics and immune response within the aortic environment.

Thoracic aortic vessels were dissected (s. section 3.3.1) and meticulously cleared of adipose tissue (compare section 3.3.2.2), with their lengths recorded before mincing. Enzymatic digestion was conducted using 1 mg/ml liberase in $HBSS^{+/+}$ for 30 minutes at 37°C, at 500 rpm. Post-digestion, aortic fragments were strained (70 µm) to achieve a single-cell suspension, and cells were pelleted (6 min with 300 g

at 4°C) and resuspended in FACS buffer (s. section 0). Cell counts for each suspended aortic sample were determined before Fc receptor blocking (anti-CD16/CD32, 10 min at RT, s. section 2.1) was performed to prevent non-specific antibody binding. The cells underwent centrifugation, and the resulting pellets were stained with a panel of fluorescence-labelled antibodies targeting cell-surface markers for immune cell phenotyping (s. section 2.1.2, 30 min, 4°C in dark).

Following staining, cells were washed and loaded onto a flow cytometer for analysis. The device, set up to handle multicolour fluorescence, recorded events from the stained single-cell suspensions.

To adjust for spectral overlaps in multicolour fluorescence studies, a compensation control was prepared using spleen cells. The spleen was finely dissected, and cells were released into suspension through gentle homogenization (40 µm). Following this, erythrocytes within the splenic cell suspension were lysed using an Ammonium-Chloride-Potassium (ACK) lysis buffer (s. section 0), clearing the sample of red blood cells, and leaving behind the white blood cells of interest. The splenocytes were then counted, resuspended in FACS buffer, and aliquoted into wells for staining. This preparation of single-stain controls involved the same fluorochrome-conjugated antibodies as used for the aortic cells, ensuring the compensation settings on the flow cytometer could be precisely calibrated.

Analysis of the labelled cells was conducted on a FACSCanto II flow cytometer, and the data were processed using FlowJo™ v10.8 software. The data acquisition focused on live, single cells, excluding dead cells by viability dye staining. A comprehensive gating strategy (s. **Figure 3-4**) was employed to identify various immune cell subsets, including lymphocytes and myeloid cells. The quantitative evaluation of the data involved normalizing the immune cell counts to the length of the respective aorta, allowing for a comparative assessment across samples as previously described [194].

Flow cytometry was performed in cooperation with Dr. Johanna Helmstädter (Laboratory of Molecular Cardiology, University Medical Center Mainz).

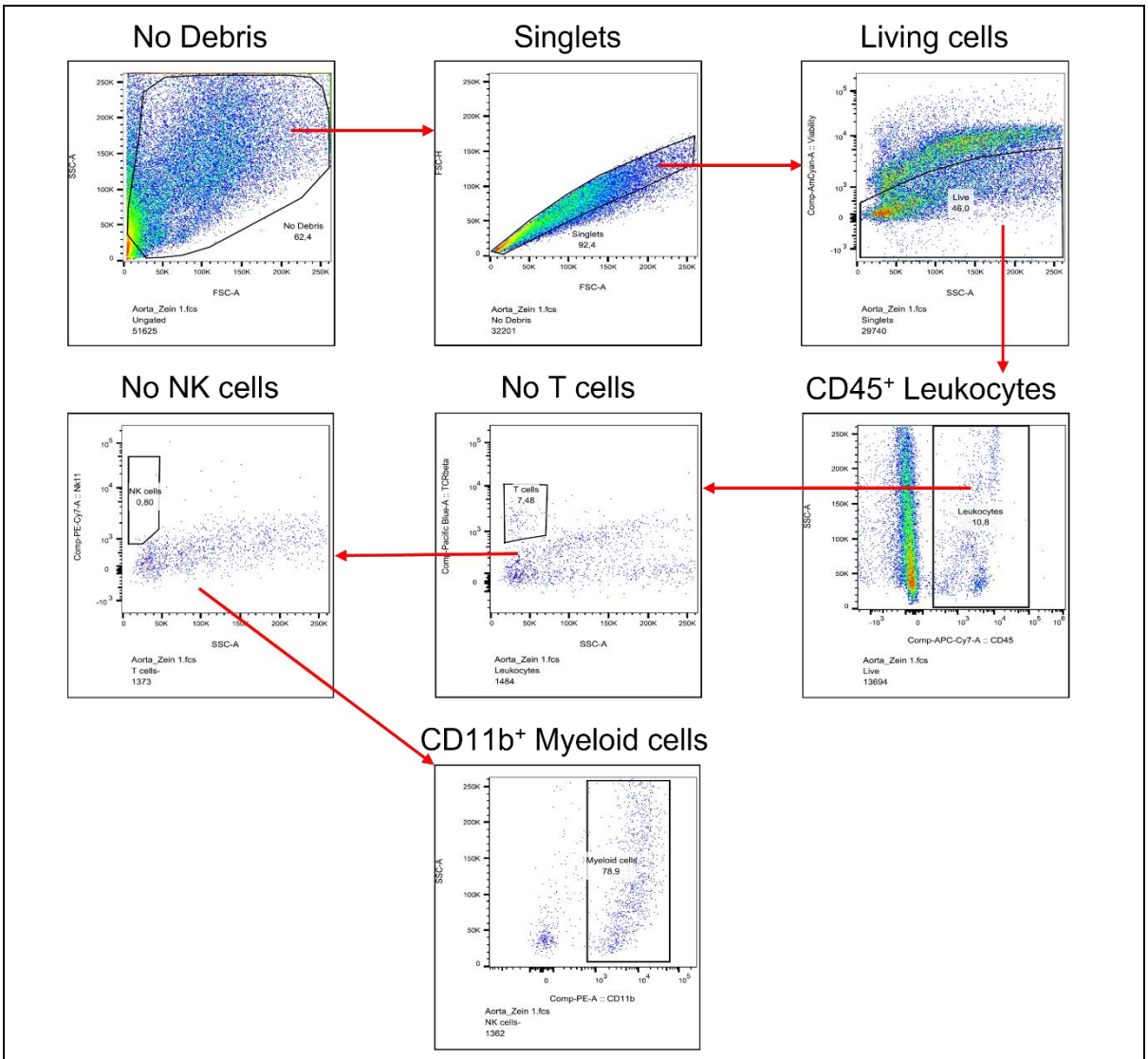

Figure 3-4: **Sequential gating strategy utilized for isolating distinct immune cell populations from murine aortic tissue**. Initial gating removed debris and aggregates, focusing on viable, single-cell events. Subsequent gates were applied to identify live leukocytes (CD45+), further delineating lymphocyte subtypes (T cells: TCRβ+ and NK cells: NK1.1+) and myeloid lineage cells (CD11b+). Adapted from Keppeler et al., 2024 [172].

3.3.3. Blood-Based

3.3.3.1. Non-Fasting Glucose Levels

The Accu-Chek Aviva system was employed for the real-time assessment of non-fasting glucose levels in whole blood, specifically during the process of tissue sampling, as detailed in section 3.3.1. This procedure was conducted in adherence to the guidelines provided by the manufacturer. Despite its primary human application, comparisons in bovine and alpaca models have demonstrated

acceptable precision with this device, indicating its potential utility in a broader research context [195, 196].

3.3.3.2. Serum Total Cholesterol Levels

Serum total cholesterol levels were determined using the cholesterol oxidase-peroxidase aminophenazone (CHOD-PAP) method, an accredited, direct, and automated enzymatic colourimetric technique, performed with the Alinity c system (Abbott) at the Institute of Clinical Chemistry and Laboratory Medicine, University Medical Center Mainz [197]. While this method is not specifically validated for murine samples, it has been successfully utilized in previous publications for similar analyses, demonstrating its applicability in research contexts [198].

3.3.3.3. Complete Blood Count (CBC)

For the complete blood count (CBC), fresh blood treated with sodium citrate as an anticoagulant (1:10 dilution) was analysed using the Sysmex XP-300 haematology analyser. This analyser provides up to 8 key blood parameters:

- white blood cells (WBC),
- red blood cells (RBC),
- haemoglobin (HGB),
- haematocrit (HCT) – the percentage of blood volume occupied by RBC,
- mean corpuscular volume (MCV) - a measure of RBC volume,
- mean corpuscular haemoglobin (MCH) - a measure of HGB per RBC,
- mean corpuscular haemoglobin concentration (MCHC) – the HGB concentration in RBC,
- and platelets (PLT).

$$with\ MCV = \frac{HCT}{RBC}, MCH = \frac{HGB}{RBC}\ and\ MCHC = \frac{HGB}{HCT}$$

The results were utilized to assess the haematological profile of the mice post-treatment and were crucial for normalizing the whole blood oxidative burst (refer to section 3.3.3.4) to the respective WBC count. It is important to note that clinical analysers, such as the Sysmex XP-300, have not been validated for use in mice [199].

3.3.3.4. Oxidative/Respiratory Burst

The whole blood oxidative burst assay evaluates leukocyte NADPH oxidase (Nox2) and myeloperoxidase (MPO) activity, serving as a marker for pro-oxidant load and inflammatory response. "Oxidative burst" and "respiratory burst" are synonymous, referring to this rapid leukocyte response. The assay follows established protocols to assess the immune defence against infection or inflammation [200].

In the tissue sampling process outlined in section 3.3.1, fresh whole blood, anticoagulated with sodium citrate in a 1:10 dilution, was taken and kept at RT. It was then further diluted (1:50) with $PBS^{+/+}$ and stimulated with 50µg/ml zymosan A extracted from the *S. cerevisiae* cell walls to provoke reactive oxygen species (ROS) production. The generation of ROS, indicative of oxidative burst, was quantitatively monitored through enhanced chemiluminescence by L-012 (100µM), recorded at 5-minute intervals using a Mithras multimode reader. The results, showing the dynamic ROS production over a 60-minute timeframe, were normalized to the white blood cell count obtained from a complete blood count (CBC by Sysmex, s. section 3.3.3.3)., thus providing a mean measure of oxidative or respiratory burst activity per leukocyte. This methodology ensures an accurate assessment of leukocyte functional response, crucial for understanding inflammatory responses and the body's innate immune mechanisms.

Oxidative Burst was performed in cooperation with Dr. Ksenija Vujačić-Mirski (Laboratory of Molecular Cardiology, University Medical Center Mainz).

3.3.3.5. Determination of NO Metabolites by Griess Test

Nitrite (NO_2^-) and nitrate ions (NO_3^-) concentrations were quantified using the ENO-20 NOx Analyzer, employing a liquid chromatography approach complemented by post-column derivatization using the Griess reagent, first described in 1858 by Peter Griess, in line with established protocols [201, 202]. The process was executed in cooperation with Prof. S. Chlopicki's group, specifically by Agnieszka Zakrzewska at the Jagiellonian Centre for Experimental Therapeutics (JCET), Jagiellonian University, Krakow, Poland.

In detail, to prepare for analysis, plasma samples underwent a methanol precipitation process at a 1:1 volume ratio, followed by centrifugation at 10,000 g for

10 minutes to isolate the supernatant for HPLC analysis. The system initially separated NO_2^- from NO_3^- using a specialized reverse-phase NO-PAK column, with subsequent reduction of NO_3^- to NO_2^- achieved using a copper-plated cadmium NO-RED column. Detection of nitrite was precisely facilitated through the Griess reaction, where sulphanilamide and n-(1-naphthyl)ethylenediamine dihydrochloride were utilized, forming a purple azo dye detectable at specific retention times. This detection was performed with a flow-through spectrophotometer at 540 nm for accurate absorbance measurement of the derivatives.

3.3.3.6. Olink Plasma Proteomics

Plasma proteomic analysis was carried out using the Olink® Target 96 Mouse Exploratory Panel (95380, v.3801) in collaboration with the Institute of Preventive Cardiology and Preventive Medicine at the University Medical Center Mainz, employing the proximity extension assay (PEA) method. This technique involves the use of pairs of oligonucleotide-labelled antibody probes that bind to their target protein. Upon proximity, these oligonucleotides hybridize and are subsequently extended and amplified, providing a highly specific and sensitive detection method. The PEA technology has been validated to ensure exceptional specificity in recognizing intended target proteins [203]. EDTA plasma, thawed just once, served as the basis for the examination. 96 target protein concentrations were quantified and expressed in normalized protein expression (NPX) units, using the Olink® NPX Manager software, which provides relative quantifications on a binary logarithmic scale. Statistical analysis of the data, including the generation of volcano plots, was conducted using the Olink® Insights Stat Analysis tool and visualized with GraphPad Prism software.

3.3.3.7. Enzyme-Linked Immunosorbent Assay (ELISA)

The enzyme-linked immunosorbent assay (ELISA), conceptualized by Eva Engvall and Peter Perlman in 1971, is a foundational technique in immunodiagnostics for detecting and quantifying specific proteins within heterogeneous samples [204]. The sandwich ELISA format, which involves the sequential use of two distinct primary antibodies targeting different epitopes of the same antigen, is particularly common. In this method, an antigen is first captured on a microtiter plate by one antibody and subsequently tagged by a second enzyme-linked antibody. The addition of a substrate leads to an enzymatic reaction that produces a colour change, which can

be measured by a plate reader. The magnitude of colour development, calibrated against a standard curve of known antigen concentrations, quantifies the antigen present in the sample.

The concentration of Interleukin-17A (IL-17A) in EDTA-treated plasma was quantified using a commercial ELISA kit (Mouse IL-17A Flex Set, 560283) following the manufacturer's guidelines (BD Biosciences, NJ, USA), as previously published [205] in collaboration with PD Dr. S. Karbach's Group.

3.3.4. RNA/DNA-Based

3.3.4.1. Quantitative/Real-Time Reverse Transcription PCR (qRT-PCR/RT-qPCR)

RNA isolation from snap-frozen tissues was performed using the acid guanidinium thiocyanate–phenol–chloroform extraction method, as established by Piotr Chomczynski and Nicoletta Sacchi [206]. For isolation of RNA from snap-frozen tissues (s. 3.3.1), small pieces were placed in GIT buffer (600 µl, s. section 0) and tissue was homogenized with a 5 mm stainless steel bead for 5-6 min at 30 Hz with the TissueLyser II. Post-homogenization, the samples underwent a lysis period of 20 minutes at -20°C to facilitate cell disruption. To this lysate, 60 µl of sodium acetate (pH 4.0), 600 µl of water-saturated phenol, and 300 µl of chloroform/isoamyl alcohol (49:1 ratio) was added, ensuring a vigorous mix through vortexing before a 15-minute ice incubation. This mixture was then centrifuged at 12,500 g for 20 minutes at 4°C, enabling phase separation where RNA is partitioned into the upper aqueous phase due to its acidic nature. Approximately 600 µl of the RNA-containing aqueous phase was carefully transferred to a new tube. RNA precipitation was achieved by adding an equal volume of isopropanol and incubating at -20°C overnight, enhancing RNA yield and purity. The RNA precipitate was subsequently gathered through centrifugation, after which the supernatant was discarded. The resultant pellet was then washed with 80% ethanol to remove any remaining impurities, followed by air-drying at room temperature to evaporate the ethanol, ensuring the pellet was ready for resuspension. The pellet was resuspended in DEPC-treated water, with solubilization achieved through incubation

at 55°C. The RNA was stored at -20°C for short-term or -80°C for long-term preservation.

RNA extraction was quantified via a UV/VIS spectrophotometer, which conducts simultaneous absorbance measurements at 260 nm (nucleic acids' absorption peak), 280 nm (proteins' absorption peak), and 230 nm (phenols and residual guanidinium thiocyanate's absorption peak). The 260 nm measurement facilitates the determination of RNA concentration, as approximately 40 ng/µl of single-stranded RNA corresponds to an optical density of 1:

RNA Concentration in ng/µl = A_{260} x dilution factor x 40

To assess the purity of the RNA extracts, absorbance ratios at 260/280 nm and 260/230 nm were evaluated. Extracts with 260/280 nm ratios within 1.8–2.0 and 260/230 nm ratios equal to or greater than 2.0 were deemed pure. For further analysis, RNA concentrations were standardized to 62.5 ng/µl using DEPC-treated water.

Quantitative real-time, reverse transcription PCR (qRT-PCR or RT-qPCR) quantifies gene expression by assessing specific mRNA levels, requiring the conversion of RNA into complementary DNA (cDNA) for analysis. This is achieved through reverse transcription using reverse transcriptase to produce cDNA from RNA. A 'one-step' approach combines cDNA synthesis and qRT-PCR in a single reaction, utilizing gene-specific primers for both processes (StepOnePlus™).

qRT-PCR operates similarly to traditional PCR, allowing for the quantification of synthesized cDNA. The technique employs TaqMan® assays, utilizing forward and reverse primers alongside a sequence-specific probe. This probe, bearing a fluorescent reporter at one end and a quencher at the other, binds within the primer-targeted sequence. Probe cleavage by Taq polymerase's exonuclease activity during PCR separates the reporter from the quencher, increasing fluorescence which correlates with the target cDNA amount.

Here, 125 ng of total RNA underwent qRT-PCR analysis using TaqMan® probe-and-primer sets (Assay IDs are listed in section 2.7) together with the QuantiTect Probe RT-PCR kit, according to the manufacturer’s instructions. Gene expression levels were quantified using the $2^{-\Delta\Delta Ct}$ method, which normalizes the cycle threshold (Ct)

values to the TATA-box binding protein (TBP), a housekeeping gene, to determine relative expression rates.

RNA Isolation and qRT-PCR were conducted with the technical assistance of Alexandra Rosenberger (Laboratory of Molecular Cardiology, University Medical Center Mainz).

3.3.5. Protein-Based

Olink Plasma Proteomics can be found in section 3.3.3.6 under Cell/Blood-based methods, as well as enzyme-linked immunosorbent assay (ELISA, 3.3.3.7).

3.3.5.1. Dot Blot

Dot blot techniques offer a practical approach in molecular biology to identify specific biomolecules, such as proteins, eliminating the need for separation through gel electrophoresis. This method is particularly useful for detecting precise protein modifications, such as tyrosine nitration identified by 3-NT, and lipid peroxidation marked by 4-HNE, utilizing specific antibodies. The process comprises several steps: it begins with the extraction of total protein from the murine tissue, followed by protein concentration measurement using the Bradford assay—a crucial step to ensure uniform protein concentrations across samples. Following this, proteins are transferred onto a membrane and quantified using enhanced chemiluminescence (ECL) and densitometric analysis. Crucially, protein expression or modification levels are normalized to the total protein content, as indicated by Ponceau S staining, ensuring a reliable comparison across samples.

Following the protocol outlined in section 3.3.1, proteins were extracted from murine tissue, specifically from the left ventricle tissue in this instance. The process involved grinding the tissue into a fine powder using a mortar and pestle that had been precooled with liquid nitrogen. This powder was then carefully transferred to tubes, kept on liquid nitrogen, and mixed with an equal volume of homogenization buffer. This buffer included Triton X-100 and protease inhibitors, as mentioned in section 0, to aid in cell lysis and prevent protein degradation. The samples were vigorously vortexed to ensure a thorough mix. After an hour of incubation on ice, allowing for the complete disruption of cell membranes, the mixtures were centrifuged at

10,000 g for 10 minutes at 4°C. The supernatant, containing the total protein extract, was then carefully separated from the insoluble debris, transferred to a fresh tube, and stored at -20°C for later use.

Protein concentrations in the samples were measured using a colorimetric assay, based on the principle that Coomassie Brilliant Blue G-250 dye binds to proteins, forming complexes that cause an absorbance shift from 465 nm to 595 nm. This shift is proportional to the protein amount present in the sample, a method first introduced by Marion M. Bradford in 1976 and hence known as the Bradford assay [207]. A standard curve was established using bovine serum albumin (BSA, up to 30 µg/ml) at various concentrations to quantify protein levels. The protein samples and BSA standards were dispensed into a 96-well plate. After introducing the Roti-Quant reagent, which includes Coomassie Brilliant Blue G-250, absorbance readings at 595 nm were obtained using a plate reader allowing for further dilution to the lowest common denominator/concentration with homogenization buffer. The uniformly diluted protein homogenates were stored at -20°C for later use.

Cardiac protein homogenates were transferred to a PBS-pre-wetted nitrocellulose membrane using a Minifold I vacuum dot-blot system [189]. After transfer, wells were rinsed with PBS, and the membrane was then dried at 60°C for an hour to ensure protein immobilization. Total protein loading per well, up to a maximum capacity of 50 µg, was verified with Ponceau S staining on the nitrocellulose membrane. Specific antibodies for 3-NT and 4-HNE were used to detect tyrosine nitration and lipid peroxidation modifications in proteins, respectively [208]. Detection and quantification of dots were performed by enhanced chemiluminescence (ECL) with peroxidase-conjugated anti-rabbit and anti-goat secondary antibodies. Densitometric quantification of antibody-specific bands was performed with a ChemiLux Imager and Gel-Pro Analyzer software. The expression level of each target-specific protein dot was normalized based on its total protein content, as determined by Ponceau S staining.

Oxidative Burst was performed in cooperation with Leonie Küster (Laboratory of Molecular Cardiology, University Medical Center Mainz).

3.4. Statistics

Data are reported as means ± standard error of the mean (SEM). Statistical analyses were conducted with GraphPad Prism version 10.2.1 for Windows. Outliers were identified and subsequently removed based on the Robust regression and Outlier removal (ROUT) method with a q-value of 1 % (0.01). The normality of distribution for continuous data sets was verified using the Shapiro-Wilk test. For data adhering to a normal distribution, two-sample comparisons were facilitated through the unpaired Student's t-test, while the Mann-Whitney test was employed for datasets that did not follow a normal distribution. Comparative analyses involving multiple groups, such as in the assessment of whole blood oxidative burst (e.g., **Figure 4-9 G**) and isometric tension dose-response curves (e.g., **Figure 4-9 A-C**), were performed using two-way ANOVA, incorporating Bonferroni's correction for post hoc testing. All data was assumed to be two-tailed. p-values < 0.05 were considered statistically significant and marked by asterisks (*p-value<0.05; **p-value<0.01; ***p-value<0.001; ****p-value<0.0001) corresponding to conventional standards.

4. Results

Results are presented primarily as scatter bar plots, if originating from zero, to illustrate individual and comparable observations from and between analysed samples. For instances where the plot origin does not start at zero, jitter plots are employed to display the individual data points. This approach ensures a clear and precise visual representation and differentiation of the findings. Parts of this thesis have previously been published in Keppeler *et al.*, 2024 [184].

4.1. Effects on the Duodenum

Although the CeD model utilized here (s. **Figure 4-1**, for more details refer to the section 3.1) aligns with previously published protocols and dissertations [173, 183, 209, 210], an examination of its effects on the small intestine via immunohistochemistry (IHC, s. section 3.3.2.4).

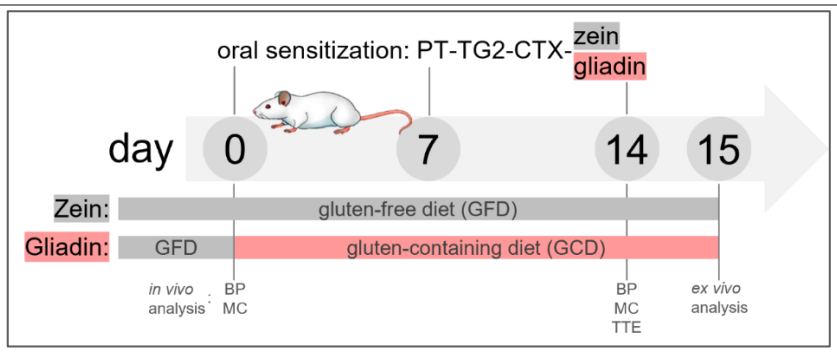

Figure 4-1: Experimental protocol overview; In the ON-study, male NOD-DQ8 mice aged between 8–12 weeks were administered three doses of deamidated zein or gliadin peptides via oral gavage, both with added cholera toxin (PT-TG2-CTX-zein/gliadin). Subsequently, mice in the gliadin treatment group were transitioned to a GCD for 14 days, while the zein group continued the GFD. Assessments of blood pressure (BP) and metabolic cage (MC) parameters were conducted on selected mice at the start (d0) and end (d14) of the experimental period. Additionally, transthoracic echocardiography (TTE) evaluation was performed at the end of the treatment, leading to further *ex vivo* analyses (for comprehensive details, consult the methods section 3). Adapted from Keppeler *et al*., 2024 [184].

The results depicted in **Figure 4-2 A-G** outline how the development of CeD was observed in the gliadin-treated mice. This is primarily indicated by a statistically significant decrease in the ratio of villous height to crypt depth (VH:CrD) within the distal duodenum (DD), a crucial histological marker of CeD.

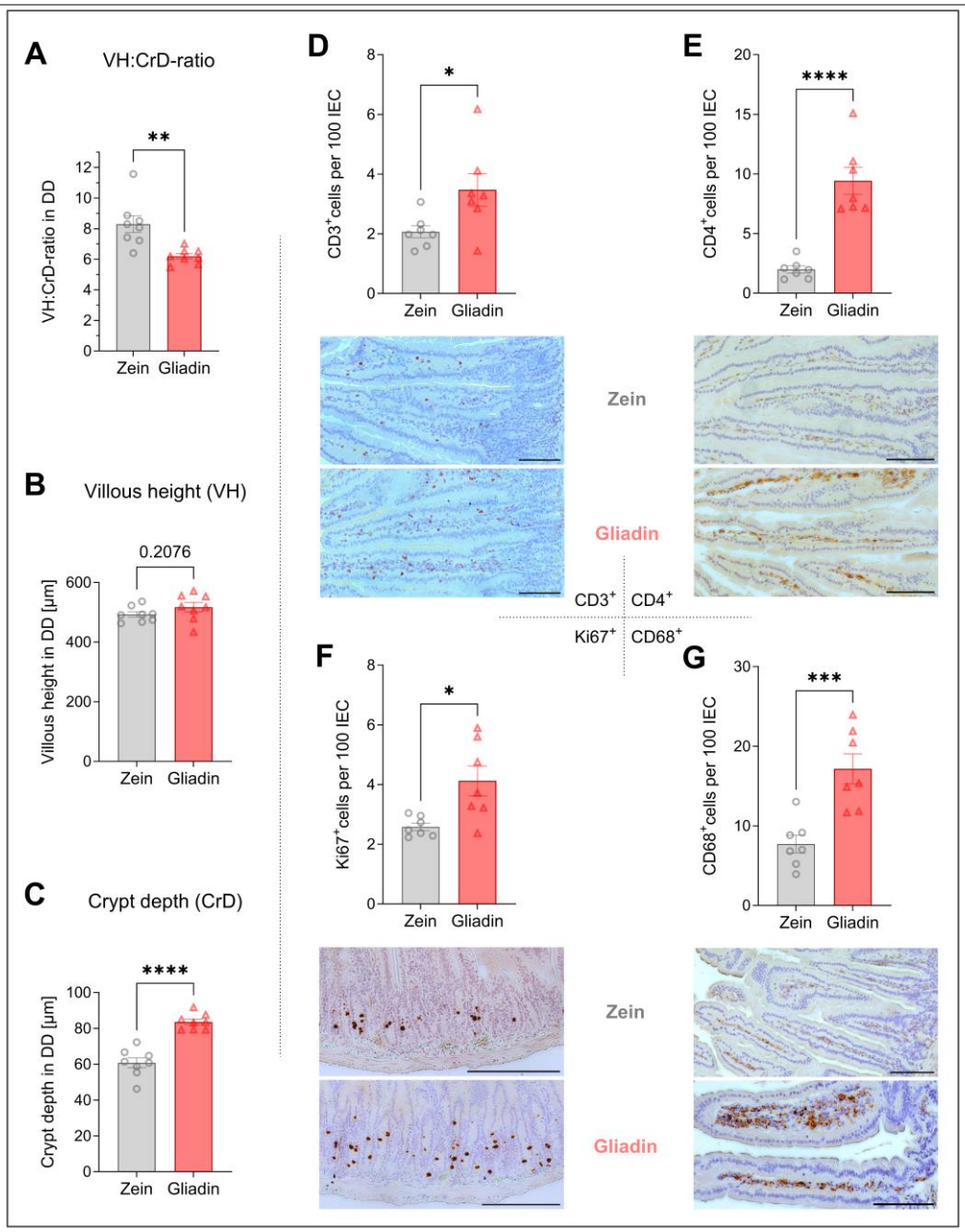

Figure 4-2: Impact of gluten on small intestinal architecture and immune response in NOD-DQ8 mice. Illustrating CeD induction through gluten exposure, this figure showcases the changes in VH:CrD, alongside the infiltration of immune cells such as $CD3^+$, $CD4^+$, $CD68^+$, and increase in proliferation ($Ki67^+$), which heightened immune activity and altered duodenal morphology characteristic of CeD, reflecting human CeD pathology.

(A) Villous height to crypt depth ratio (VH:CrD) in DD determined by the quotient of **(B)** villous height (VH) to **(C)** crypt depth (CrD). Immunohistochemical analysis (IHC) of **(D)** $CD3^+$ positive intraepithelial lymphocytes (IELs), **(E)** $CD4^+$ T cells, **(F)** $Ki67^+$ proliferating cells and **(G)** $CD68^+$ cells per 100 intestinal epithelial cells (IEC) together with exemplary stainings of the FFPE DD cross sections (scale bars represent 100 µm).

(A)-(C) Unpaired t-test; n=8, **(D)-(G)** unpaired t-test; n=7. Data are means±SEM. *p<0.05; **p<0.01; ***p<0.001; ****p<0.0001. Adapted from Keppeler *et al.*, 2024 [184].

In contrast, the control group fed with zein exhibited no signs of CeD induction, maintaining normal VH:CrD ratios, similar to those of healthy controls. Results indicated that although no significant difference in villous height (VH) was detected across the groups, suggesting the absence of villous atrophy, a notable increase in crypt depth (CrD) was observed in the Gliadin group compared to the Zein group. This suggests a pronounced proliferation or regeneration of the crypts, indicative of crypt hyperplasia.

Quantitatively, the Gliadin group had an average VH:CrD ratio of 6.2, marked by a statistically significant reduction of 2.1 (p-value=0.0025). On the other hand, the zein group, with an average VH:CrD ratio of 8.3, showed no signs of CeD induction. Although the VH did not exhibit a significant difference (p-value=0.2076), the CrD in the Gliadin group was significantly higher by 22.8 µm (p-value<0.0001), with an average of 83.6 µm compared to the zein group's average of 60.8 µm.

In the additional analysis of duodenal sections from gliadin-treated mice compared with zein-control mice, quantitative immunohistochemistry revealed an increase in $CD3^+$ intraepithelial lymphocytes, $CD4^+$ T cells, and $CD68^+$ macrophages in the lamina propria, alongside crypt cell hyperplasia evidenced by Ki67 staining. These changes are indicative of elevated cell proliferation rates, mirroring key markers of human CeD and thus validating the model's efficacy in simulating the disease [211, 212] (**Figure 4-2 D-G**).

Specifically, the Gliadin group exhibited an increase in $CD3^+$ cells from 2 to 3.4 (a +1.4 change, p-value=0.0325, **Figure 4-2 D**), $CD4^+$ T cells from 2 to 9.4 (+7.4 change, p-value<0.0001, **Figure 4-2 E**), and $Ki67^+$ proliferation marker from 2.6 to 4.1 per 100 IECs (+1.5 change, p-value=0.0113, **Figure 4-2 F**). Additionally, $CD68^+$ macrophages surged from 7.7 to 17.2, marking a +9.5 change per 100 IECs (p-value=0.001, **Figure 4-2 G**). Each of these increments underscores the immune response characteristic of CeD in the gliadin-challenged mice. For clarity, all data are presented as the count of specific marker-positive cells per 100 intestinal epithelial cells (IECs), offering a standardized metric for assessing the extent of immune cell infiltration and proliferation within the duodenal epithelium.

In the small intestine of NOD-DQ8 mice subjected to gliadin treatment was a statistically significant elevation in the expression of inflammatory cytokines, notably tumor necrosis factor-alpha (*Tnfa*), interferon-gamma (*Ifng*), interleukin-6 (*Il6*), and

interleukin-17A (*Il17a*) mRNA, in comparison to zein controls. This increase was accompanied by an upregulation of cytochrome b-245 (*Cybb*) transcripts, coding for the heavy chain of the superoxide-producing enzyme NADPH oxidase 2 (Nox2), indicating also a rise in oxidative stress within the DD, as depicted in **Figure 4-3 A-E.**

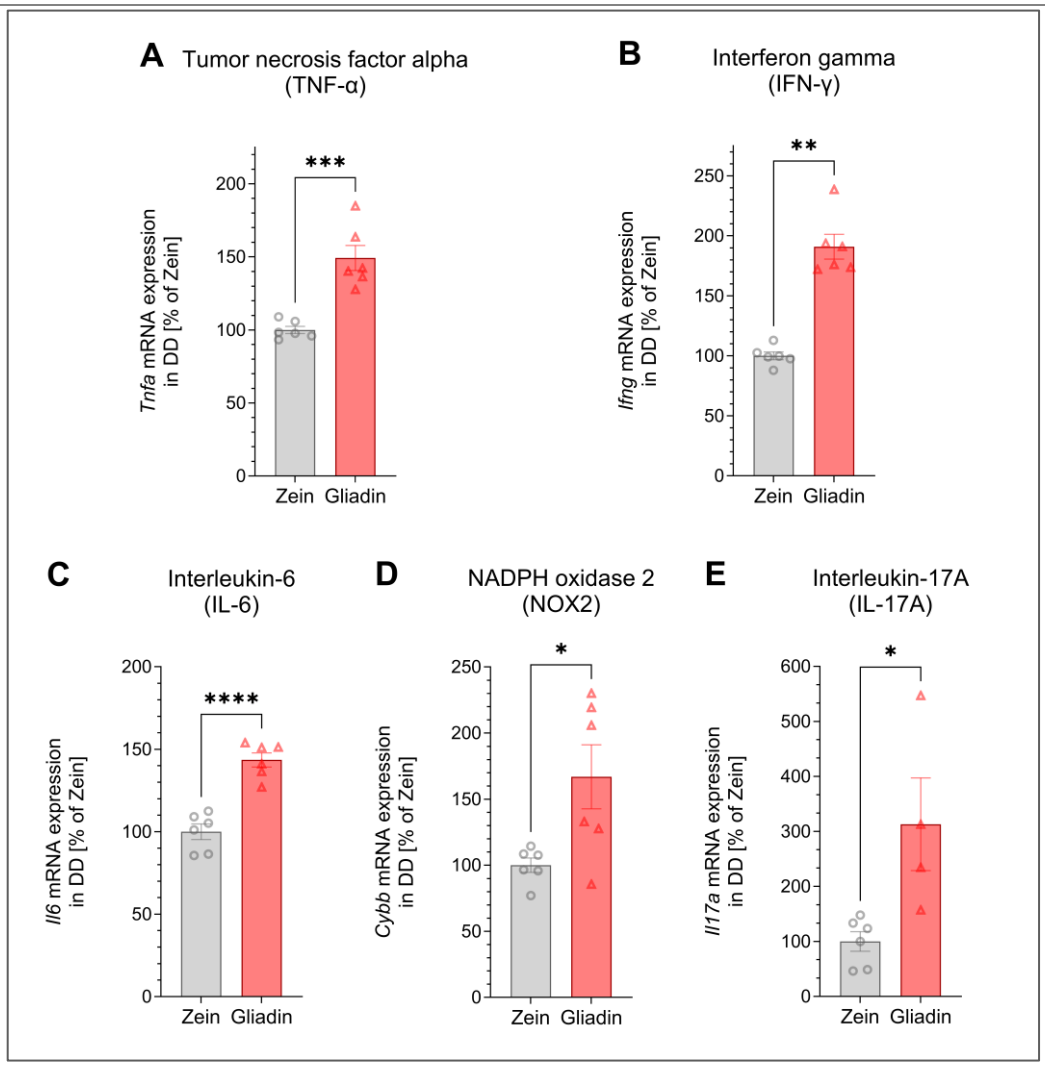

Figure 4-3: Enhanced inflammatory response in the DD of gliadin-treated mice. This figure illustrates the notable rise in pro-inflammatory cytokines and markers of oxidative stress, highlighting the transcriptional dynamics that mimic CeD pathology.

(A) Tumor necrosis factor alpha (*Tnfa*), **(B)** Interferon gamma (*Ifng*), **(C)** Interleukin-6 (*Il6*), **(D)** NADPH oxidase 2 (*Cybb*) **(E)** Interleukin-17A (*Il17a*) mRNA expression was measured by qRT-PCR in DD.

(A) Unpaired t-test; n=6, **(B)** Mann-Whitney test; n=6, **(C)-(D)** unpaired t-test; n=6, **(E)** unpaired t-test; n(Z)=6, n(G)=4. Data are means±SEM. *p<0.05; **p<0.01; ***p<0.001; ****p<0.0001. Adapted from Keppeler *et al.*, 2024 [184].

Precisely, *Tnfa* mRNA transcription levels rose to 149.2% with a p-value of 0.0003 (**Figure 4-3 A**), *Ifng* to 183.6% with a p-value of 0.0022 (**Figure 4-3 B**), *Il6* to 143.5% with a p-value of <0.0001 (**Figure 4-3 C**), *Cybb* (encoding for Nox2) to 167% with a p-value of 0.0223 (**Figure 4-3 D**), and *Il17a* significantly increased to 313.1% with a p-value of 0.0162 (**Figure 4-3 E**), all normalized against the zein control group set at 100%. Together with histological evidence of CeD-like changes, these results indicate a two-week gliadin treatment in genetically susceptible NOD-DQ8 mice led not only to specific immune cell infiltration in the duodenal epithelium and lamina propria but also to a marked increase in pro-inflammatory cytokine expression. This showcases the immune and inflammatory reactions consistent with CeD pathology.

4.2. Systemic Effects of Gliadin Treatment

In gliadin-treated NOD-DQ8 mice, there was an observed increase in both systolic and diastolic BPs, which did not correspond with the development of cardiac hypertrophy. Alongside these cardiovascular changes, the gliadin-treated mice exhibited a trend towards reduced weight gain compared to their control counterparts, while serum total cholesterol levels experienced a significant elevation. Despite these variations, glucose homeostasis, as indicated by non-fasting blood glucose levels, remained constant and unaffected in the mice with CeD. These outcomes, including BP, weight changes, total cholesterol levels, and glucose homeostasis, are detailed comprehensively in **Figure 4-4 A-F.** Glucose levels were specifically measured to rule out the spontaneous development of T1D, a condition for which the genetic NOD background (Non-Obese Diabetic) of this mouse line is known [213].

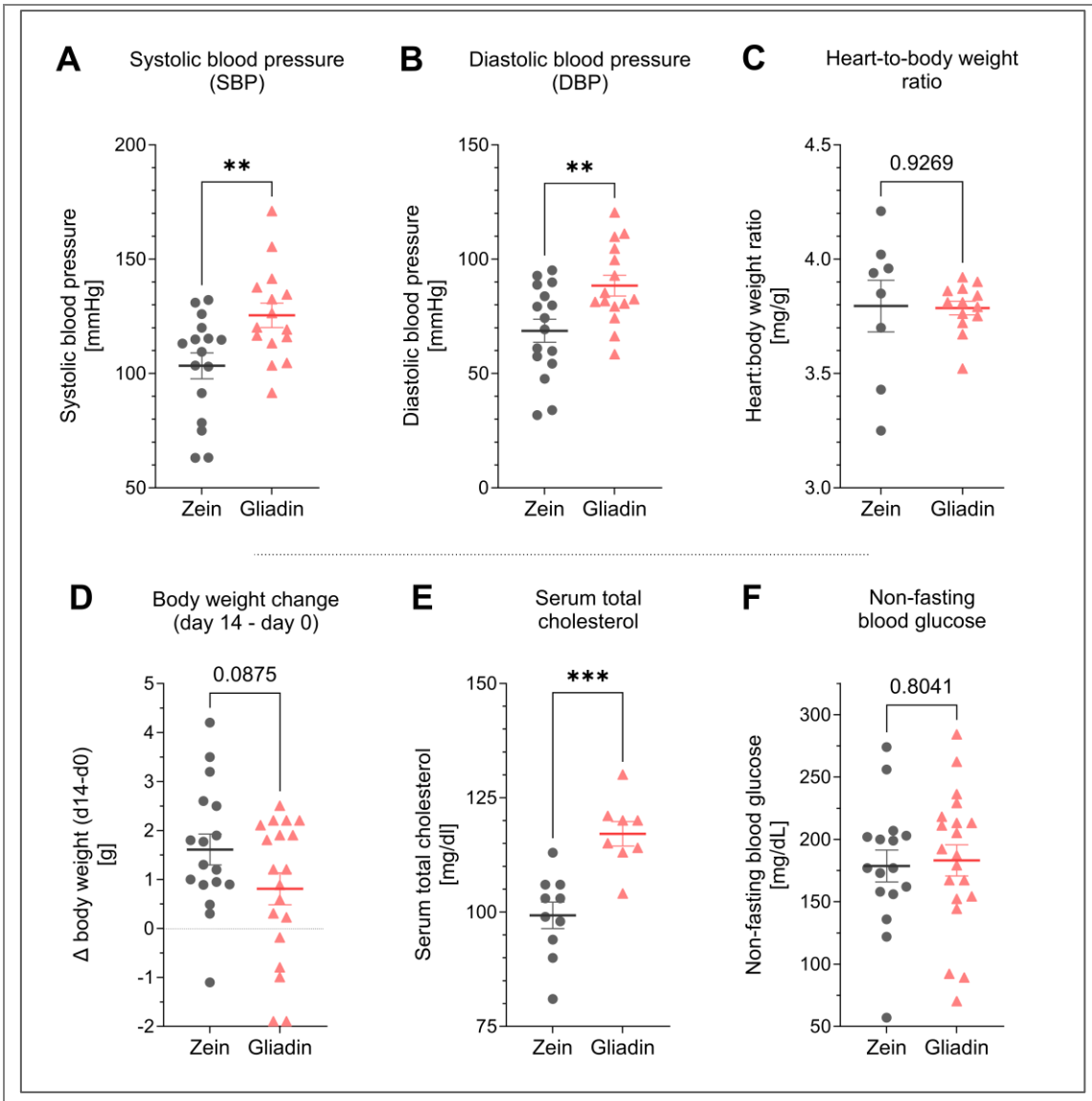

Figure 4-4: Comprehensive effects of gliadin treatment: elevated BP and total cholesterol levels and maintained glucose homeostasis.

(A) Systolic and **(B)** diastolic BP measured by non-invasive tail-cuff at the end of the treatment (day 14). **(C)** Heart-to-body weight ratio and **(D)** body weight changes during the treatment (day 14 – day 0). **(E)** Serum total cholesterol levels and **(F)** non-fasting blood glucose levels were evaluated in whole blood *ex vivo* (day 15).

(A)-(B) Unpaired t-test; n(Z)=16, n(G)=15, **(C)** unpaired t-test; n(Z)=8, n(G)=13, **(D)** unpaired t-test; n(Z)=17, n(G)=19, **(E)** unpaired t-test; n(Z)=10, n(G)=8, **(F)** unpaired t-test; n(Z)=16, n(G)=20. Data are means±SEM. **p<0.01; ***p<0.001. Adapted from Keppeler *et al.*, 2024 [184].

Specifically, systolic BP experienced a marked increase, rising by 22.1 mmHg from 103.4 mmHg in the zein group to 125.5 mmHg in the Gliadin group, a statistically significant change (p-value=0.0084, **Figure 4-4 A**). Diastolic BP also increased by 19.7 mmHg, from 68.7 mmHg to 88.4 mmHg (p-value=0.0071, **Figure 4-4 B**). Despite these shifts in cardiovascular metrics, the heart-to-body weight ratio showed

no significant alteration (p-value=0.9269, **Figure 4-4 C**), suggesting the absence of cardiac hypertrophy. Weight gain in the Gliadin group slightly decreased, with a reduction of 0.8 g compared to a 1.6 g increase in the zein group, though this difference did not reach statistical significance (p-value=0.0875, **Figure 4-4 D**). Total cholesterol levels saw a considerable rise by 17.8 mg/dl, moving from 99.3 mg/dl in the zein group to 117.1 mg/dl in the Gliadin group (p-value=0.0004, **Figure 4-4 E**). Glucose levels, crucially measured to exclude the potential spontaneous onset of diabetes, showed no significant change (p-value=0.8041, **Figure 4-4 F**).

4.2.1. Metabolic Cages: 24-Hour Observation

In this investigation, as illustrated in **Figure 4-5 A-E**, mice were individually housed in metabolic cages for 24-hour periods at two critical time points: before the beginning of treatment on day 0 (d0) and at its end on day 14 (d14). The objective was to precisely assess food and water intake relative to body weight, to identify any differences in intake between the groups. On day 0, before any treatment had begun, no differences were expected—and indeed observed—between the groups, serving merely to illustrate the baseline scattering of data across individuals. This initial measurement confirmed uniformity in conditions prior to the experimental intervention.

It's important to note that during these 24-hour metabolic cage confinements, mice experienced stress due to limited nesting material and restricted access to food, leading to weight loss. This stress-induced weight loss is distinct from the weight changes observed over the normal 14-day experiment period and should not be directly compared (for more details s. section 3.2.2). The findings from this period showed no significant differences in relative body weight loss, water, food, and caloric intake between gliadin-treated and control groups, suggesting that the gliadin-induced physiological changes observed post-treatment were not due to differences in dietary intake. Moreover, both the GFD and GCD were analysed in terms of their macronutrient composition and metabolizable energy. This was done to confirm that the observed physiological effects were a direct result of the gliadin treatment, eliminating nutritional differences as a contributing factor (refer to **Figure 4-5 F**, and section 3.1.4 for detailed information).

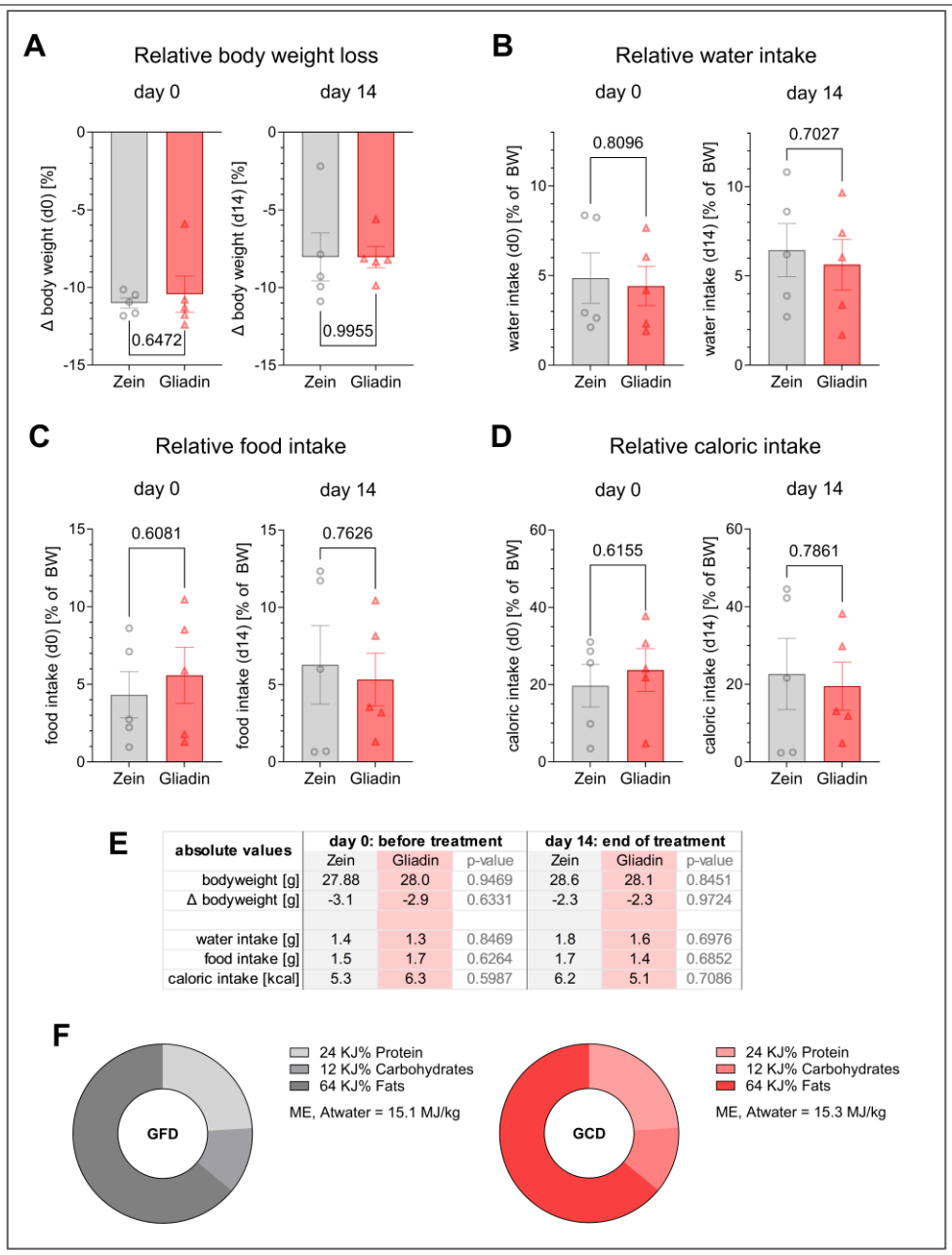

absolute values	day 0: before treatment			day 14: end of treatment		
	Zein	Gliadin	p-value	Zein	Gliadin	p-value
bodyweight [g]	27.88	28.0	0.9469	28.6	28.1	0.8451
Δ bodyweight [g]	-3.1	-2.9	0.6331	-2.3	-2.3	0.9724
water intake [g]	1.4	1.3	0.8469	1.8	1.6	0.6976
food intake [g]	1.5	1.7	0.6264	1.7	1.4	0.6852
caloric intake [kcal]	5.3	6.3	0.5987	6.2	5.1	0.7086

Figure 4-5: 24-hour observation in metabolic cages revealed no significant differences.

Relative measurements within 24 hours of single mice in a metabolic cage of **(A)** relative body weight loss **(B)** relative water intake **(C)** relative food intake and **(D)** their relative caloric intake, all in relation to their initial body weight (BW) before the start and the absolute values depicted in **(E)** and changes regarding the parameters of **(A)** to **(D)**. **(F)** Macronutrient composition and the metabolizable energy (ME) provided by both experimental diets (GFD, GCD, compare section 3.1.4).

During the experiment, mice were individually housed in metabolic cages for 24 hours. The confinement in these cages, with limited nesting material and restricted food access, induced stress and resulted in weight loss. This weight loss cannot be directly compared to the normal 14-day experiment. **(A)**-**(E)** Unpaired t-test; n=5, data are means±SEM. Adapted from Keppeler *et al.*, 2024 [184].

4.3. Impact on Cardiac Function, mRNA Expression and Oxidative and Nitro-Oxidative Stress

In the investigation of the impact on cardiac function, mRNA expression, and oxidative and nitro-oxidative stress, the aim was to understand the general effects on the heart after a two-week gliadin treatment.

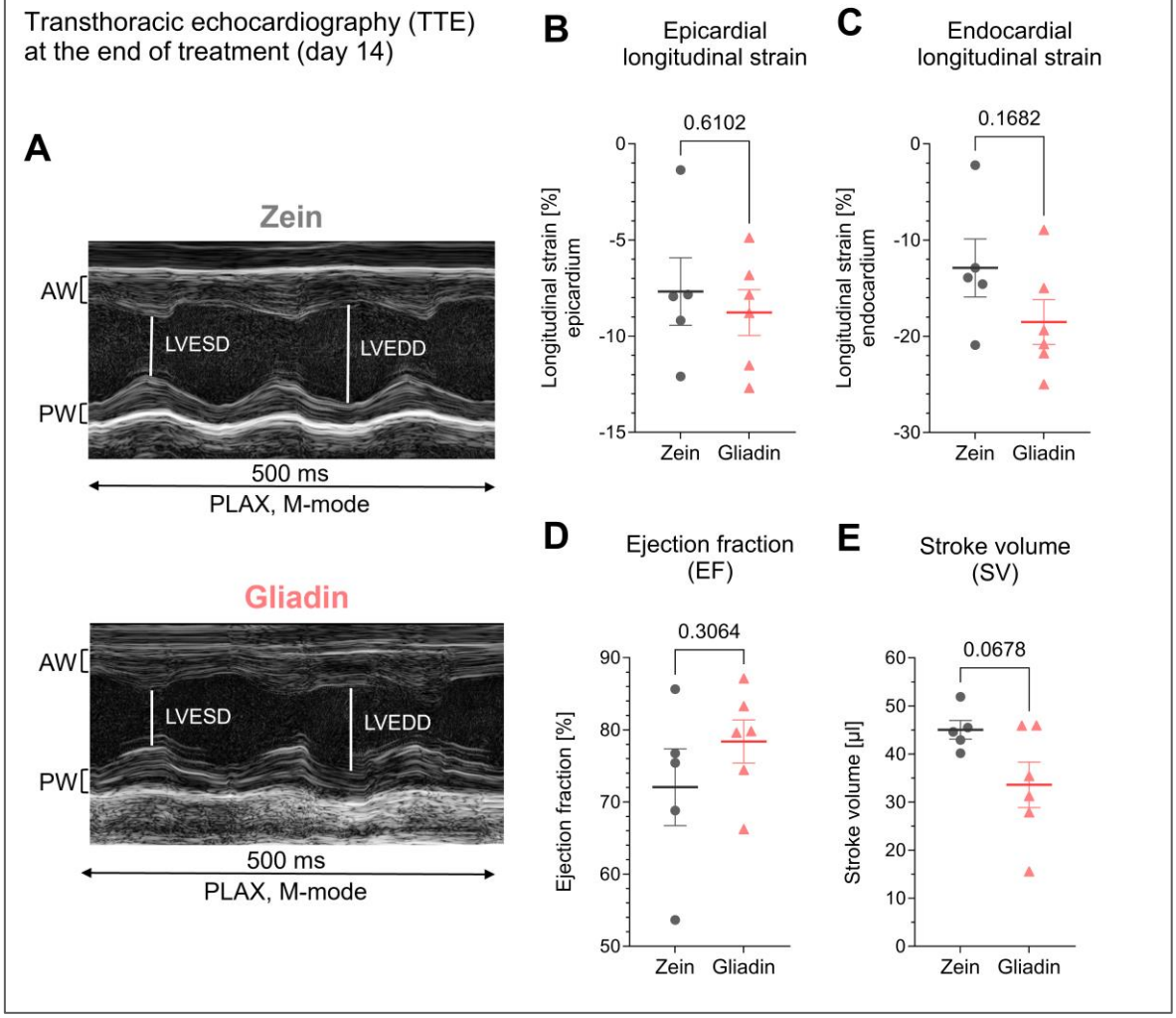

Figure 4-6: Effects of active murine CeD on cardiac function.

Analysis of transthoracic echocardiography (TTE) at day 14 of the treatment with **(A)** representative M-mode parasternal long axis (PLAX)-images with their left ventricular end-systolic (LVESD) and left ventricular end-diastolic diameter (LVEDD), as well as their anterior (AW) and posterior wall (PW) displayed **(B)** epicardial longitudinal strain and **(C)** endocardial longitudinal strain, **(D)** ejection fraction, **(E)** stroke volume (SV), (for additional parameters, s. **Table 4-1**). **(B)-(E)** Unpaired t-test; n(Z)=5, n(G)=6. Data are means±SEM. Adapted from Keppeler *et al.*, 2024 [184].

Cardiac assessments by transthoracic echocardiography (TTE) revealed that key parameters such as the longitudinal strain of the epicardium and endocardium, ejection fraction (EF), and stroke volume (SV) remained within normal ranges for both groups, as shown in **Figure 4-6 B-E**. However, trends indicated by TTE pointed to reduced diastolic volume (refer to Table 4-1), suggesting the potential beginning cardiac effects of the gliadin treatment.

Table 4-1: Table to Figure 4-6: Detailed cardiac functional parameters from TTE in NOD-DQ8 mice. Additional TTE data, comparing the zein-treated control group to the gliadin-treated group. Parameters include heart rate (HR), diameters, volumes, EF, fractional shortening, cardiac output (CO), and left ventricular mass and wall thicknesses. P-values indicate statistical comparisons between the two treatment groups with unpaired t-tests. Adapted from Keppeler *et al*., 2024 [184]. Abbreviations: LV – left ventricular, AW – anterior wall, PW – posterior wall.

Parameter	**Units**	Zein		Gliadin		**P-value**
Heart Rate (HR)	bpm	357.10	± 31.85	340.58	± 18.81	0.6525
Systolic Diameter	mm	2.25	± 0.22	1.77	± 0.21	0.1464
Diastolic Diameter	mm	3.83	± 0.1	3.24	± 0.24	0.0665
Systolic Volume	µl	18.47	± 4.9	10.50	± 2.99	0.1827
Diastolic Volume	µl	63.49	± 4.16	44.09	± 7.41	0.0597
Stroke Volume (SV)	µl	45.02	± 1.94	33.59	± 4.72	0.0678
Ejection Fraction (EF)	%	72.05	± 5.33	78.38	± 2.99	0.3064
Fractional Shortening	%	41.50	± 4.38	46.30	± 2.64	0.3545
Cardiac Output (CO)	ml/min	16.20	± 1.99	11.35	± 1.55	0.0821
LV Mass	mg	161.87	± 19.58	146.82	± 8.22	0.4684
LV Mass Cor	mg	129.49	± 15.66	117.46	± 6.58	0.4684
Systolic LVAW	mm	1.56	± 0.12	1.58	± 0.1	0.8726
Diastolic LVAW	mm	0.92	± 0.1	0.93	± 0.09	0.9455
Systolic LVPW	mm	1.60	± 0.13	1.90	± 0.11	0.0916
Diastolic LVPW	mm	1.17	± 0.19	1.43	± 0.13	0.2713

Gene expression experiments via qRT-PCR showed an increase in the transcript levels of *Vcam1* and *Cybb* (Nox2), within the left ventricular tissue, suggesting an upsurge in cardiac inflammation (**Figure 4-7 A-B**). This elevation in inflammatory markers was corroborated by increased ROS, as indicated by enhanced fluorescence in DHE-stained cardiac cryosections, and the presence of (nitro-)oxidative stress markers, specifically 4-HNE and 3-NT, in left ventricular tissue (**Figure 4-7 C-E**).

In detail, quantitative analysis showed a significant rise in these inflammatory and (nitro-) oxidative stress markers in the Gliadin group compared to controls, with *Vcam1* expression levels reaching 140.8% (p-value=0.0001, **Figure 4-7 A**), *Cybb* (Nox2) expression increasing to 167.1% (p-value=0.0018, **Figure 4-7 B**), DHE fluorescence climbing to 121.2% (p-value=0.0057, **Figure 4-7 C**), 4-HNE levels rising to 160% (p-value=0.0019, **Figure 4-7 D**), and 3-NT levels up to 139.7% (p-value=0.0387, **Figure 4-7 E**), all relative to the Zein group normalized to 100%.

Despite these indicators of increased inflammation and (nitro-)oxidative stress, cardiac function as measured by traditional TTE, did not show significant impairment, indicating a complex interplay between acute CeD and cardiac health that may not immediately affect cardiac performance but highlights underlying molecular changes.

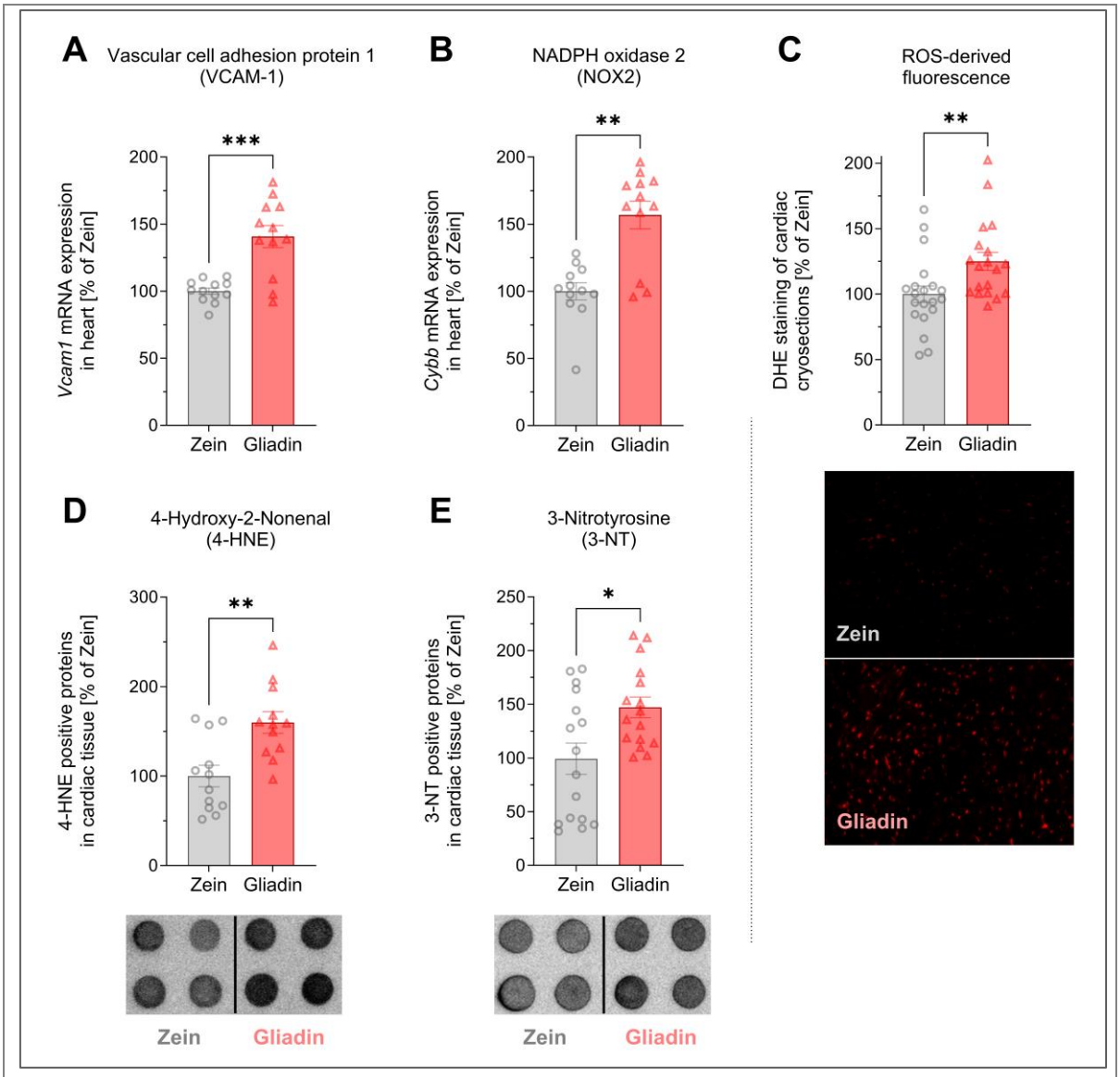

Figure 4-7: Effects of active CeD on cardiac gene expression and oxidative and nitro-oxidative stress.

(A) *Vcam1* and **(B)** *Cybb* (Nox2) mRNA expression were measured by qRT-PCR with cardiac left ventricular tissue. **(C)** ROS-formation was visualized by DHE-stainings of left ventricular cardiac cryosections, with exemplary photomicrographs (ROS=red fluorescence) shown below. **(D)** 4-HNE and **(E)** 3-NT positive proteins in cardiac tissue, with exemplary dot blot images shown below.

(A) Unpaired t-test; n=12, **(B)** Mann-Whitney test; n=12, **(C)** Mann-Whitney test; n(Z)=19, n(G)=20, **(D)** unpaired t-test; n=12, **(E)** Mann-Whitney test; n=16. Data are means±SEM. *p<0.05; **p<0.01; ***p<0.001. Adapted from Keppeler *et al.*, 2024 [184].

4.3.1. Impact on mRNA Expression in the Brain

Within the scope of this study, while the primary focus was not on neurological effects, an exploratory assessment of brain tissue revealed elevated levels of pro-inflammatory and oxidative stress markers in the brain following gliadin treatment. The brain tissue analysis was conducted solely through this method, with no other supporting neurological investigations, given the study's emphasis on other systemic effects.

Markers such as tumor necrosis factor-alpha (Tnfα), *Cybb* (Nox2), as well as *Nos1* (nNOS) and *Nos2* (iNOS) were found to be increased in the Gliadin group compared to controls (**Figure 4-8 A-D**). The rises in these markers align with patterns observed in other cardiovascular risk factors, such as noise and particulate matter, suggesting that gliadin's impact might extend to the brain's inflammatory state via the gut-to-brain axis, thus underscoring a possible systemic effect [215-217].

Quantitatively, *Tnfα* levels in the Gliadin group were elevated to 151.2% of control levels, with a p-value narrowly missing significance at 0.0528 (**Figure 4-8 A**). *Cybb* (Nox2) saw an increase to 150.4% of control, showing high significance (p-value<0.0001, **Figure 4-8 B**). *Nos2* (iNOS) levels were 123.0% of control, with statistical significance (p-value=0.0140, **Figure 4-8 C**), and *Nos1* (nNOS) increased to 119.5% of control, also significant (p-value=0.0358, **Figure 4-8 D**).

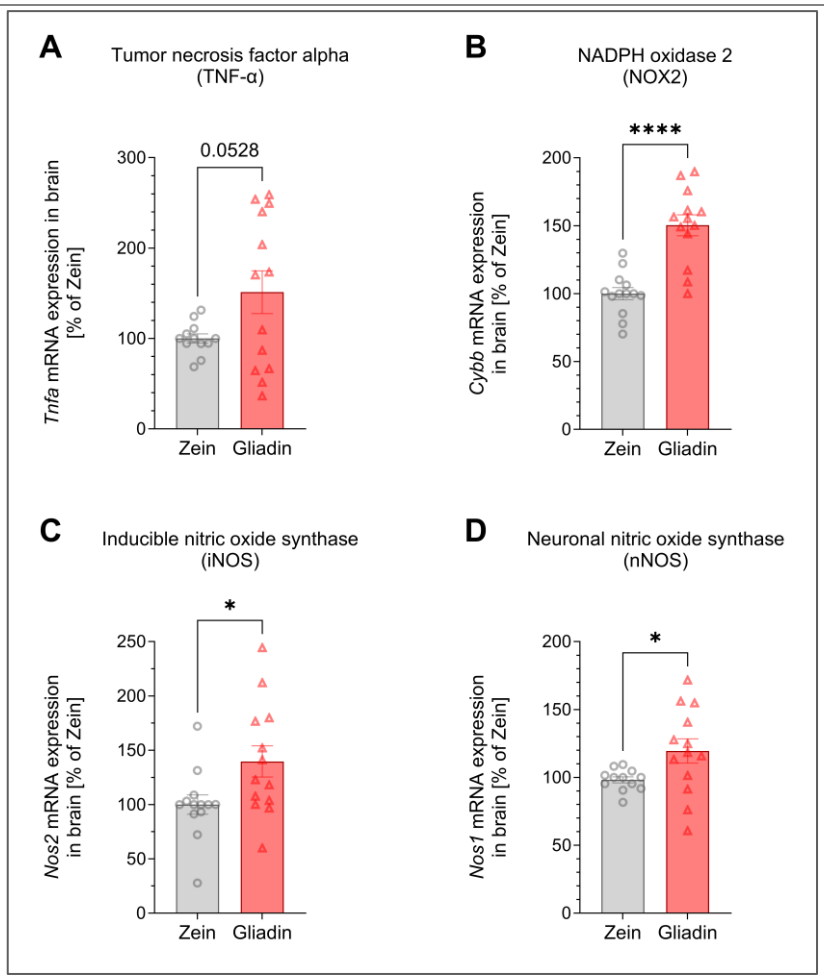

Figure 4-8: Transcript levels of pro-inflammatory markers in brain tissues.

mRNA expression of **(A)** Tumor necrosis factor α (*Tnfa*), **(B)** *Cybb* (Nox2), **(C)** *Nos2* (iNOS), and **(D)** *Nos1* (nNOS) mRNA expression was measured by qRT-PCR with brain tissue.

(A) Unpaired t-test; n(Z)=12, n(G)=13, **(B)** unpaired t-test; n= 13, **(C)** Mann-Whitney test; n=13, **(D)** unpaired t-test; n(Z)=12, n(G)=13. Data are means±SEM. *P<0.05; ****P<0.0001. Adapted from Keppeler *et al.*, 2024 [184].

4.4. Impact on Vascular Function, and Nitro-Oxidative Stress in Vascular and Blood

The treatment of NOD-DQ8 mice with gliadin, in contrast to zein-treated controls, led to significant impairments in vascular function. This was evidenced by isometric tension studies which showed a decrease in both endothelial-dependent relaxation, following acetylcholine (ACh) administration, and endothelial-independent relaxation, after nitroglycerin (GTN) application, within the Gliadin group. Although significant variances were noted in the contraction response to 25 mM potassium

chloride (KCl), the overall progression of response curves between the two groups did not diverge significantly, pointing to vascular impairment in the gliadin-treated mice.

Further investigations into oxidative stress responses unveiled an increased whole blood oxidative burst in the gliadin-treated mice following zymosan A (L-012) stimulation, indicating an upregulation of Nox2 in leukocytes. This was paralleled by a rise in plasma levels of nitrite and notably nitrate, suggesting increased immune cell activity, particularly of iNOS-expressing leukocytes, which together underscore the systemic impacts of gliadin treatment extending beyond gastrointestinal inflammation to influence vascular health.

In detail, the capacity for endothelial-dependent relaxation, as induced by ACh, was significantly reduced in gliadin-treated mice, dropping to 73.1% from a higher baseline of 84.3% observed in the zein control group. Similarly, the ability for endothelial-independent relaxation triggered by GTN also diminished, falling to 86.2% from 93.4% of the control group. When examining the contraction response to KCl at a concentration of 20mM, the gliadin-treated group exhibited an increased response rate of 33.4% compared to 25.6% in the control group, a difference marked by a notable p-value of 0.0005, although this did not suggest any functional disparities between the groups.

Additionally, the study measured plasma levels of nitrate and nitrite as indicators of oxidative stress. Nitrate levels in the plasma of gliadin-treated mice saw a notable increase, surging by 9.7 μM to reach 25.8 μM from the baseline of 16.1 μM in the control group (p-value=0.0315). Plasma nitrite levels experienced a similar rise, increasing by 0.13 μM to 0.31 μM from an initial 0.18 μM in the control group (p-value=0.0016). Furthermore, the oxidative burst measured at 60 minutes after stimulation revealed a significant uptick in the gliadin-treated group, reaching 1686 counts/s, a substantial increase from the 859 counts/s observed in the zein-treated control group.

Together, these outcomes highlight that gliadin treatment leads to vascular dysfunction and an elevation in oxidative and nitro-oxidative stress, affirming the systemic effects of gliadin and underlining the critical importance of vascular assessment in this study.

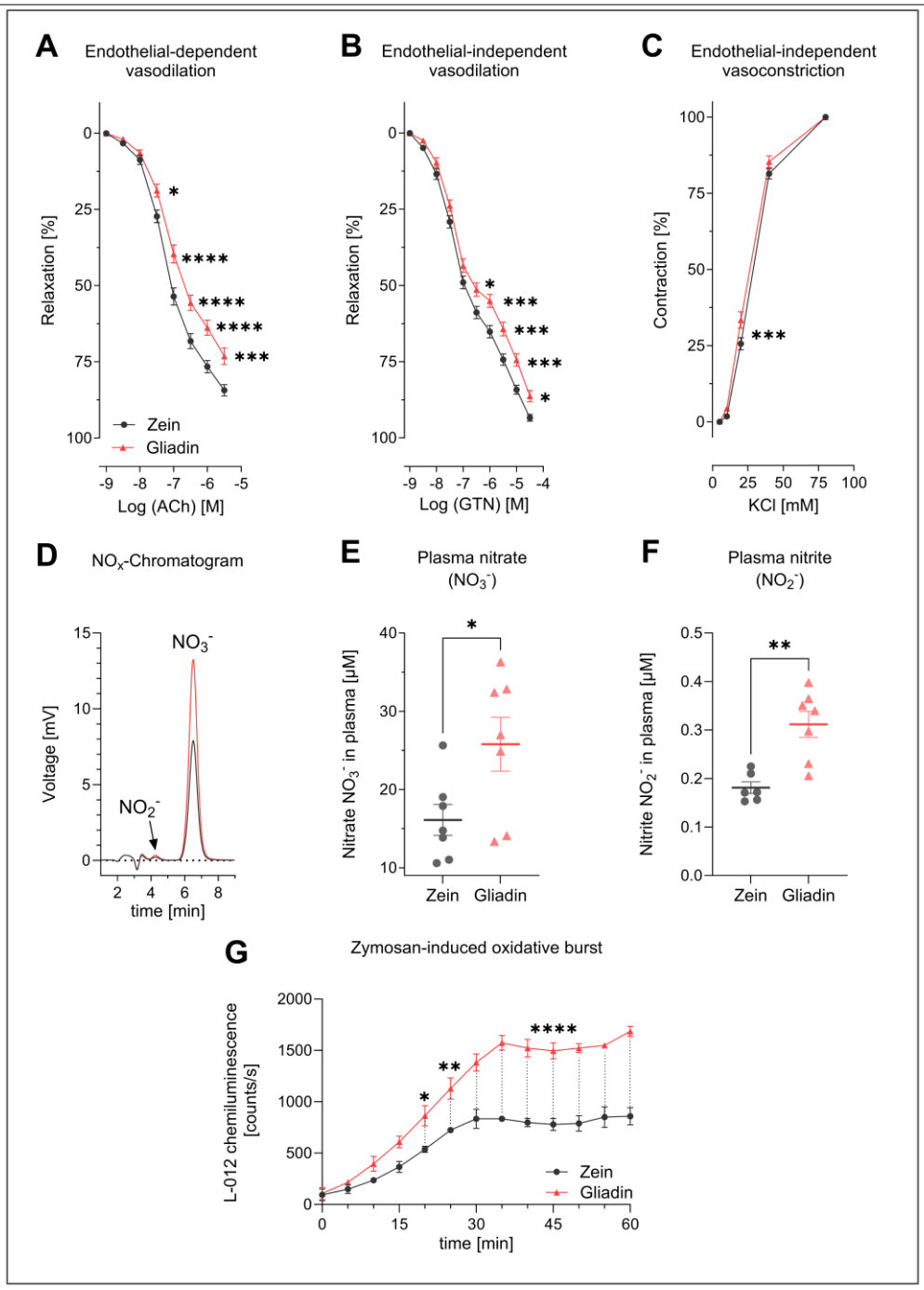

Figure 4-9: Impact of active CeD on both endothelial-dependent and -independent vascular function, as well as whole blood nitro-oxidative and oxidative stress.

Isometric tension studies of **(A)** Endothelium-dependent (ACh) and **(B)** -independent (GTN) relaxation and **(C)** contraction (KCl) of thoracic aorta rings. **(D)** Exemplary chromatograms of the HPLC analysis to detect **(E)** nitrate (NO_3^-) and **(F)** nitrite (NO_2^-) in plasma. **(G)** Time course of whole blood oxidative burst determined by L-012 ECL after zymosan A stimulation.

(A)-(C) Two-way ANOVA and Bonferroni multiple comparison test; n(Z)=30, n(G)=36, **(E)-(F)** unpaired t-test; n=7, **(G)** two-way ANOVA and Bonferroni multiple comparison test; n=2. Data are means±SEM. *p<0.05; **p<0.01; ***p<0.001; ****p<0.0001. Adapted from Keppeler *et al.*, 2024 [184].

When comparing the results normalized against the control group treated with zein, set as the baseline at 100%, there were notable increases in specific markers indicating changes in vascular stress responses. Protein-tyrosine nitration levels (3-NT), in the gliadin-treated group, were significantly elevated to 187.1%, as shown in **Figure 4-10 A** (p-value=0.0159), indicative of elevated superoxide/peroxynitrite levels. Additionally, DHE staining also showed a significant rise to 119.7% in the Gliadin group compared to the control (p-value=0.0108), as depicted in **Figure 4-10 B**, indicating a rise in ROS formation in the vasculature.

These observations collectively reveal the extensive effects of CeD on vascular health in mice, emphasizing the significant rise in both nitro-oxidative and oxidative stress markers in the vascular system due to gliadin exposure.

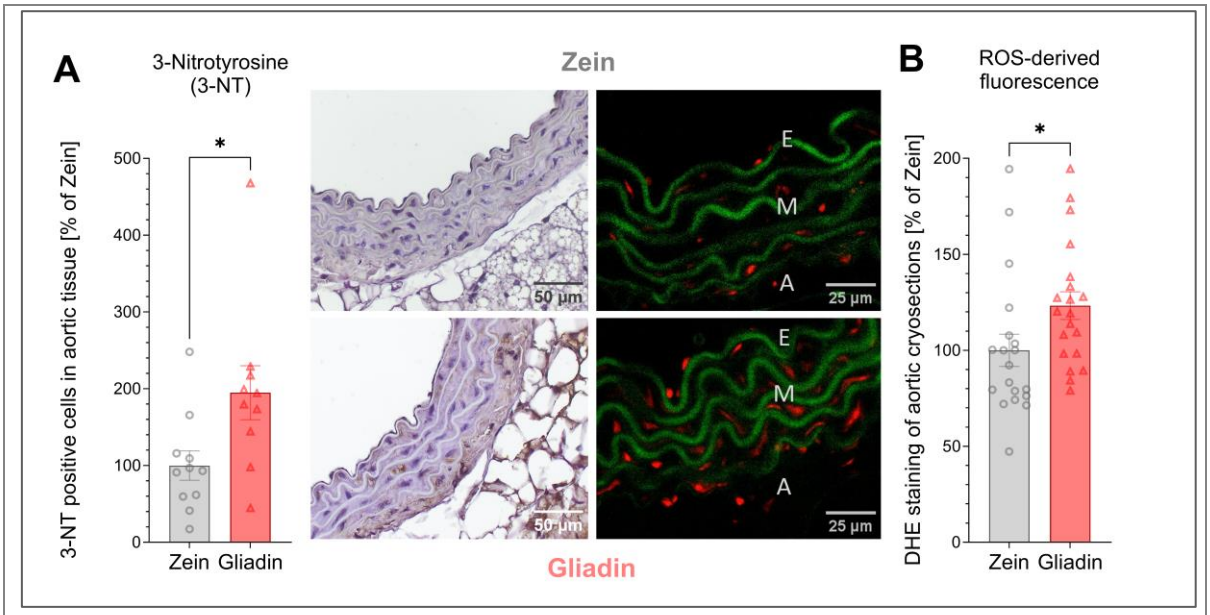

Figure 4-10: Impact of active CeD on vascular nitro-oxidative and oxidative stress .

(A) Densitometrical quantification of IHC of thoracic aortic rings for 3-NT positive proteins together with exemplary images on the right. **(B)** Aortic DHE-stained cryosections visualising ROS formation within the aortic wall, with exemplary photomicrographs shown on the left. Elastic lamina (green autofluorescence); ROS=red fluorescence; E-endothelium; M-tunica media; A-tunica adventitia.

(A) Mann-Whitney test; n(Z)=11, n(G)=10, **(B)** Mann-Whitney test; n(Z)=19, n(G)=20. Data are means±SEM. *p<0.05. Adapted from Keppeler *et al*., 2024 [184].

4.4.1. Comparison between PVAT vs. EWAT

Adipose tissue is increasingly recognized as a metabolically active organ, with perivascular adipose tissue (PVAT) attracting particular attention for its paracrine impact on adjacent vascular structures [218, 219]. This section sought to determine if PVAT, closely associated with the aorta, exhibits distinct characteristics compared to epididymal white adipose tissue (EWAT), potentially offering insights into the vascular inflammatory milieu. The focus was on assessing mRNA expression levels of leptin (Lep) and CD11b, markers potentially indicative of inflammatory and metabolic activity.

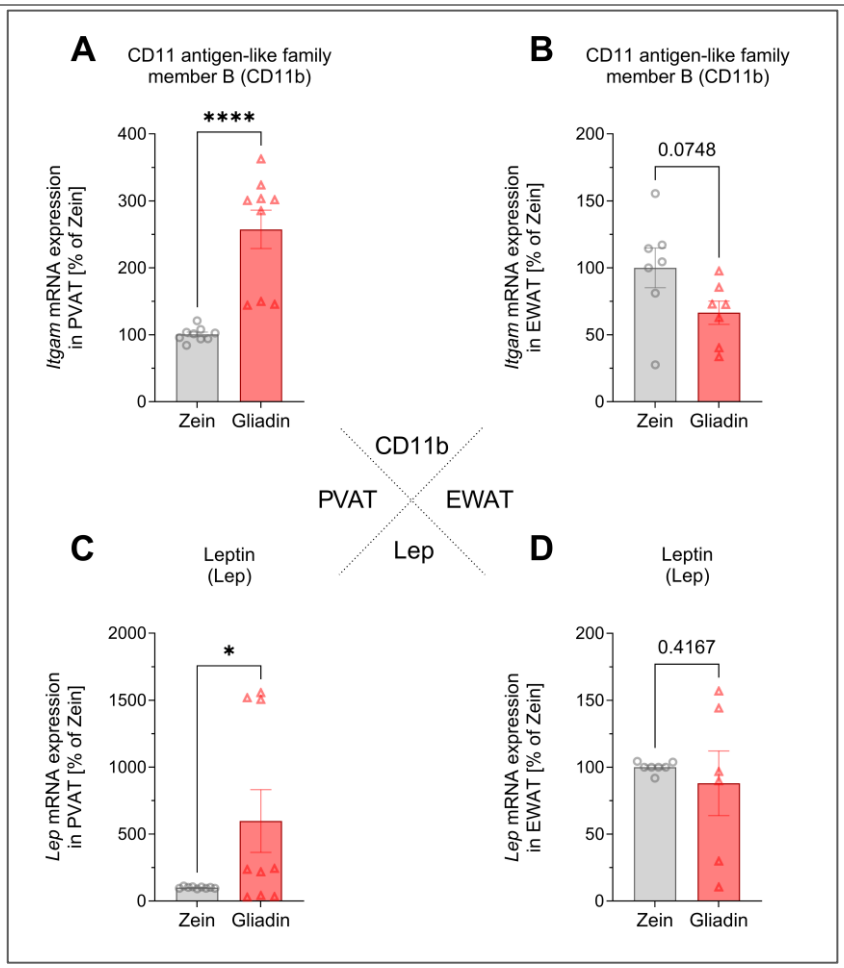

Figure 4-11 Comparison of mRNA expression of pro-inflammatory markers in PVAT and EWAT.

mRNA expression levels of **(A)** *Itgam* (CD11b) in PVAT compared to **(B)** EWAT. **(C)** *Lep* (Leptin) in PVAT compared to **(D)** EWAT. All were measured by qRT-PCR with the respective tissue.

(A) Mann-Whitney test; n=9, **(B)** unpaired t-test; n=7, **(C)** unpaired t-test; n=9, **(D)** Mann-Whitney test; n(Z)=7, n(G)=6. Data are means±SEM. *P<0.05; ****P<0.0001. Adapted from Keppeler *et al.*, 2024 [184].

Analysing the effects of gliadin treatment on adipose tissues, as depicted in **Figure 4-11 A-D**, reveals significant differential responses between PVAT and EWAT, normalized against the control Zein group set at 100%. CD11b mRNA expression in PVAT soared to 300.5% (p-value<0.0001), indicating a potential increase in inflammatory response or immune cell activity, whereas in EWAT, the slight decrease to 66.5% was not statistically significant, suggesting stable inflammation levels. Leptin mRNA expression in PVAT significantly jumped to 598.0%. In contrast, leptin expression in EWAT remained relatively unchanged at 93.3%, showing that EWAT's endocrine function was largely unaffected.

4.5. Aortic Immune Cell Infiltration and Inflammatory Transcript Expression

Statistically significant upregulation was observed in the mRNA expression of several key molecules integral to vascular inflammation and immune response.

In detail, normalized against the control Zein group, established at a baseline of 100%, the analysis showed *VCAM1* mRNA levels upregulated to 164.2%, indicating enhanced vascular cell adhesion potentially facilitating immune cell migration (p-value=0.006, **Figure 4-12 A**). *Nos2* (iNOS) mRNA expression also saw a notable increase to 232.2%, pointing to a rise in NO production, critical in the inflammatory process (p-value=0.007, **Figure 4-12 B**). Moreover, *Tnfα* mRNA levels rose to 211.2% (p-value=0.0006, **Figure 4-12 C**).

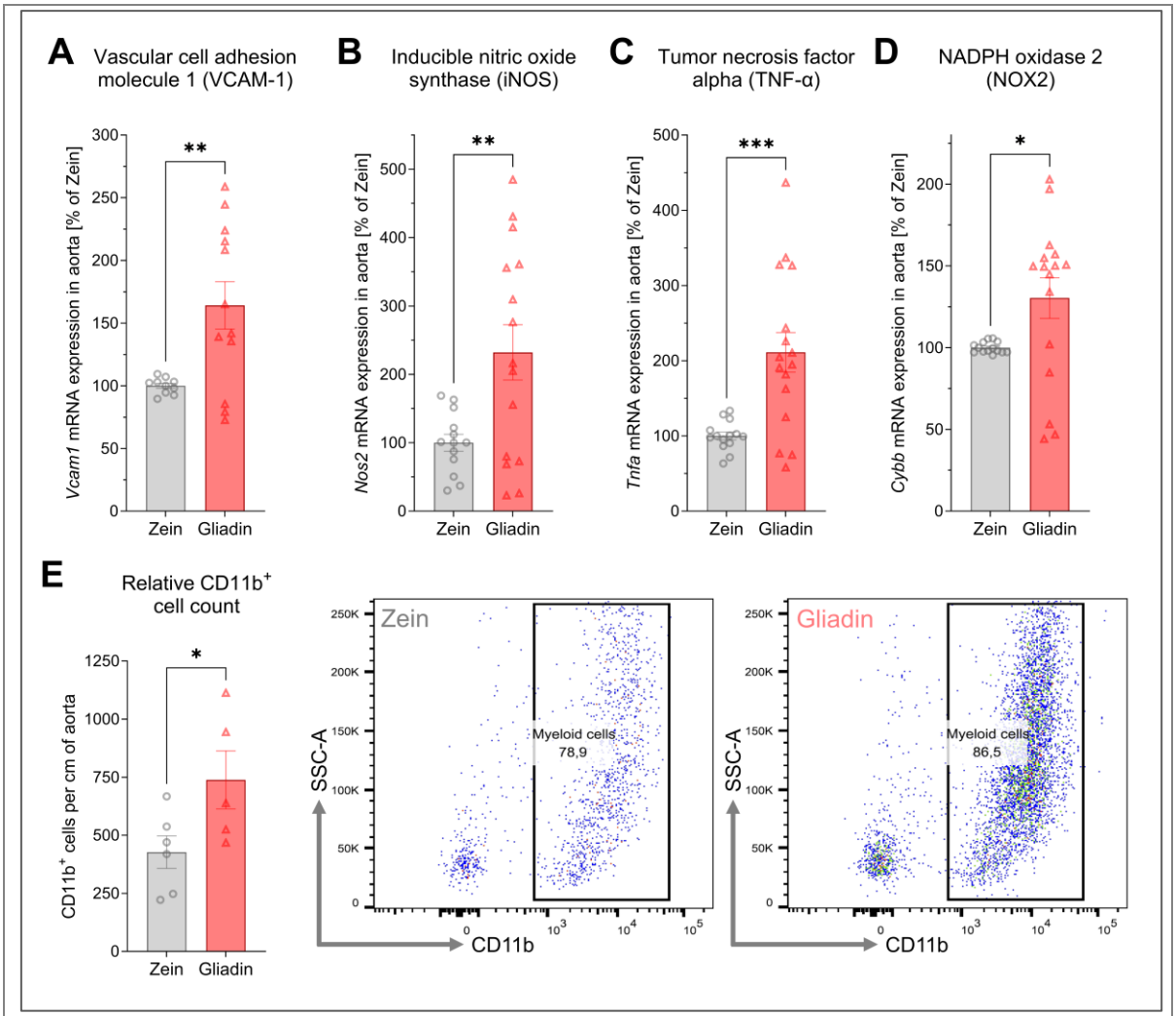

Figure 4-12: Active celiac disease (CeD) promotes the infiltration of immune cells into the aorta and the expression of inflammatory transcripts.

(A) *Vcam1*, **(B)** *Nos2* (iNOS), **(C)** *Tnfα*, and **(D)** *Cybb* (Nox2) mRNA measured by qRT-PCR in aortic tissue. **(E)** Flow cytometry of aortic single-cell suspensions showed CD11b⁺ myeloid cells (per cm) within the aortic wall (CD11b marker against side scatter area (SSC-A)), with exemplary original plots shown on the right.

(A) Unpaired t-test; n(Z)=10, n(G)=12, **(B)** unpaired t-test; n(Z)=13, n(G)=15, **(C)** unpaired t-test; n(Z)=14, n(G)=16, **(D)** Mann-Whitney test; n(Z)=14, n(G)=16, **(E)** unpaired t-test; n(Z)=6, n(G)=5. Data are means±SEM. *P<0.05; **P<0.01; ***P<0.001. Adapted from Keppeler *et al*., 2024 [184].

Additionally, *Cybb* (Nox2) mRNA expression was elevated to 149.7%, indicative of an augmented generation of ROS, contributing to oxidative stress (p-value=0.0308, **Figure 4-12 D**). Complementary to these molecular findings, flow cytometry analysis quantified a significant rise in the infiltration of CD11b⁺ myeloid cells within the aortic wall, from 427.2 cells/cm in the control to 738.2 cells/cm in the Gliadin group, demonstrating a pronounced immune presence (p-value=0.0487, **Figure 4-12 E**).

These comprehensive results highlight the extensive systemic inflammatory response elicited by gliadin treatment, characterised by significant upregulation of key inflammatory markers and enhanced immune cell infiltration.

4.6. Remission-Study: After 14 Days of Recovery on GFD

Following a two-week dietary intervention with either a gluten-containing diet (GCD) or a gluten-free control diet (GFD), mice were subsequently given an additional 14 days on a GFD to assess potential recovery effects in the group previously fed with gluten (referred to as the OFF-study, illustrated in **Figure 4-13 A**; for comparison, s. ON-study in **Figure 4-1**).

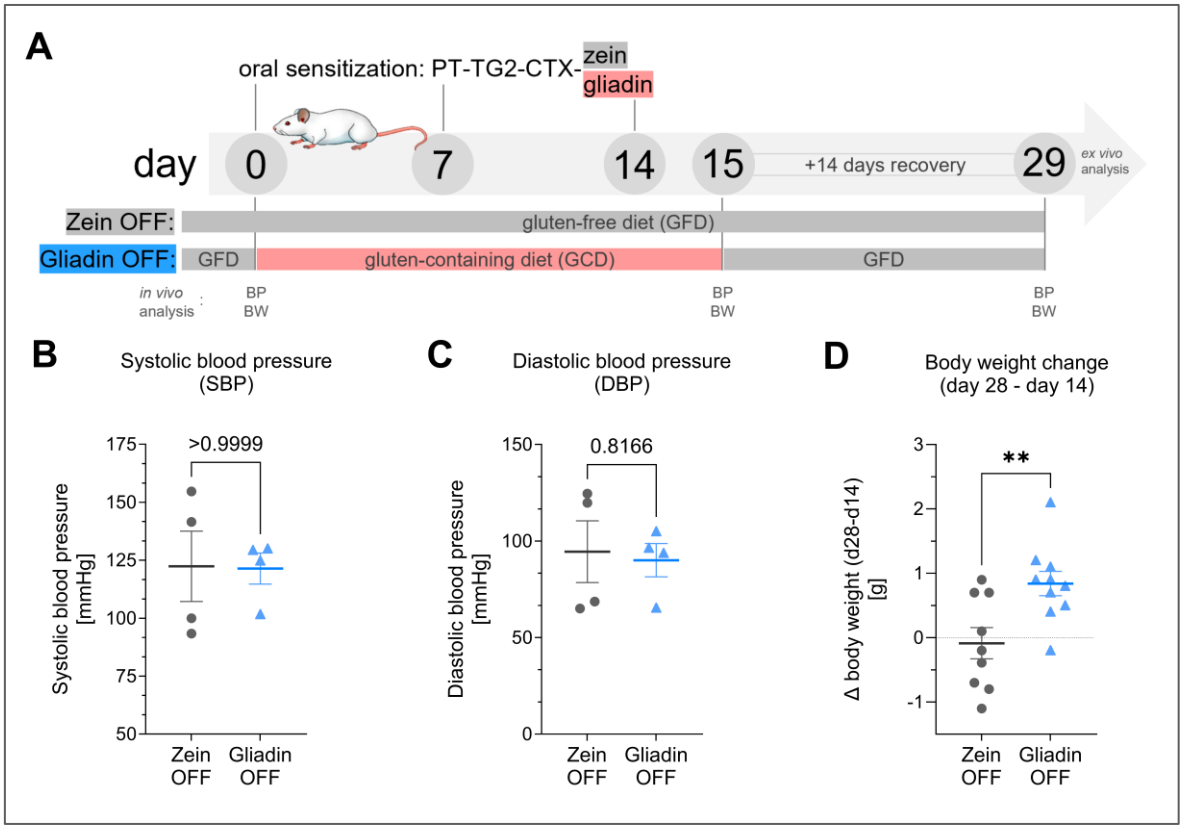

Figure 4-13: Remission of CeD after 14 days on a GFD recovers cardiovascular phenotype.

(A) OFF-study treatment scheme; 14 days of recovery on GFD following the ON-study treatment (compare **Figure 4-1**). **(B)** Systolic and **(C)** diastolic BP were measured by NIBP on day 28. **(D)** Body weight changes within 14 days of recovery (day 28 – day 14).

(B) Mann-Whitney test; n=4, **(C)** unpaired t-test; n=4, **(D)** unpaired t-test; n(Z)=9, n(G)=10. Data are means±SEM. **p<0.01. Adapted from Keppeler *et al.*, 2024 [184].

At the end of this period, measurements indicated no significant difference in systolic and diastolic BP between the groups (**Figure 4-13 B-C**, for BP comparison, s. **Figure 4-4 A-B**). Furthermore, the initially reduced weight gain observed in the gluten group was reversed following the dietary switch back to GFD, indicating a recovery from the gluten-induced effects (**Figure 4-13 D**, for initial weight change, s. **Figure 4-4 D**).

In detail, results at the end of the OFF-study showed systolic BP readings of 120.8 mmHg for the Zein group and 127.0 mmHg for the formerly gluten-fed group (p-value>0.9999, **Figure 4-13 B**). Diastolic BP levels were 94.5 mmHg for zein and 90.1 mmHg for the formerly gluten group, which seemed comparable (**Figure 4-13 C**, p-value=0.8166). However, the delta in body weight significantly differed, with the Zein group showing a slight decrease (-0.1 g) and the formerly gluten group gaining weight (0.8 g), highlighting more than a recovery in weight gain (p-value=0.0073, **Figure 4-13 D**).

Following the dietary switch, the improvement observed extended beyond weight recovery to encompass vascular functions and oxidative stress levels. This notable return to baseline conditions was evident in endothelial-independent relaxation responses to GTN and endothelial-dependent responses to ACh (ACh: 86.4% in Zein vs. 81% in Gliadin, p-value=0.6326, **Figure 4-14 A**; GTN: 93.2% in Zein vs. 89.8% in Gliadin, p-value=0.9231, **Figure 4-14 B**). Additionally, plasma levels of nitrite ($NO2^-$) and nitrate ($NO3^-$), along with oxidative stress markers indicated by DHE staining in aortic cryosections, all reverted to levels observed in control mice (**Figure 4-14 A-H**). Such findings underscore the body's ability to recover from gluten-induced disruptions, with a comprehensive restoration of endothelial function, body weight, and reduction in nitro-oxidative stress within the vasculature, all achieved within two weeks of returning to a GFD.

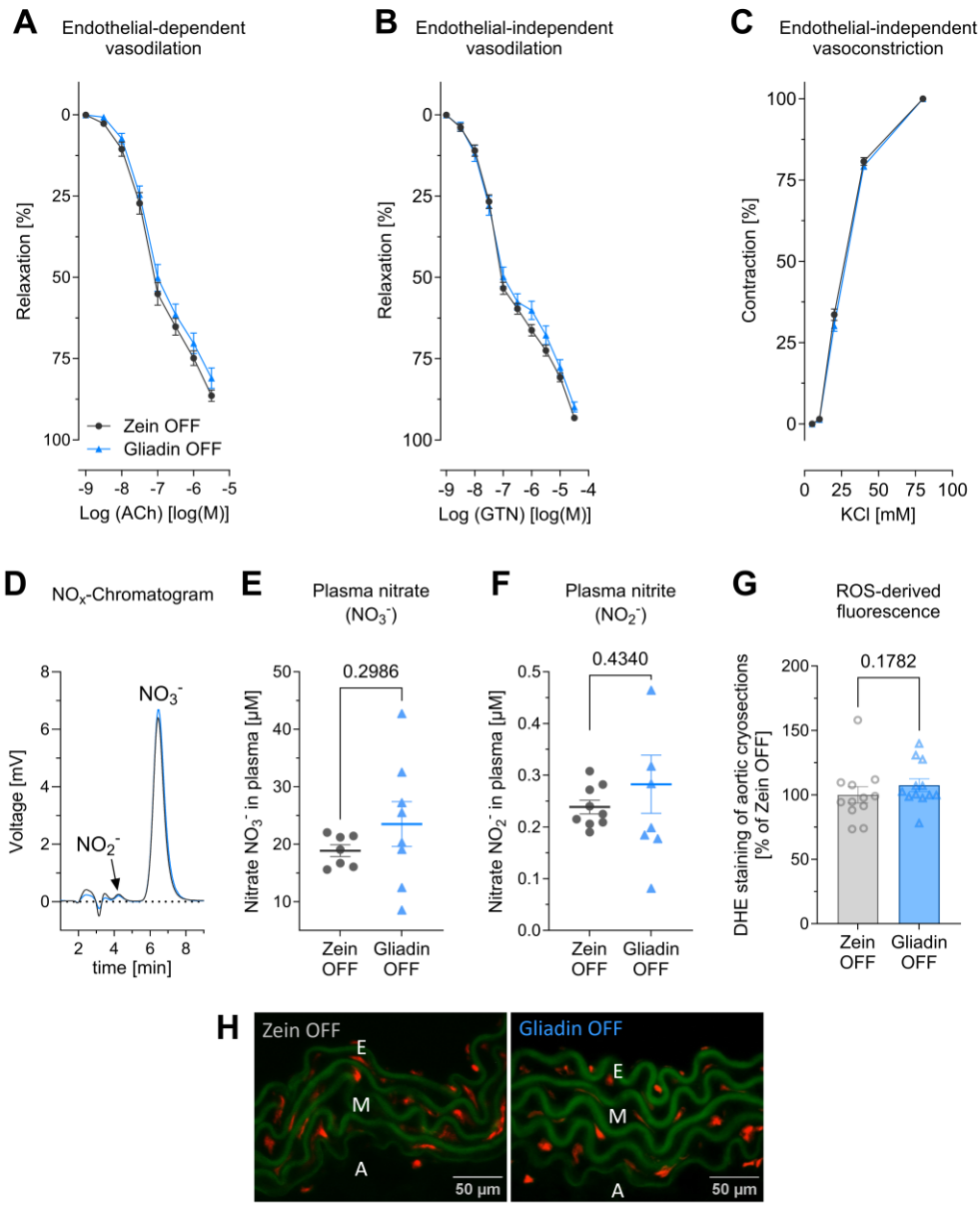

Figure 4-14: Remission of CeD after 14 days on a GFD restores the normal cardiovascular phenotype.

(A) Endothelium-dependent (ACh) relaxation,**(B)** endothelium-independent (GTN) relaxation, and **(C)** constriction (KCl). **(D)** Representative chromatograms of high-performance liquid chromatography (HPLC) analysis to detect **(E)** nitrate ($NO3^-$) and **(F)** nitrite ($NO2^-$) in plasma. **(G)** Aortic cryosections stained with DHE were used to detect ROS in the vascular wall. **(H)** Exemplary photomicrographs are shown below the densitometrical analysis. Elastic lamina (green autofluorescence); ROS-formation (red fluorescence; E-endothelium; M-tunica media; A-tunica adventitia).

(A)-(C) Two-way ANOVA and Bonferroni multiple comparison test; n=12, **(E)-(F)** unpaired t-test; n(Z,OFF)=7, n(G,OFF)=8, **(H)** Mann-Whitney test; n=12. Data are means±SEM. Adapted from Keppeler *et al.*, 2024 [184].

4.7. Impact on inflammatory Biomarkers revealed via Plasma Proteomics

The Olink plasma proteomics analysis aimed to identify potential plasma biomarkers that could elucidate the mechanisms through which intestinal inflammation induced by gluten exposure transitions into vascular inflammation. A significant finding from this study was the upregulation of IL-17A in mice on a GCD compared to controls, suggesting a systemic inflammatory response that could bridge intestinal and vascular inflammation. The volcano plot from the proteomics data, along with a detailed table, presents IL-17A as the most notably upregulated protein, with other proteins such as IL10, Fas, Dlk1, and CCL5 also showing increased levels, albeit to a lesser extent (**Figure 4-15 A-B**; for a detailed proteomics overview, s. Appendix **Table 5-1**). Conversely, proteins such as Notch3, Lpl, and Casp3 were found at reduced levels in the gluten-fed group. None of these changes were statistically significant.

To further verify these findings, a mouse IL-17A ELISA confirmed the significant elevation of plasma IL-17A in gluten-fed NOD-DQ8 mice, highlighting its potential role in mediating the observed systemic inflammatory response (**Figure 4-15 C**). Baseline IL-17A levels in control mice were at 45.8, which rose significantly to 81.8 in Gliadin ON mice. Following a switch back to a gluten-free diet (Gliadin OFF), IL-17A levels decreased to 61.2, indicating partial mitigation of the inflammatory response. Statistical analyses underscored a significant difference between the control and Gliadin ON groups (p-value=0.0273), whereas the reduction from Gliadin ON to OFF did not reach statistical significance (p-value=0.2718). This pattern suggests that the inflammatory effects initiated by gluten exposure are partially reversible.

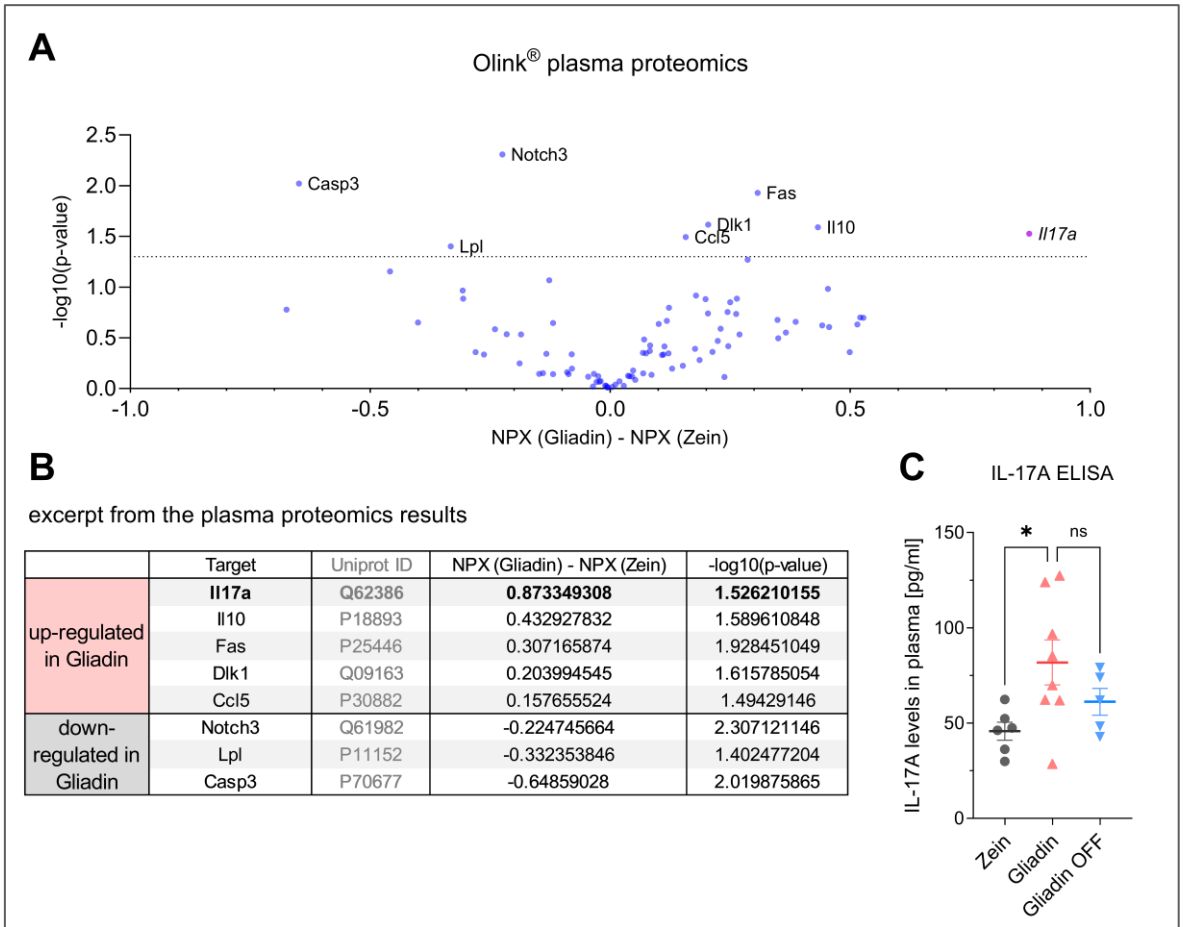

	Target	Uniprot ID	NPX (Gliadin) - NPX (Zein)	-log10(p-value)
up-regulated in Gliadin	**Il17a**	Q62386	**0.873349308**	**1.526210155**
	Il10	P18893	0.432927832	1.589610848
	Fas	P25446	0.307165874	1.928451049
	Dlk1	Q09163	0.203994545	1.615785054
	Ccl5	P30882	0.157655524	1.49429146
down-regulated in Gliadin	Notch3	Q61982	-0.224745664	2.307121146
	Lpl	P11152	-0.332353846	1.402477204
	Casp3	P70677	-0.64859028	2.019875865

Figure 4-15: Plasma proteomics suggests that IL-17A links intestinal and vascular inflammation.

(A) Volcano plot of Olink plasma proteomics showing the targets closest to statistical significance (-log10(p-value)>1.3), also detailed in the **(B)** table below with the normalised protein expression (NPX). **(C)** Plasma levels of IL-17A after 14 days of zein and gliadin treatment and after 14 days of remission (ns, p-value=0.2717).

(A/B) Unpaired t-test; n(Z)=11, n(G)=13, **(C)** one-way ANOVA and Dunnett's comparison test; n(Z)=6, n(G)=8; n(G,OFF)=5. Data are means±SEM. *p<0.05. Adapted from Keppeler *et al.*, 2024 [184].

5. Discussion

In this thesis, a CeD model in NOD-DQ8 mice was employed to investigate the effects of gliadin treatment both within the intestine and systemically, especially examining its influence on cardiovascular health. The examination of the small intestine revealed a significant increase in the expression of inflammatory cytokines, immune cell infiltration into the lamina propria, crypt hyperplasia and a reduction in VH:CrD ratio. This confirmed the successful induction of CeD in the model.

Beyond the intestinal impact, systemic parameters were investigated, revealing notable alterations induced by gliadin treatment. These included elevated systolic and diastolic BPs, reduction in weight gain, and a notable rise in serum total cholesterol, underscoring the widespread systemic nature of CeD development. The metabolic cage experiments confirmed these systemic effects were not attributable to dietary intake differences, while equivalent diet composition ensured that nutritional variances did not influence the observed physiological impacts.

Echocardiography indicated that the CeD induction did not significantly impair cardiac function despite evidence of increased inflammation and oxidative and nitro-oxidative stress within the heart. These cardiac observations were paramount, especially considering the potential for spontaneous myocarditis associated with the NOD-DQ8 genotype, which was ruled out to attribute observed changes directly to gliadin treatment.

Further, semi-quantitative IHC (3-NT staining) and DHE-staining (a surrogate parameter of ROS formation) of the aortic wall highlighted enhanced oxidative and nitro-oxidative stress, contributing to the vascular dysfunction observed in gliadin-treated mice. This endothelial-dependent and independent dysfunction primarily affects relaxation rather than contraction. Additionally, significant increases in various (pro-)inflammatory and oxidative stress markers, along with myeloid immune cell infiltration, underscore the adverse effects of CeD on vascular health. These effects are revealed through the exploration of aortic endothelial function and oxidative stress responses in blood. Adipose tissue analysis between PVAT and EWAT revealed differential involvement in response to gliadin treatment, suggesting that the pro-inflammatory environment in the vasculature influences PVAT. This interplay further contributes to an overall pro-inflammatory environment in the

vascular systems and their surroundings. Following this and a general systemic pro-inflammatory state the brain tissue showed evidence of increased inflammatory gene expression.

Concluding the findings, the Olink plasma proteomics analysis suggested IL-17A among other proteins as key mediators potentially linking intestinal inflammation to vascular and systemic effects. However, none of the targets reached statistical significance. This was reinforced by ELISA results confirming IL-17A upregulation in gliadin-treated mice, with a partial reversal observed after returning to a GFD, suggesting the reversible nature of gliadin-induced systemic and vascular changes.

To further assess the reversibility, mice were switched to GFD for an additional 14 days. The results showed no significant differences in BP compared to the control group. Weight gain in the gluten-fed group normalized after switching to GFD. Vascular functions and oxidative stress levels also improved, with endothelial relaxation responses and oxidative stress markers returning to baseline. These findings highlight the body's ability to recover from the CeD-induced disruptions within two weeks on a GFD.

A summary of the systemic and vascular effects observed during gliadin treatment in the ON study, incorporating current knowledge on CeD onset (s. Section 1.2.3), is illustrated in the central scheme (s. **Figure 5-1** and **Figure 5-2**), providing a visual representation of the key findings discussed above. The upcoming sections will delve deeper into these findings. The next section will further explore the clinical implications and comparative effects of gliadin on the small intestine, systemic health, and the cardiovascular system. Following that, the discussion will focus on the mechanisms through which systemic inflammation propagates to the cardiovascular system. Finally, insights into the chosen murine model, as well as the limitations of the study and suggestions for alternative approaches for future research will be provided.

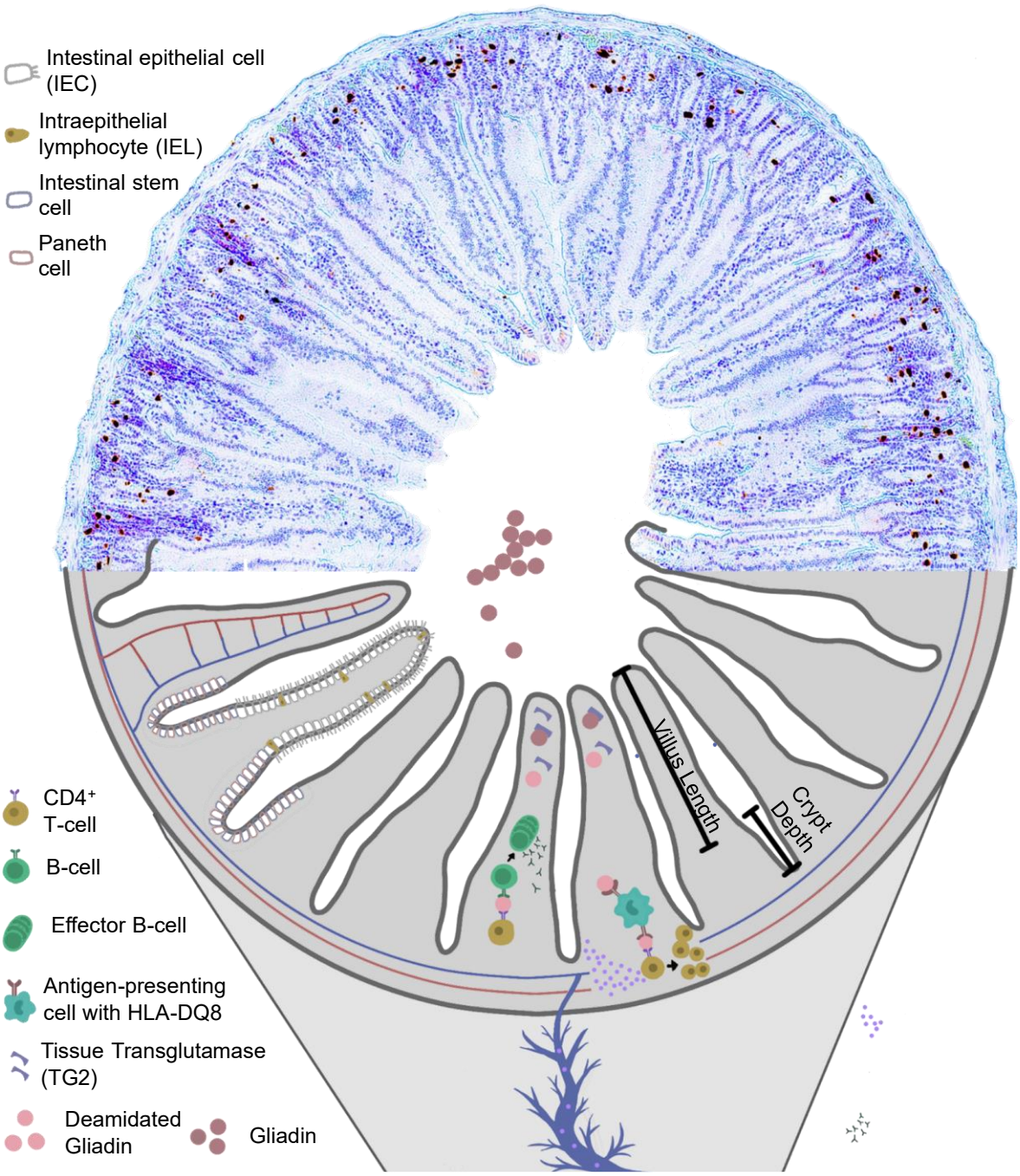

Figure 5-1: Central Scheme, part 1: This illustrates the pathophysiological process triggered by CeD. Gluten, containing indigestible gliadin, is absorbed in the duodenum. In the lamina propria, gliadin undergoes deamidation, enabling it to bind to DQ8 antigens on APCs, which initiates an immune response involving T and B cells. This immune activation can result in intestinal modifications such as villous atrophy, crypt hyperplasia, and intraepithelial lymphocytosis. We identified signs of intestinal inflammation, a reduced VH:CrD ratio, and an upregulation of pro-inflammatory cytokines. While no immediate cardiac dysfunction was observed, there was a noted increase in systolic and diastolic BP, markers of lipid peroxidation, and nitro-oxidative stress. Consumption of gliadin also negatively impacted vascular function, leading to enhanced vascular nitro-oxidative stress. Additionally, there was an increase in oxidative burst, nitrate, and nitrite levels, along with elevated IL-17A plasma levels. These findings highlight the systemic effects of active CeD on oxidative stress and the body's inflammatory state.

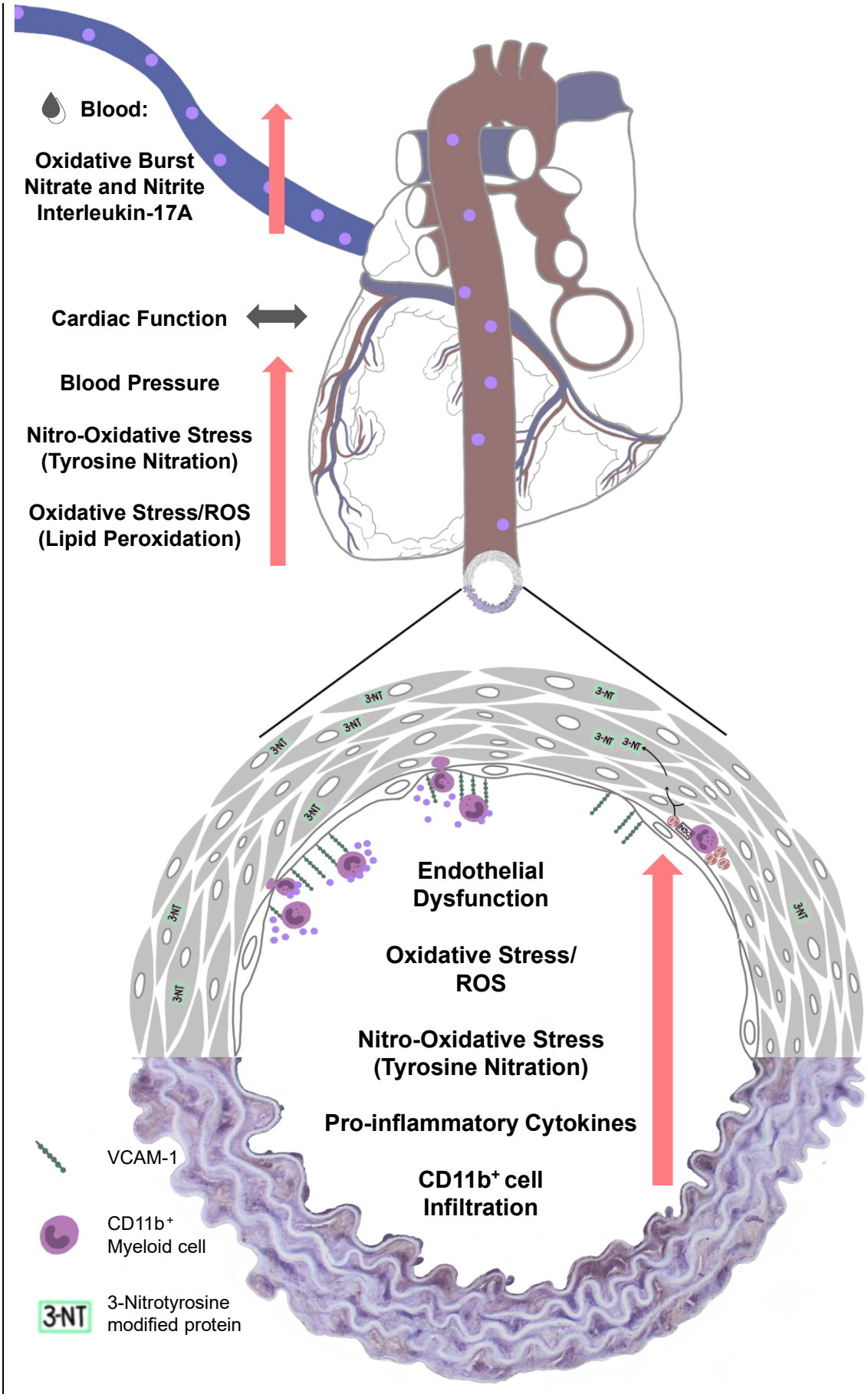

Figure 5-2: Central Scheme, part 2, for description s. **Figure 5-1** (part 1 on the previous page).

5.1. Clinical Correlation and Comparative Analysis of Gliadin-Induced Effects on the Small Intestine, Systemic Health, and Cardiovascular System

In this thesis, a CeD model using NOD-DQ8 mice was employed to investigate the effects of gliadin treatment within the intestine and systemically, focusing on cardiovascular health. While some measured effects have been extensively studied in clinical settings, this chapter aims to contextualise the preclinical results within a broader clinical framework.

The preclinical model demonstrated that gliadin treatment significantly increased inflammatory cytokine expression and lamina propria immune cell infiltration, notably IELs. A crucial finding was the reduction in the VH:CrD ratio, a hallmark of intestinal damage in CeD. Interestingly, despite these inflammatory changes, no significant difference in VH was observed between the gliadin-treated group and the control group. This suggests that the most severe form of villous atrophy when CeD is usually diagnosed in patients, is not present in this model at least not after two weeks of treatment. However, the gliadin-treated group exhibited a significant increase in CrD, indicating upregulated cell proliferation as a compensatory response to inflammation.

This mirrors the crypt hyperplasia observed in human CeD, where the intestine attempts to repair itself in response to gluten-induced damage. The Marsh score is a clinical tool used to assess the extent of gluten-induced intestinal damage. Recognizing the limitations of applying this clinical score directly to murine models, the observed histological changes, specifically hyperplastic crypts without villous atrophy, may tentatively be classified as Marsh class 2. According to the Oslo classification, this can be interpreted as subclinical, symptomatic, or classical CeD [220-223].

The development of anti-TG2 antibodies is a crucial indicator in the diagnosis and progression of CeD. These antibodies are often the first-choice diagnostic tool due to the invasiveness of biopsy sampling for duodenal histological assessment. Here, anti-TG2 antibodies were not detectable (data not shown) after two weeks of treatment, which was likely due to the short timeframe being insufficient for NOD-DQ8 mice to mount a specific antibody response following initial exposure to

(deamidated) gliadin. Various pre-clinical studies have shown that anti-TG2 antibodies typically become detectable after prolonged gluten exposure in genetically predisposed mice. DR3-DQ2 transgenic mice developed anti-TG2 antibodies approximately 7–8 weeks after starting a gluten-containing diet, with prior immune sensitization also achieved through pepsin-trypsin-digested gliadin and cholera toxin administration [224]. Similarly, HLA-DQ8 mice treated with indomethacin demonstrated significant serum levels of anti-TG2 antibodies after 30 days of gluten exposure, but not after 10 days. Therefore, longer studies are essential to comprehensively understand the dynamics of antibody production and persistence in CeD. Short-term studies, like this are insufficient to capture the full scope of the immune response and the progression of autoimmune markers and instead focus on early disease development [225, 226].

While pre-clinical models provide valuable insights under controlled conditions, translating these findings to clinical practice presents unique challenges. Clinical data, and nutritional studies in particular, face common challenges with CeD patients due to the time-sensitive nature of key data points, such as the time point of diagnosis relative to study inclusion and the initiation of gluten restriction, as well as adherence to the GFD and its quality. Too early implementation of gluten restrictions before proper diagnosis often complicates clinical practice. While it is ideal for cohorts to be as homogeneous as possible, the reality is often complex and influenced by numerous contributing factors, making the standardization seen in pre-clinical settings difficult to achieve in clinical practice. Additionally, the clinical presentation of CeD is highly variable among patients regarding intestinal and extra-intestinal symptoms, indicating significant individual differences that complicate the ability to draw uniform conclusions [159, 168].

Beyond gastrointestinal symptoms, CeD can also impact systemic parameters. Systemic parameters such as BP and serum cholesterol levels were significantly altered by gliadin treatment compared to the control (s. section 4.2). Clinical studies have shown mixed results, with a tendency towards a lower prevalence of classical cardiovascular risk factors among CeD patients. This observation, previously discussed in section 1.3, partly motivated the initial assessments of cardiovascular risk in CeD patients [147].

This study showed increased systolic and diastolic BP levels after the initiation of CeD on GCD compared to the control mice, with the same levels observed in both groups after two weeks on GFD. Clinical studies have shown mixed results regarding BP levels in CeD patients, with most studies focusing on the changes after the switch to GFD. Therefore, there is limited data on hypertension in CeD patients.

Two clinical studies published in 2016 found statistically significant increases in BP: Stein *et al.* reported systolic BP levels of 116 vs. 125 mmHg, and Bayar *et al.* reported levels of 121 vs. 126 mmHg. According to the 2017 AHA Guidelines, these values are considered elevated but are not yet in the hypertensive range. Conversely, Conroy *et al.* reported lower systolic BP in CeD patients compared to controls, with both groups exhibiting stage 1 hypertension (138 vs. 136 mmHg) [167, 227-229].

The impact of the switch to a GFD on BP is somewhat clearer and has been addressed in a meta-analysis by Potter *et al.*. De Marchi *et al.* and Riezzo *et al.* reported no statistically significant change in BP after the initiation of a GFD, while Tortora *et al.* reported an increase in both systolic and diastolic BP (systolic; from 113 to 118 mmHg and diastolic; from 75 to 78 mmHg), with both being considered normal BP levels according to AHA [227, 230, 231].

Overall, there is no clear consensus regarding the prevalence of hypertension in CeD patients pre- and post-GFD. This inconsistency may be due to differences in study design, patient populations, and adherence to and quality of the GFD. Additionally, as previously discussed, the stage of disease in CeD patients during diagnosis and study inclusion is not comparable to the early stage of CeD achieved in the treatment of the mice. Therefore, the BP levels observed in clinical studies are likely not directly comparable to those seen in the experimental model.

This also applies to other systemic cardiovascular risk factors, such as plasma total cholesterol. Wolf *et al.* noted that blood lipoprotein profiles in mice differ significantly from those in humans, highlighting challenges in translating animal data to humans. In most clinical studies, an impairment and subsequent normalization of the lipid profile following a GFD in CeD patients has been reported. This dyslipidaemia, present before GFD, is characterised by hypocholesterolaemia, likely due to malabsorption as a consequence of duodenal destruction. Conversely, Cakir *et al.*

reported significantly higher plasma total cholesterol levels (85 vs. 175 mg/dL, p-value<0.001). This study also included subclinical patients classified as Marsh I to the CeD cohort, who exhibit less duodenal destruction. Furthermore, an association between the systemic immune inflammation index and newly diagnosed adult CeD has been observed, which may also be potentially linked to CVD [230, 232-237].

Regarding the observed experimental endothelial-dependent and independent dysfunction in gliadin-treated mice, there are several surrogate parameters for subclinical atherosclerosis, such as flow-mediated dilation (FMD), aortic stiffness, and carotid intima-media thickness (IMT), which have been investigated in various clinical studies. In the study by Sari *et al.*, FMD was found to be significantly lower in CeD patients compared to controls (10.61 ± 2.64% vs. 13.09 ± 2.9%, p-value=0.0003), while endothelium-independent vasodilation in the brachial artery before and after nitroglycerin administration showed only a trend toward significance (p-value=0.09 and 0.07, respectively). De Marchi *et al.* reported an increased baseline IMT in CeD patients (0.082 ± 0.011 vs. 0.058 ± 0.012 cm, p-value<0.005) and decreased endothelium-dependent dilation (9.3 ± 1.3 vs. 11.2 ± 1.2%, p-value<0.05) compared to controls, with noted improvement following gluten abstinence [153, 154, 229].

These parameters consistently indicate early atherogenesis in CeD patients before gluten abstinence. The literature on cardiovascular complications in CeD patients is not completely consistent yet and has already been introduced in section 1.3. The effects of continuous duodenal destruction and inflammation in cases of non-responsive or refractory CeD, or due to delayed diagnosis, have not been particularly investigated so far. In summary, most studies report that CeD, along with other systemic implications, influences cardiovascular health negatively. The interplay between chronic inflammation, immune responses, and nutritional deficiencies in CeD patients contributes to a complex cardiovascular risk profile. While a GFD generally offers substantial benefits in reducing cardiovascular risks over the long term. As demonstrated by the OFF-study (s. section 4.6), returning gliadin-treated mice to a GFD mostly reversed the systemic and vascular changes, including the previously discussed alterations of BP and endothelial function by gliadin treatment [147-168, 228, 229, 238-241]. Future therapeutic interventions

should also be evaluated for their effects on extra-intestinal manifestations, including cardiovascular risk.

The NOD-DQ8 CeD mouse model provided valuable insights into the cardiovascular effects of gliadin in CeD, mirroring several clinical findings. While limitations exist, such as the need for long-term studies and consideration of gender differences (s. section 5.4), the model serves as a relevant tool for studying early disease mechanisms and potential therapeutic interventions.

5.2. Mechanism of Systemic Inflammatory Response and Propagation to the Cardiovascular System

The impact of gliadin-induced inflammation extends beyond the small intestine, affecting systemic health and the cardiovascular system. This study highlights the need to further investigate the mechanisms underlying these effects, particularly how intestinal inflammation propagates to distant organs. Comparative analysis with other disease models has provided key insights into the broader systemic effects of gliadin exposure. However, the precise pathways through which gliadin-induced inflammation contributes to cardiovascular dysfunction remain partially understood, necessitating further research.

In the NOD-DQ8 mouse model of CeD, gliadin treatment induced significant intestinal inflammation, marked by increased cytokine expression, immune cell infiltration, and epithelial barrier dysfunction. At the molecular level, gliadin exposure in genetically susceptible individuals triggers an immune response involving both innate and adaptive pathways. A key factor in this process is the release of zonulin, which modulates tight junctions and increases intestinal permeability, commonly referred to as ‘leaky gut’. In this study, permeability was further increase by cholera toxin in the oral gavage, ensuring gliadin reached lamina propria efficiently. This allowed gliadin peptides and other luminal antigens to cross into the lamina propria, where they encountered APCs and initiated an immune response. This inflammation triggered the release of pro-inflammatory cytokines such as TNF-α, IL-1β, and IL-17A, and the activation of immune cells, including cytotoxic Th1 $CD4^+$ T cells, $CD68^+$ monocytes/macrophages, and $CD3^+$ IELs. The autoantigen tissue TG2 deamidates, increasing their immunogenicity and further stimulating the immune response (s. section 1.2.3) [128, 176, 242]. These cytokines and immune cells enter the

bloodstream, creating a systemic pro-inflammatory state that affects multiple organs, including the vasculature, PVAT, brain, and heart. The dissemination of cytokines and immune cells establishes a pro-inflammatory environment, contributing to the extra-intestinal manifestations of CeD. Clinical studies suggest that IL-17A plays a role in this inflammatory cascade, supporting its potential link between local intestinal immune activation and broader systemic consequences. Monteleone *et al.* reported elevated IL-17A expression in the duodenal mucosa of active CeD patients, suggesting that gliadin exposure induces its production. IL-17A was primarily produced by CD4+ and CD4+CD8+ T cells, with IL-21 acting as a key regulator, supporting a Th17-driven immune response in CeD. These findings align with the systemic inflammatory mechanisms described in this study, reinforcing the hypothesis that IL-17A links intestinal inflammation to systemic immune activation and potential vascular dysfunction [243]. Another often-discussed factor in this context is nutritional deficiencies due to malabsorption. Although gliadin-treated mice showed a trend towards reduced weight gain, this did not meet the criteria for Grade I - mild malnutrition according to Gomez's classification, which is defined as less than 90% of the body weight compared to controls. Therefore, the focus remains on inflammation rather than malnutrition [244].

Among the systemic cytokines released, IL-17A plays a crucial role in vascular inflammation in gliadin-treated mice. By activating NF-κB signalling, IL-17A increases VCAM-1 expression, promoting endothelial activation and facilitating immune cell recruitment. This inflammatory response enhances oxidative stress and impairs endothelial function, similar to mechanisms observed in autoimmune diseases such as psoriasis and RA, where IL-17A-driven inflammation is linked to increased cardiovascular risk. In this study, IL-17A expression was significantly elevated in duodenal tissue and plasma during gliadin treatment, decreasing upon gliadin withdrawal in the OFF-study. Elevated IL-17A levels also contributed to the recruitment of inflammatory cells, such as CD11b+ myeloid cells, CD8+ T cells, and γδ T cells, to the vascular subendothelium, further aggravating vascular dysfunction [245-247].

Infiltrating immune cells further worsen vascular dysfunction by increasing oxidative and nitro-oxidative stress. Superoxide production via Nox2 and subsequent peroxynitrite ($ONOO^-$) formation contribute to endothelial damage, impairing NO bioavailability and vascular relaxation. IL-17A has also been implicated in the

downregulation of eNOS via RhoA activation, further reducing endothelial NO production. Nitro-oxidative stress leads to DNA strand breaks, lipid peroxidation (4-HNE), and protein modifications via tyrosine nitration (3-NT), exacerbating vascular dysfunction. A comparable mechanism has been observed in type 1 diabetes (T1D), where tyrosine nitration of prostacyclin synthase reduces enzymatic activity, increases apoptosis, and enhances endothelial adhesion molecule expression—pathways that may similarly contribute to gliadin-induced vascular inflammation [248-254].

Beyond CeD, IL-17A plays a central role in autoimmune diseases with elevated cardiovascular risk. In psoriasis, chronic IL-17A-driven skin inflammation is associated with systemic endothelial dysfunction, contributing to an increased prevalence of hypertension and atherosclerosis. Similarly, in RA, IL-17A promotes vascular inflammation by enhancing monocyte and T cell recruitment to the endothelium, accelerating endothelial dysfunction and plaque formation. The role of IL-17A in atherogenesis remains complex. While IL-17A is widely recognized as a pro-inflammatory mediator, some studies suggest it may stabilize atherosclerotic plaques, preventing rupture and thrombosis. This dual role indicates that the impact of IL-17A may be context-dependent, influenced by disease stage and comorbidities. However, in chronic inflammatory diseases such as CeD, psoriasis, and RA, IL-17A's overall effect appears to be pro-atherogenic, contributing to systemic vascular dysfunction [243, 246, 247, 255, 256].

Finally, this leads to a general endothelial dysfunction, characterised by impaired vasodilation, and increased vascular stiffness. In the long run, these factors contribute to the development of CVD. The study observed that gliadin-treated mice exhibited elevated BP, which goes along with the potential vascular stiffness and impaired endothelial function. The pro-inflammatory environment also extends to other organs such as the brain and heart. In the heart, increased inflammation and oxidative stress can lead to impaired cardiac function, which was so far only mildly affected.

In the vascular tissue, oxidative stress could also promote the uncoupling of eNOS, producing superoxide instead of NO and further exacerbating endothelial dysfunction. After the 2 weeks of treatment, there was no evidence of an uncoupled eNOS, but the overall circumstances warranted attention. Another potential

mechanism involving IL-17A on the other hand could be the downregulation of eNOS, directly leading to reduced NO-availability. This process might be mediated by RhoA activation by the signalling pathway. Elevated IL-17A levels activate Rho-kinase activator RhoA, which leads to the phosphorylation of the inhibitory eNOS residue threonine 495 [257-259].

IL-17A appears to be a central mediator linking intestinal inflammation to systemic and vascular inflammation in CeD. Its role in cardiovascular dysfunction aligns with its effects in other autoimmune diseases, such as psoriasis and RA, where it promotes endothelial dysfunction and inflammatory cell recruitment.

This study underscores the link between intestinal inflammation and systemic cardiovascular dysfunction, with IL-17A emerging as a central mediator. The observed vascular dysfunction, including endothelial activation, oxidative stress, and increased BP, mirrors mechanisms seen in other inflammatory diseases, emphasizing the broader relevance of IL-17A-driven inflammation. Future research should explore IL-17A as a potential therapeutic target and assess the long-term reversibility of gliadin-induced vascular dysfunction. Further investigation into additional mediators of the gut-vascular axis could refine intervention strategies aimed at mitigating extra-intestinal complications in CeD. Methodological considerations and study limitations are discussed in a dedicated chapter (s. section 5.4).

5.3. Background of the Murine Disease Model and Alternatives for Future Studies

In this thesis, the NOD-DQ8 mouse model was employed to investigate CeD due to its humanised immune response characteristics. The NOD (Non-Obese Diabetic) mouse strain is genetically modified to express the human HLA-DQ8 gene (HLA-DQA103:01; DQB103:02), a key factor in CeD immune responses. Additionally, their endogenous mouse class II genes ($A\beta^{0/0}$) are deleted, making them a widely used model for studying autoimmune diseases (AIDs) such as CeD [122, 173, 260].

Galipeau *et al.* found that NOD-DQ8 mice develop severe insulitis only after depletion of CD25+ FoxP3+ T regulatory cells (Tregs), highlighting the importance of immune regulation in this model. However, it is essential to note that the genetic background of these mice also predisposes them to spontaneous myocarditis and

gluten-induced dermatitis herpetiformis, particularly in long-term investigations. In this study, these conditions were meticulously ruled out by monitoring blood sugar levels and cardiac function to attribute observed changes directly to CeD development. Notably, skin changes were not observed during the 2 week treatment period, while Marietta *et al.* reported that mice developed skin rashes after 2–5 months of gluten ingestion [173, 174, 214].

Taneja *et al.* reported that predominantly female NOD-DQ8 mice, with a mean age of 18 ± 3 weeks, are susceptible to the spontaneous development of myocarditis and cardiomyopathy with high morbidity, which could confound results and limit the interpretation and feasibility of long-term data, especially regarding cardiovascular read-outs [214]. The NOD-DQ8 model effectively replicates many aspects of CeD and provides valuable insights into early disease mechanisms. While the NOD-DQ8 model provides valuable insights into CeD pathophysiology, its limitations, and broader implications are discussed in detail in the dedicated limitations chapter (s. section 5.4).

Various models are used to study CeD, each with distinct advantages and limitations. Spontaneous models like Irish Setter dogs and Rhesus macaques provide valuable insights but face practical constraints. Other inducible models such as HLA-DQ2-DR3 are useful for studying immune responses to gluten, though they do not exhibit enteropathy. An interesting alternative model is the HLA-DQ8-IL-15-D^d-villin mouse, with the same haplotype as NOD-DQ8, but with a C57BL/6 background and additional IL-15 intestinal overexpression. This additional IL-15 overexpression is required for the development of villous atrophy, resulting in a more pronounced form of CeD. Since IL-15 is a pro-inflammatory and pro-atherosclerotic cytokine, its overexpression in this model raises concerns about potential cardiovascular effects that may not be directly attributable to CeD. However, increased intestinal IL-15 expression is a well-documented feature of CeD pathophysiology in humans [261-267].

A combination of *in vivo*, *in vitro*, and *in silico* approaches is essential for understanding CeD pathogenesis. However, translating findings from animal models to clinical applications remains a challenge, requiring validation in diverse patient populations to ensure relevance and treatment efficacy. The complexity of CeD in humans necessitates extensive clinical investigations and the collection of

robust human data. Clinical studies involving diverse patient populations are crucial to validate the relevance of experimental findings and to ensure the safety and efficacy of new treatments [268, 269].

5.4. Limitations of the Study

This chapter consolidates the study's key limitations, addressing methodological constraints, model-specific considerations, and broader translational challenges.

The NOD-DQ8 mouse model effectively replicates key aspects of CeD, such as immune cell infiltration and crypt hyperplasia (s. section 4.1). However, its genetic predisposition to additional autoimmune conditions, including T1D and spontaneous myocarditis, may confound cardiovascular findings (refer to section 5.3). This makes it challenging to isolate CeD-specific effects, particularly in long-term studies. Moreover, as HLA-DQ2 is the predominant genotype in CeD patients, the NOD-DQ8 model represents only a subset of genetic susceptibility, limiting its translational applicability. Therefore, when using this model, researchers must account for potential co-developing AIDs, especially in extended studies, increasing experimental complexity.

Additionally, while sex differences were addressed in a separate study, this study focused exclusively on male mice. Previous research from our group demonstrated sex-specific cardiovascular effects in CeD, with male mice developing a disease phenotype, whereas female mice exhibited vascular resilience [270]. These findings highlight the need for sex-specific research in CeD to improve cardiovascular risk assessment and intervention strategies.

Moreover, although the model effectively replicates early-stage intestinal inflammation, it does not fully capture all clinical CeD manifestations, such as anti-TG2 antibody presence or diarrhoea (s. section 5.1). Additionally, it does not reflect non-responsive CeD (NRCeD), which remains a challenge in human patient management (s. section 1.2).

While IL-17A was identified as a key mediator linking gut and vascular inflammation, other cytokines, such as TNF-α and IL-1β, may also contribute to endothelial dysfunction and systemic inflammation. Future studies should explore their roles to establish a more comprehensive mechanistic framework. Additionally, given the

influence of diet on the gut microbiome and its systemic effects, investigating microbiome composition alongside inflammatory markers would provide further insight into CeD-induced cardiovascular risk.

Methodological constraints also present challenges. While the transition from a GCD to a GFD was well-controlled, it does not fully reflect real-world dietary adherence or the long-term effects of gluten withdrawal. The two-week intervention may not capture chronic cardiovascular adaptations. Additionally, blood pressure was measured using indirect methods, which are standard for small animals but may lack the precision of invasive techniques. Reliable results require extensive operator training. Similarly, vascular function was assessed in isolated aortic segments, which do not fully account for in vivo haemodynamic influences such as blood flow and neurohumoral regulation.

Although this study bridges preclinical and clinical observations, extrapolating findings from animal models to human patients remains a challenge due to interspecies differences. For example, murine blood lipoprotein profiles differ significantly from those of humans, impacting cardiovascular risk assessment (s. section 5.2, Wolf et al. [237]). Additionally, the study primarily focused on cardiovascular outcomes, whereas the potential implications of CeD-induced systemic inflammation for other autoimmune diseases were not explored in detail.

The study design and scope present additional limitations. The sample size, though sufficient for detecting significant differences, may limit the robustness of subgroup analyses. Moreover, gluten exposure was the sole environmental factor investigated, whereas other triggers, such as infections or stress, were not considered.

Future studies should refine experimental designs and methodological approaches to address the remaining knowledge gaps. Investigating sex-specific cardiovascular responses by including both male and female animals will provide insights into the role of biological differences in CeD progression. Expanding the duration of dietary interventions will help clarify whether gliadin-induced cardiovascular dysfunction is fully reversible or leads to long-term alterations. Additionally, a more comprehensive assessment of microvascular function, metabolic changes, and cardiac remodelling will improve the mechanistic understanding of CeD-related cardiovascular effects.

Translating these findings into human cohort studies will be essential to confirm their clinical relevance and guide therapeutic strategies.

5.5. Relevance of the Results and Future Perspectives to Investigate Cardiovascular Consequences of CeD

This thesis provides new insights into the relationship between CeD and cardiovascular health. Using the NOD-DQ8 mouse model, this study demonstrates that both active and non-active CeD conditions contribute to systemic effects, including vascular dysfunction, oxidative stress, and inflammation. These findings strengthen the understanding of CeD as a systemic disorder with potential cardiovascular consequences, aligning with clinical observations of increased cardiovascular risk in CeD patients.

The demonstration of measurable cardiovascular impairments in the NOD-DQ8 mouse model highlights the importance of systemic inflammation as a contributor to vascular dysfunction in CeD. Specifically, the role of nitro-oxidative stress and the identification of IL-17A as a potential key mediator establish important mechanistic links between intestinal inflammation and cardiovascular outcomes. These findings underscore the need for integrated therapeutic approaches targeting both the local intestinal environment and systemic inflammatory pathways to mitigate cardiovascular risk.

Furthermore, the study's results emphasize the potential reversibility of CeD-induced cardiovascular impairments through dietary intervention, such as adherence to a GFD. This has direct clinical implications, reinforcing the importance of early diagnosis and strict dietary management in preventing long-term systemic complications. The research bridges the gap between preclinical and clinical observations, providing a basis for future translational studies.

Future Perspectives might be:

- Model Optimisation and Validation: Future studies should refine the NOD-DQ8 model to better replicate cardiovascular manifestations in CeD patients, including variations in disease severity and sex-based differences.

- Mechanistic Pathway Exploration: Further investigation is needed into IL-17A's role in systemic inflammation, along with other immune mediators that may contribute to vascular dysfunction.
- Longitudinal and Interventional Studies: Long-term studies should assess whether cardiovascular impairments persist or reverse with dietary or pharmacological interventions. Adjunctive therapies alongside a GFD could offer new treatment avenues.
- Clinical Translation: The translational value of these findings should be validated in clinical settings by identifying biomarkers for cardiovascular risk in CeD. Collaboration with clinicians is essential for integrating these insights into diagnostics and treatment protocols.
- Broader Implications: This research underscores the role of systemic inflammation in autoimmune diseases beyond CeD. Investigating shared pathways between gut and vascular health in other AIDs could identify new therapeutic targets.

In summary, this study provides a foundation for understanding the cardiovascular consequences of CeD and highlights potential therapeutic targets. By addressing the systemic nature of CeD, these findings contribute to broader efforts to mitigate cardiovascular risks in autoimmune diseases. Future research should build on these insights to develop integrated prevention, diagnostic, and treatment strategies, ultimately improving patient outcomes.

VII. References

1. World Health Organization (WHO), Cardiovascular diseases. https://www.who.int/health-topics/cardiovascular-diseases#tab=tab_1 (accessed 08.04.2024)
2. World Health Organization (WHO), Noncommunicable diseases. https://www.who.int/health-topics/noncommunicable-diseases#tab=tab_1 (accessed 08.04.2024)
3. Linus Pauling Institute, M. I. C. Cardiovascular Disease. https://lpi.oregonstate.edu/mic/health-disease/cardiovascular-disease (accessed 09.04.2024)
4. Cosselman, K. E., Navas-Acien, A. & Kaufman, J. D. (2015). Environmental factors in cardiovascular disease. Nat Rev Cardiol. **12**, 627-642. https://doi.org/10.1038/nrcardio.2015.152.
5. Heart arrhythmia. https://www.mayoclinic.org/diseases-conditions/heart-arrhythmia/symptoms-causes/syc-20350668 (accessed 03.05.2024)
6. (2019/2021). World Health Organization (WHO), International Classification of Diseases, Eleventh Revision (ICD-11). World Health Organization (WHO).
7. Yusuf, S., Reddy, S., Ounpuu, S. & Anand, S. (2001). Global burden of cardiovascular diseases: Part I: general considerations, the epidemiologic transition, risk factors, and impact of urbanization. Circulation. **104**, 2746-2753. https://doi.org/10.1161/hc4601.099487.
8. (2023). World Health Organization (WHO), World health statistics 2023: monitoring health for the SDGs, Sustainable Development Goals. World Health Organization (WHO).
9. Roth, G. A., Mensah, G. A., Johnson, C. O., Addolorato, G., Ammirati, E., Baddour, L. M., Barengo, N. C., Beaton, A. Z., Benjamin, E. J., Benziger, C. P., Bonny, A., Brauer, M., Brodmann, M., Cahill, T. J., Carapetis, J., Catapano, A. L., Chugh, S. S., Cooper, L. T., Coresh, J., Criqui, M., DeCleene, N., Eagle, K. A., Emmons-Bell, S., Feigin, V. L., Fernandez-Sola, J., Fowkes, G., Gakidou, E., Grundy, S. M., He, F. J., Howard, G., Hu, F., Inker, L., Karthikeyan, G., Kassebaum, N., Koroshetz, W., Lavie, C., Lloyd-Jones, D., Lu, H. S., Mirijello, A., Temesgen, A. M., Mokdad, A., Moran, A. E., Muntner, P., Narula, J., Neal, B., Ntsekhe, M., Moraes de Oliveira, G., Otto, C., Owolabi, M., Pratt, M., Rajagopalan, S., Reitsma, M., Ribeiro, A. L. P., Rigotti, N., Rodgers, A., Sable, C., Shakil, S., Sliwa-Hahnle, K., Stark, B., Sundstrom, J., Timpel, P., Tleyjeh, I. M., Valgimigli, M., Vos, T., Whelton, P. K., Yacoub, M., Zuhlke, L., Murray, C., Fuster, V. & Group, G.-N.-J. G. B. o. C. D. W. (2020). Global Burden of Cardiovascular Diseases and Risk Factors, 1990-2019: Update From the GBD 2019 Study. J Am Coll Cardiol. **76**, 2982-3021. https://doi.org/10.1016/j.jacc.2020.11.010.
10. Gersh, B. J., Sliwa, K., Mayosi, B. M. & Yusuf, S. (2010). Novel therapeutic concepts: the epidemic of cardiovascular disease in the developing world: global implications. Eur Heart J. **31**, 642-648. https://doi.org/10.1093/eurheartj/ehq030.
11. (2023). World Heart Report 2023: Confronting the World's Number One Killer.
12. Disease, G. B. D., Injury, I. & Prevalence, C. (2018). Global, regional, and national incidence, prevalence, and years lived with disability for 354 diseases and injuries for 195 countries and territories, 1990-2017: a systematic analysis for the Global Burden of Disease (GBD) Study 2017. Lancet. **392**, 1789-1858. https://doi.org/10.1016/S0140-6736(18)32279-7.

13. Yusuf, S., Reddy, S., Ounpuu, S. & Anand, S. (2001). Global burden of cardiovascular diseases: Part II: variations in cardiovascular disease by specific ethnic groups and geographic regions and prevention strategies. Circulation. **104**, 2855-2864. https://doi.org/10.1161/hc4701.099488.
14. Bloom, D. E., Cafiero, E.T., Jané-Llopis, E., Abrahams-Gessel, S., Bloom, L.R., Fathima, S., Feigl, A.B., Gaziano, T., Mowafi, M., Pandya, A., Prettner, K., Rosenberg, L., Seligman, B., Stein, A.Z., & Weinstein, C. (2011). The Global Economic Burden of Noncommunicable Diseases. Geneva: World Economic Forum. World Economic Forum.
15. Khan, M. A., Hashim, M. J., Mustafa, H., Baniyas, M. Y., Al Suwaidi, S., AlKatheeri, R., Alblooshi, F. M. K., Almatrooshi, M., Alzaabi, M. E. H., Al Darmaki, R. S. & Lootah, S. (2020). Global Epidemiology of Ischemic Heart Disease: Results from the Global Burden of Disease Study. Cureus. **12**, e9349. https://doi.org/10.7759/cureus.9349.
16. United Nations (UN), Goals 3 - Ensure healthy lives and promote well-being for all at all ages. https://sdgs.un.org/goals/goal3#overview (accessed 09.04.2024)
17. Li, Y., Cao, G. Y., Jing, W. Z., Liu, J. & Liu, M. (2023). Global trends and regional differences in incidence and mortality of cardiovascular disease, 1990-2019: findings from 2019 global burden of disease study. Eur J Prev Cardiol. **30**, 276-286. https://doi.org/10.1093/eurjpc/zwac285.
18. Sacco, R. L., Roth, G. A., Reddy, K. S., Arnett, D. K., Bonita, R., Gaziano, T. A., Heidenreich, P. A., Huffman, M. D., Mayosi, B. M., Mendis, S., Murray, C. J. L., Perel, P., Piñeiro, D. J., Smith, S. C., Taubert, K. A., Wood, D. A., Zhao, D. & Zoghbi, W. A. (2016). The Heart of 25 by 25: Achieving the Goal of Reducing Global and Regional Premature Deaths From Cardiovascular Diseases and Stroke. Circulation. **133**, e674-e690. https://doi.org/doi:10.1161/CIR.0000000000000395.
19. Stary, H. C., Chandler, A. B., Dinsmore, R. E., Fuster, V., Glagov, S., Insull, W., Jr., Rosenfeld, M. E., Schwartz, C. J., Wagner, W. D. & Wissler, R. W. (1995). A definition of advanced types of atherosclerotic lesions and a histological classification of atherosclerosis. A report from the Committee on Vascular Lesions of the Council on Arteriosclerosis, American Heart Association. Circulation. **92**, 1355-1374. https://doi.org/10.1161/01.cir.92.5.1355.
20. Sanz, J. & Fayad, Z. A. (2008). Imaging of atherosclerotic cardiovascular disease. Nature. **451**, 953-957. https://doi.org/10.1038/nature06803.
21. Libby, P., Buring, J. E., Badimon, L., Hansson, G. K., Deanfield, J., Bittencourt, M. S., Tokgozoglu, L. & Lewis, E. F. (2019). Atherosclerosis. Nat Rev Dis Primers. **5**, 56. https://doi.org/10.1038/s41572-019-0106-z.
22. Frak, W., Wojtasinska, A., Lisinska, W., Mlynarska, E., Franczyk, B. & Rysz, J. (2022). Pathophysiology of Cardiovascular Diseases: New Insights into Molecular Mechanisms of Atherosclerosis, Arterial Hypertension, and Coronary Artery Disease. Biomedicines. **10**. https://doi.org/10.3390/biomedicines10081938.
23. Libby, P. (2021). The changing landscape of atherosclerosis. Nature. **592**, 524-533. https://doi.org/10.1038/s41586-021-03392-8.
24. Bernard, I., Limonta, D., Mahal, L. K. & Hobman, T. C. (2020). Endothelium Infection and Dysregulation by SARS-CoV-2: Evidence and Caveats in COVID-19. Viruses. **13**. https://doi.org/10.3390/v13010029.
25. Celermajer, D. S., Sorensen, K. E., Gooch, V. M., Spiegelhalter, D. J., Miller, O. I., Sullivan, I. D., Lloyd, J. K. & Deanfield, J. E. (1992). Non-invasive detection

of endothelial dysfunction in children and adults at risk of atherosclerosis. Lancet. **340**, 1111-1115. https://doi.org/10.1016/0140-6736(92)93147-f.
26. Clarkson, P., Celermajer, D. S., Powe, A. J., Donald, A. E., Henry, R. M. & Deanfield, J. E. (1997). Endothelium-dependent dilatation is impaired in young healthy subjects with a family history of premature coronary disease. Circulation. **96**, 3378-3383. https://doi.org/10.1161/01.cir.96.10.3378.
27. Drexler, H., Hayoz, D., Munzel, T., Just, H., Zelis, R. & Brunner, H. R. (1993). Endothelial function in congestive heart failure. Am Heart J. **126**, 761-764. https://doi.org/10.1016/0002-8703(93)90926-z.
28. Panza, J. A., Quyyumi, A. A., Brush, J. E., Jr. & Epstein, S. E. (1990). Abnormal endothelium-dependent vascular relaxation in patients with essential hypertension. N Engl J Med. **323**, 22-27. https://doi.org/10.1056/NEJM199007053230105.
29. Brandes, R. P. (2014). Endothelial dysfunction and hypertension. Hypertension. **64**, 924-928. https://doi.org/10.1161/HYPERTENSIONAHA.114.03575.
30. Dzau, V. J. (2004). Markers of malign across the cardiovascular continuum: interpretation and application. Circulation. **109**, IV1-2. https://doi.org/10.1161/01.CIR.0000133445.78855.aa.
31. Cohn, J. N., Quyyumi, A. A., Hollenberg, N. K. & Jamerson, K. A. (2004). Surrogate markers for cardiovascular disease: functional markers. Circulation. **109**, IV31-46. https://doi.org/10.1161/01.CIR.0000133442.99186.39.
32. Steven, S., Frenis, K., Oelze, M., Kalinovic, S., Kuntic, M., Bayo Jimenez, M. T., Vujacic-Mirski, K., Helmstadter, J., Kroller-Schon, S., Munzel, T. & Daiber, A. (2019). Vascular Inflammation and Oxidative Stress: Major Triggers for Cardiovascular Disease. Oxid Med Cell Longev. **2019**, 7092151. https://doi.org/10.1155/2019/7092151.
33. Godo, S. & Shimokawa, H. (2017). Endothelial Functions. Arterioscler Thromb Vasc Biol. **37**, e108-e114. https://doi.org/10.1161/ATVBAHA.117.309813.
34. Daiber, A., Steven, S., Weber, A., Shuvaev, V. V., Muzykantov, V. R., Laher, I., Li, H., Lamas, S. & Munzel, T. (2017). Targeting vascular (endothelial) dysfunction. Br J Pharmacol. **174**, 1591-1619. https://doi.org/10.1111/bph.13517.
35. Vanhoutte, P. M., Zhao, Y., Xu, A. & Leung, S. W. (2016). Thirty Years of Saying NO: Sources, Fate, Actions, and Misfortunes of the Endothelium-Derived Vasodilator Mediator. Circ Res. **119**, 375-396. https://doi.org/10.1161/CIRCRESAHA.116.306531.
36. De Hert, S. (2012). Physiology of hemodynamic homeostasis. Best Pract Res Clin Anaesthesiol. **26**, 409-419. https://doi.org/10.1016/j.bpa.2012.10.004.
37. Wolin, M. S., Ahmad, M. & Gupte, S. A. (2005). The sources of oxidative stress in the vessel wall. Kidney Int. **67**, 1659-1661. https://doi.org/10.1111/j.1523-1755.2005.00257.x.
38. Ohara, Y., Peterson, T. E. & Harrison, D. G. (1993). Hypercholesterolemia increases endothelial superoxide anion production. J Clin Invest. **91**, 2546-2551. https://doi.org/10.1172/JCI116491.
39. Drummond, G. R. & Sobey, C. G. (2014). Endothelial NADPH oxidases: which NOX to target in vascular disease? Trends Endocrinol Metab. **25**, 452-463. https://doi.org/10.1016/j.tem.2014.06.012.
40. Brandes, R. P. & Kreuzer, J. (2005). Vascular NADPH oxidases: molecular mechanisms of activation. Cardiovasc Res. **65**, 16-27. https://doi.org/10.1016/j.cardiores.2004.08.007.

41. Forstermann, U. & Munzel, T. (2006). Endothelial nitric oxide synthase in vascular disease: from marvel to menace. Circulation. **113**, 1708-1714. https://doi.org/10.1161/CIRCULATIONAHA.105.602532.
42. Forstermann, U. & Sessa, W. C. (2012). Nitric oxide synthases: regulation and function. Eur Heart J. **33**, 829-837, 837a-837d. https://doi.org/10.1093/eurheartj/ehr304.
43. Nathan, C. & Xie, Q. W. (1994). Nitric oxide synthases: roles, tolls, and controls. Cell. **78**, 915-918. https://doi.org/10.1016/0092-8674(94)90266-6.
44. Zhazykbayeva, S., Pabel, S., Mugge, A., Sossalla, S. & Hamdani, N. (2020). The molecular mechanisms associated with the physiological responses to inflammation and oxidative stress in cardiovascular diseases. Biophys Rev. **12**, 947-968. https://doi.org/10.1007/s12551-020-00742-0.
45. Wenzel, P., Kossmann, S., Munzel, T. & Daiber, A. (2017). Redox regulation of cardiovascular inflammation - Immunomodulatory function of mitochondrial and Nox-derived reactive oxygen and nitrogen species. Free Radic Biol Med. **109**, 48-60. https://doi.org/10.1016/j.freeradbiomed.2017.01.027.
46. Mourouzis, K., Oikonomou, E., Siasos, G., Tsalamadris, S., Vogiatzi, G., Antonopoulos, A., Fountoulakis, P., Goliopoulou, A., Papaioannou, S. & Tousoulis, D. (2020). Pro-inflammatory Cytokines in Acute Coronary Syndromes. Curr Pharm Des. **26**, 4624-4647. https://doi.org/10.2174/1381612826666200413082353.
47. Zhang, H., Park, Y., Wu, J., Chen, X., Lee, S., Yang, J., Dellsperger, K. C. & Zhang, C. (2009). Role of TNF-alpha in vascular dysfunction. Clin Sci (Lond). **116**, 219-230. https://doi.org/10.1042/CS20080196.
48. Hohensinner, P. J., Niessner, A., Huber, K., Weyand, C. M. & Wojta, J. (2011). Inflammation and cardiac outcome. Curr Opin Infect Dis. **24**, 259-264. https://doi.org/10.1097/QCO.0b013e328344f50f.
49. Cybulsky, M. I., Iiyama, K., Li, H., Zhu, S., Chen, M., Iiyama, M., Davis, V., Gutierrez-Ramos, J. C., Connelly, P. W. & Milstone, D. S. (2001). A major role for VCAM-1, but not ICAM-1, in early atherosclerosis. J Clin Invest. **107**, 1255-1262. https://doi.org/10.1172/JCI11871.
50. Cybulsky, M. I. & Gimbrone, M. A., Jr. (1991). Endothelial expression of a mononuclear leukocyte adhesion molecule during atherogenesis. Science. **251**, 788-791. https://doi.org/10.1126/science.1990440.
51. Zhang, H., Chen, J., Liu, X., Awar, L., McMickle, A., Bai, F., Nagarajan, S. & Yu, S. (2013). IL-17 induces expression of vascular cell adhesion molecule through signalling pathway of NF-kappaB, but not Akt1 and TAK1 in vascular smooth muscle cells. Scand J Immunol. **77**, 230-237. https://doi.org/10.1111/sji.12030.
52. Elyasi, A., Voloshyna, I., Ahmed, S., Kasselman, L. J., Behbodikhah, J., De Leon, J. & Reiss, A. B. (2020). The role of interferon-gamma in cardiovascular disease: an update. Inflamm Res. **69**, 975-988. https://doi.org/10.1007/s00011-020-01382-6.
53. Schroecksnadel, K., Frick, B., Winkler, C. & Fuchs, D. (2006). Crucial role of interferon-gamma and stimulated macrophages in cardiovascular disease. Curr Vasc Pharmacol. **4**, 205-213. https://doi.org/10.2174/157016106777698379.
54. Yudkin, J. S., Kumari, M., Humphries, S. E. & Mohamed-Ali, V. (2000). Inflammation, obesity, stress and coronary heart disease: is interleukin-6 the link? Atherosclerosis. **148**, 209-214. https://doi.org/10.1016/s0021-9150(99)00463-3.

55. Nordlohne, J. & von Vietinghoff, S. (2019). Interleukin 17A in atherosclerosis - Regulation and pathophysiologic effector function. Cytokine. **122**, 154089. https://doi.org/10.1016/j.cyto.2017.06.016.
56. Lin, Q. Y., Bai, J., Zhang, Y. L. & Li, H. H. (2023). Integrin CD11b Contributes to Hypertension and Vascular Dysfunction Through Mediating Macrophage Adhesion and Migration. Hypertension. **80**, 57-69. https://doi.org/10.1161/HYPERTENSIONAHA.122.20328.
57. Wu, H., Gower, R. M., Wang, H., Perrard, X. Y., Ma, R., Bullard, D. C., Burns, A. R., Paul, A., Smith, C. W., Simon, S. I. & Ballantyne, C. M. (2009). Functional role of CD11c+ monocytes in atherogenesis associated with hypercholesterolemia. Circulation. **119**, 2708-2717. https://doi.org/10.1161/CIRCULATIONAHA.108.823740.
58. Kibel, A., Lukinac, A. M., Dambic, V., Juric, I. & Selthofer-Relatic, K. (2020). Oxidative Stress in Ischemic Heart Disease. Oxid Med Cell Longev. **2020**, 6627144. https://doi.org/10.1155/2020/6627144.
59. Oparil, S. & Oberman, A. (1999). Nontraditional cardiovascular risk factors. Am J Med Sci. **317**, 193-207. https://doi.org/10.1097/00000441-199903000-00010.
60. Force, U. S. P. S. T. (2009). Using nontraditional risk factors in coronary heart disease risk assessment: U.S. Preventive Services Task Force recommendation statement. Ann Intern Med. **151**, 474-482. https://doi.org/10.7326/0003-4819-151-7-200910060-00008.
61. Lin, J. S., Evans, C. V., Johnson, E., Redmond, N., Coppola, E. L. & Smith, N. (2018). Nontraditional Risk Factors in Cardiovascular Disease Risk Assessment: Updated Evidence Report and Systematic Review for the US Preventive Services Task Force. JAMA. **320**, 281-297. https://doi.org/10.1001/jama.2018.4242.
62. Cimmino, G., Natale, F., Alfieri, R., Cante, L., Covino, S., Franzese, R., Limatola, M., Marotta, L., Molinari, R., Mollo, N., Loffredo, F. S. & Golino, P. (2023). Non-Conventional Risk Factors: "Fact" or "Fake" in Cardiovascular Disease Prevention? Biomedicines. **11**. https://doi.org/10.3390/biomedicines11092353.
63. Munzel, T., Daiber, A., Steven, S., Tran, L. P., Ullmann, E., Kossmann, S., Schmidt, F. P., Oelze, M., Xia, N., Li, H., Pinto, A., Wild, P., Pies, K., Schmidt, E. R., Rapp, S. & Kroller-Schon, S. (2017). Effects of noise on vascular function, oxidative stress, and inflammation: mechanistic insight from studies in mice. Eur Heart J. **38**, 2838-2849. https://doi.org/10.1093/eurheartj/ehx081.
64. Munzel, T., Schmidt, F. P., Steven, S., Herzog, J., Daiber, A. & Sorensen, M. (2018). Environmental Noise and the Cardiovascular System. J Am Coll Cardiol. **71**, 688-697. https://doi.org/10.1016/j.jacc.2017.12.015.
65. Kyrou, I. & Tsigos, C. (2007). Stress mechanisms and metabolic complications. Horm Metab Res. **39**, 430-438. https://doi.org/10.1055/s-2007-981462.
66. Radfar, A., Ferreira, M. M., Sosa, J. P. & Filip, I. (2021). Emergent Crisis of COVID-19 Pandemic: Mental Health Challenges and Opportunities. Front Psychiatry. **12**, 631008. https://doi.org/10.3389/fpsyt.2021.631008.
67. deVries, M. W. & Wilkerson, B. (2003). Stress, work and mental health: a global perspective. Acta Neuropsychiatr. **15**, 44-53. https://doi.org/10.1034/j.1601-5215.2003.00017.x.
68. Wild, C. P. (2005). Complementing the genome with an "exposome": the outstanding challenge of environmental exposure measurement in molecular

epidemiology. Cancer Epidemiol Biomarkers Prev. **14**, 1847-1850. https://doi.org/10.1158/1055-9965.EPI-05-0456.
69. Daiber, A., Lelieveld, J., Steven, S., Oelze, M., Kroller-Schon, S., Sorensen, M. & Munzel, T. (2019). The "exposome" concept - how environmental risk factors influence cardiovascular health. Acta Biochim Pol. **66**, 269-283. https://doi.org/10.18388/abp.2019_2853.
70. Munzel, T., Miller, M. R., Sorensen, M., Lelieveld, J., Daiber, A. & Rajagopalan, S. (2020). Reduction of environmental pollutants for prevention of cardiovascular disease: it's time to act. Eur Heart J. https://doi.org/10.1093/eurheartj/ehaa745.
71. Vrijheid, M. (2014). The exposome: a new paradigm to study the impact of environment on health. Thorax. **69**, 876-878. https://doi.org/10.1136/thoraxjnl-2013-204949.
72. Khambhati, J., Allard-Ratick, M., Dhindsa, D., Lee, S., Chen, J., Sandesara, P. B., O'Neal, W., Quyyumi, A. A., Wong, N. D., Blumenthal, R. S. & Sperling, L. S. (2018). Re: The art of cardiovascular risk assessment. Clinical Cardiology 2018;41(5):677-684. Clin Cardiol. **41**, 1111. https://doi.org/10.1002/clc.22998.
73. Khambhati, J., Allard-Ratick, M., Dhindsa, D., Lee, S., Chen, J., Sandesara, P. B., O'Neal, W., Quyyumi, A. A., Wong, N. D., Blumenthal, R. S. & Sperling, L. S. (2018). The art of cardiovascular risk assessment. Clin Cardiol. **41**, 677-684. https://doi.org/10.1002/clc.22930.
74. Stewart, J., Manmathan, G. & Wilkinson, P. (2017). Primary prevention of cardiovascular disease: A review of contemporary guidance and literature. JRSM Cardiovasc Dis. **6**, 2048004016687211. https://doi.org/10.1177/2048004016687211.
75. Ettehad, D., Emdin, C. A., Kiran, A., Anderson, S. G., Callender, T., Emberson, J., Chalmers, J., Rodgers, A. & Rahimi, K. (2016). Blood pressure lowering for prevention of cardiovascular disease and death: a systematic review and meta-analysis. Lancet. **387**, 957-967. https://doi.org/10.1016/S0140-6736(15)01225-8.
76. Cosentino, F., Grant, P. J., Aboyans, V., Bailey, C. J., Ceriello, A., Delgado, V., Federici, M., Filippatos, G., Grobbee, D. E., Hansen, T. B., Huikuri, H. V., Johansson, I., Juni, P., Lettino, M., Marx, N., Mellbin, L. G., Ostgren, C. J., Rocca, B., Roffi, M., Sattar, N., Seferovic, P. M., Sousa-Uva, M., Valensi, P., Wheeler, D. C. & Group, E. S. C. S. D. (2020). 2019 ESC Guidelines on diabetes, pre-diabetes, and cardiovascular diseases developed in collaboration with the EASD. Eur Heart J. **41**, 255-323. https://doi.org/10.1093/eurheartj/ehz486.
77. Patrono, C. & Baigent, C. (2019). Role of aspirin in primary prevention of cardiovascular disease. Nat Rev Cardiol. **16**, 675-686. https://doi.org/10.1038/s41569-019-0225-y.
78. Marso, S. P., Daniels, G. H., Brown-Frandsen, K., Kristensen, P., Mann, J. F., Nauck, M. A., Nissen, S. E., Pocock, S., Poulter, N. R., Ravn, L. S., Steinberg, W. M., Stockner, M., Zinman, B., Bergenstal, R. M., Buse, J. B., Committee, L. S. & Investigators, L. T. (2016). Liraglutide and Cardiovascular Outcomes in Type 2 Diabetes. N Engl J Med. **375**, 311-322. https://doi.org/10.1056/NEJMoa1603827.
79. Ussher, J. R. & Drucker, D. J. (2023). Glucagon-like peptide 1 receptor agonists: cardiovascular benefits and mechanisms of action. Nat Rev Cardiol. **20**, 463-474. https://doi.org/10.1038/s41569-023-00849-3.

80. Fitchett, D., Inzucchi, S. E., Cannon, C. P., McGuire, D. K., Scirica, B. M., Johansen, O. E., Sambevski, S., Kaspers, S., Pfarr, E., George, J. T. & Zinman, B. (2019). Empagliflozin Reduced Mortality and Hospitalization for Heart Failure Across the Spectrum of Cardiovascular Risk in the EMPA-REG OUTCOME Trial. Circulation. **139**, 1384-1395. https://doi.org/10.1161/CIRCULATIONAHA.118.037778.
81. Packer, M. (2023). SGLT2 inhibitors: role in protective reprogramming of cardiac nutrient transport and metabolism. Nat Rev Cardiol. **20**, 443-462. https://doi.org/10.1038/s41569-022-00824-4.
82. Lingvay, I., Brown-Frandsen, K., Colhoun, H. M., Deanfield, J., Emerson, S. S., Esbjerg, S., Hardt-Lindberg, S., Hovingh, G. K., Kahn, S. E., Kushner, R. F., Lincoff, A. M., Marso, S. P., Fries, T. M., Plutzky, J., Ryan, D. H. & Group, S. S. (2023). Semaglutide for cardiovascular event reduction in people with overweight or obesity: SELECT study baseline characteristics. Obesity (Silver Spring). **31**, 111-122. https://doi.org/10.1002/oby.23621.
83. Bugger, H. & Zirlik, A. (2021). Anti-inflammatory Strategies in Atherosclerosis. Hamostaseologie. **41**, 433-442. https://doi.org/10.1055/a-1661-0020.
84. Thau, H., Neuber, S., Emmert, M. Y. & Nazari-Shafti, T. Z. (2024). Targeting Lipoprotein(a): Can RNA Therapeutics Provide the Next Step in the Prevention of Cardiovascular Disease? Cardiol Ther. **13**, 39-67. https://doi.org/10.1007/s40119-024-00353-w.
85. Ridker, P. M., Everett, B. M., Thuren, T., MacFadyen, J. G., Chang, W. H., Ballantyne, C., Fonseca, F., Nicolau, J., Koenig, W., Anker, S. D., Kastelein, J. J. P., Cornel, J. H., Pais, P., Pella, D., Genest, J., Cifkova, R., Lorenzatti, A., Forster, T., Kobalava, Z., Vida-Simiti, L., Flather, M., Shimokawa, H., Ogawa, H., Dellborg, M., Rossi, P. R. F., Troquay, R. P. T., Libby, P., Glynn, R. J. & Group, C. T. (2017). Antiinflammatory Therapy with Canakinumab for Atherosclerotic Disease. N Engl J Med. **377**, 1119-1131. https://doi.org/10.1056/NEJMoa1707914.
86. Nidorf, S. M., Fiolet, A. T. L., Mosterd, A., Eikelboom, J. W., Schut, A., Opstal, T. S. J., The, S. H. K., Xu, X. F., Ireland, M. A., Lenderink, T., Latchem, D., Hoogslag, P., Jerzewski, A., Nierop, P., Whelan, A., Hendriks, R., Swart, H., Schaap, J., Kuijper, A. F. M., van Hessen, M. W. J., Saklani, P., Tan, I., Thompson, A. G., Morton, A., Judkins, C., Bax, W. A., Dirksen, M., Alings, M., Hankey, G. J., Budgeon, C. A., Tijssen, J. G. P., Cornel, J. H., Thompson, P. L. & LoDoCo2 Trial, I. (2020). Colchicine in Patients with Chronic Coronary Disease. N Engl J Med. **383**, 1838-1847. https://doi.org/10.1056/NEJMoa2021372.
87. (2023). Heart Procedures and Surgeries. https://www.heart.org/en/health-topics/heart-attack/treatment-of-a-heart-attack/cardiac-procedures-and-surgeries (accessed 16.06.2024)
88. Eckel, R. H., Jakicic, J. M., Ard, J. D., de Jesus, J. M., Houston Miller, N., Hubbard, V. S., Lee, I. M., Lichtenstein, A. H., Loria, C. M., Millen, B. E., Nonas, C. A., Sacks, F. M., Smith, S. C., Jr., Svetkey, L. P., Wadden, T. A., Yanovski, S. Z. & American College of Cardiology/American Heart Association Task Force on Practice, G. (2014). 2013 AHA/ACC guideline on lifestyle management to reduce cardiovascular risk: a report of the American College of Cardiology/American Heart Association Task Force on Practice Guidelines. J Am Coll Cardiol. **63**, 2960-2984. https://doi.org/10.1016/j.jacc.2013.11.003.

89. Yusuf, S., Hawken, S., Ounpuu, S., Dans, T., Avezum, A., Lanas, F., McQueen, M., Budaj, A., Pais, P., Varigos, J., Lisheng, L. & Investigators, I. S. (2004). Effect of potentially modifiable risk factors associated with myocardial infarction in 52 countries (the INTERHEART study): case-control study. Lancet. **364**, 937-952. https://doi.org/10.1016/S0140-6736(04)17018-9.
90. Ockene, I. S. & Miller, N. H. (1997). Cigarette smoking, cardiovascular disease, and stroke: a statement for healthcare professionals from the American Heart Association. American Heart Association Task Force on Risk Reduction. Circulation. **96**, 3243-3247. https://doi.org/10.1161/01.cir.96.9.3243.
91. Ahmad, A. F., Dwivedi, G., O'Gara, F., Caparros-Martin, J. & Ward, N. C. (2019). The gut microbiome and cardiovascular disease: current knowledge and clinical potential. Am J Physiol Heart Circ Physiol. **317**, H923-H938. https://doi.org/10.1152/ajpheart.00376.2019.
92. Whelton, P. K., Carey, R. M., Aronow, W. S., Casey, D. E., Jr., Collins, K. J., Dennison Himmelfarb, C., DePalma, S. M., Gidding, S., Jamerson, K. A., Jones, D. W., MacLaughlin, E. J., Muntner, P., Ovbiagele, B., Smith, S. C., Jr., Spencer, C. C., Stafford, R. S., Taler, S. J., Thomas, R. J., Williams, K. A., Sr., Williamson, J. D. & Wright, J. T., Jr. (2018). 2017 ACC/AHA/AAPA/ABC/ACPM/AGS/APhA/ASH/ASPC/NMA/PCNA Guideline for the Prevention, Detection, Evaluation, and Management of High Blood Pressure in Adults: Executive Summary: A Report of the American College of Cardiology/American Heart Association Task Force on Clinical Practice Guidelines. Hypertension. **71**, 1269-1324. https://doi.org/10.1161/HYP.0000000000000066.
93. Arnett, D. K., Blumenthal, R. S., Albert, M. A., Buroker, A. B., Goldberger, Z. D., Hahn, E. J., Himmelfarb, C. D., Khera, A., Lloyd-Jones, D., McEvoy, J. W., Michos, E. D., Miedema, M. D., Munoz, D., Smith, S. C., Jr., Virani, S. S., Williams, K. A., Sr., Yeboah, J. & Ziaeian, B. (2019). 2019 ACC/AHA Guideline on the Primary Prevention of Cardiovascular Disease: A Report of the American College of Cardiology/American Heart Association Task Force on Clinical Practice Guidelines. Circulation. **140**, e596-e646. https://doi.org/10.1161/CIR.0000000000000678.
94. Goff, D. C., Jr., Lloyd-Jones, D. M., Bennett, G., Coady, S., D'Agostino, R. B., Gibbons, R., Greenland, P., Lackland, D. T., Levy, D., O'Donnell, C. J., Robinson, J. G., Schwartz, J. S., Shero, S. T., Smith, S. C., Jr., Sorlie, P., Stone, N. J., Wilson, P. W., Jordan, H. S., Nevo, L., Wnek, J., Anderson, J. L., Halperin, J. L., Albert, N. M., Bozkurt, B., Brindis, R. G., Curtis, L. H., DeMets, D., Hochman, J. S., Kovacs, R. J., Ohman, E. M., Pressler, S. J., Sellke, F. W., Shen, W. K., Smith, S. C., Jr., Tomaselli, G. F. & American College of Cardiology/American Heart Association Task Force on Practice, G. (2014). 2013 ACC/AHA guideline on the assessment of cardiovascular risk: a report of the American College of Cardiology/American Heart Association Task Force on Practice Guidelines. Circulation. **129**, S49-73. https://doi.org/10.1161/01.cir.0000437741.48606.98.
95. Visseren, F. L. J., Mach, F., Smulders, Y. M., Carballo, D., Koskinas, K. C., Back, M., Benetos, A., Biffi, A., Boavida, J. M., Capodanno, D., Cosyns, B., Crawford, C., Davos, C. H., Desormais, I., Di Angelantonio, E., Franco, O. H., Halvorsen, S., Hobbs, F. D. R., Hollander, M., Jankowska, E. A., Michal, M., Sacco, S., Sattar, N., Tokgozoglu, L., Tonstad, S., Tsioufis, K. P., van Dis, I., van Gelder, I. C., Wanner, C., Williams, B., Societies, E. S. C. N. C. & Group, E. S. C. S. D. (2021). 2021 ESC Guidelines on cardiovascular disease

prevention in clinical practice. Eur Heart J. **42**, 3227-3337. https://doi.org/10.1093/eurheartj/ehab484.

96. Konstantinides, S. V., Meyer, G., Becattini, C., Bueno, H., Geersing, G. J., Harjola, V. P., Huisman, M. V., Humbert, M., Jennings, C. S., Jimenez, D., Kucher, N., Lang, I. M., Lankeit, M., Lorusso, R., Mazzolai, L., Meneveau, N., Ainle, F. N., Prandoni, P., Pruszczyk, P., Righini, M., Torbicki, A., Van Belle, E., Zamorano, J. L., The Task Force for the, d. & management of acute pulmonary embolism of the European Society of, C. (2019). 2019 ESC Guidelines for the diagnosis and management of acute pulmonary embolism developed in collaboration with the European Respiratory Society (ERS): The Task Force for the diagnosis and management of acute pulmonary embolism of the European Society of Cardiology (ESC). Eur Respir J. **54**. https://doi.org/10.1183/13993003.01647-2019.
97. e.V., D. G. f. K. D.-H. u. K. (2024). Leitlinien. https://leitlinien.dgk.org/leitlinien/ (accessed 15.06.2024)
98. Pisetsky, D. S. (2023). Pathogenesis of autoimmune disease. Nat Rev Nephrol. **19**, 509-524. https://doi.org/10.1038/s41581-023-00720-1.
99. Lenti, M. V., Rossi, C. M., Melazzini, F., Gastaldi, M., Bugatti, S., Rotondi, M., Bianchi, P. I., Gentile, A., Chiovato, L., Montecucco, C., Corazza, G. R. & Di Sabatino, A. (2022). Seronegative autoimmune diseases: A challenging diagnosis. Autoimmun Rev. **21**, 103143. https://doi.org/10.1016/j.autrev.2022.103143.
100. Rose, N. R. (2016). Prediction and Prevention of Autoimmune Disease in the 21st Century: A Review and Preview. Am J Epidemiol. **183**, 403-406. https://doi.org/10.1093/aje/kwv292.
101. Conrad, N., Misra, S., Verbakel, J. Y., Verbeke, G., Molenberghs, G., Taylor, P. N., Mason, J., Sattar, N., McMurray, J. J. V., McInnes, I. B., Khunti, K. & Cambridge, G. (2023). Incidence, prevalence, and co-occurrence of autoimmune disorders over time and by age, sex, and socioeconomic status: a population-based cohort study of 22 million individuals in the UK. Lancet. **401**, 1878-1890. https://doi.org/10.1016/S0140-6736(23)00457-9.
102. Dou, D. R., Zhao, Y., Belk, J. A., Zhao, Y., Casey, K. M., Chen, D. C., Li, R., Yu, B., Srinivasan, S., Abe, B. T., Kraft, K., Hellstrom, C., Sjoberg, R., Chang, S., Feng, A., Goldman, D. W., Shah, A. A., Petri, M., Chung, L. S., Fiorentino, D. F., Lundberg, E. K., Wutz, A., Utz, P. J. & Chang, H. Y. (2024). Xist ribonucleoproteins promote female sex-biased autoimmunity. Cell. **187**, 733-749 e716. https://doi.org/10.1016/j.cell.2023.12.037.
103. Dolgin, E. (2024). Why autoimmune disease is more common in women: X chromosome holds clues. Nature. **626**, 466. https://doi.org/10.1038/d41586-024-00267-6.
104. Tukiainen, T., Villani, A. C., Yen, A., Rivas, M. A., Marshall, J. L., Satija, R., Aguirre, M., Gauthier, L., Fleharty, M., Kirby, A., Cummings, B. B., Castel, S. E., Karczewski, K. J., Aguet, F., Byrnes, A., Consortium, G. T., Laboratory, D. A., Coordinating Center -Analysis Working, G., Statistical Methods groups-Analysis Working, G., Enhancing, G. g., Fund, N. I. H. C., Nih/Nci, Nih/Nhgri, Nih/Nimh, Nih/Nida, Biospecimen Collection Source Site, N., Biospecimen Collection Source Site, R., Biospecimen Core Resource, V., Brain Bank Repository-University of Miami Brain Endowment, B., Leidos Biomedical-Project, M., Study, E., Genome Browser Data, I., Visualization, E. B. I., Genome Browser Data, I., Visualization-Ucsc Genomics Institute, U. o. C. S. C., Lappalainen, T., Regev, A., Ardlie, K. G., Hacohen, N. & MacArthur, D. G.

(2017). Landscape of X chromosome inactivation across human tissues. Nature. **550**, 244-248. https://doi.org/10.1038/nature24265.
105. Ngo, S. T., Steyn, F. J. & McCombe, P. A. (2014). Gender differences in autoimmune disease. Front Neuroendocrinol. **35**, 347-369. https://doi.org/10.1016/j.yfrne.2014.04.004.
106. Tozzoli, R., Sorrentino, M. C. & Bizzaro, N. (2013). Detecting multiple autoantibodies to diagnose autoimmune co-morbidity (multiple autoimmune syndromes and overlap syndromes): a challenge for the autoimmunologist. Immunol Res. **56**, 425-431. https://doi.org/10.1007/s12026-013-8418-7.
107. Miyauchi, E., Shimokawa, C., Steimle, A., Desai, M. S. & Ohno, H. (2023). The impact of the gut microbiome on extra-intestinal autoimmune diseases. Nat Rev Immunol. **23**, 9-23. https://doi.org/10.1038/s41577-022-00727-y.
108. Iversen, R. & Sollid, L. M. (2023). The Immunobiology and Pathogenesis of Celiac Disease. Annu Rev Pathol. **18**, 47-70. https://doi.org/10.1146/annurev-pathmechdis-031521-032634.
109. Schuppan, D. (2016). Zöliakie. Bundesgesundheitsblatt - Gesundheitsforschung - Gesundheitsschutz. **59**, 827-835. https://doi.org/10.1007/s00103-016-2364-1.
110. Jabri, B. & Terhorst, C. (2014). Editorial overview: Autoimmunity. Curr Opin Immunol. **31**, v-vii. https://doi.org/10.1016/j.coi.2014.10.010.
111. Pashnina, I. A., Krivolapova, I. M., Fedotkina, T. V., Ryabkova, V. A., Chereshneva, M. V., Churilov, L. P. & Chereshnev, V. A. (2021). Antinuclear Autoantibodies in Health: Autoimmunity Is Not a Synonym of Autoimmune Disease. Antibodies (Basel). **10**. https://doi.org/10.3390/antib10010009.
112. Dinse, G. E., Parks, C. G., Weinberg, C. R., Co, C. A., Wilkerson, J., Zeldin, D. C., Chan, E. K. L. & Miller, F. W. (2020). Increasing Prevalence of Antinuclear Antibodies in the United States. Arthritis Rheumatol. **72**, 1026-1035. https://doi.org/10.1002/art.41214.
113. Singh, P., Arora, A., Strand, T. A., Leffler, D. A., Catassi, C., Green, P. H., Kelly, C. P., Ahuja, V. & Makharia, G. K. (2018). Global Prevalence of Celiac Disease: Systematic Review and Meta-analysis. Clin Gastroenterol Hepatol. **16**, 823-836 e822. https://doi.org/10.1016/j.cgh.2017.06.037.
114. Fasano, A., Berti, I., Gerarduzzi, T., Not, T., Colletti, R. B., Drago, S., Elitsur, Y., Green, P. H., Guandalini, S., Hill, I. D., Pietzak, M., Ventura, A., Thorpe, M., Kryszak, D., Fornaroli, F., Wasserman, S. S., Murray, J. A. & Horvath, K. (2003). Prevalence of celiac disease in at-risk and not-at-risk groups in the United States: a large multicenter study. Arch Intern Med. **163**, 286-292. https://doi.org/10.1001/archinte.163.3.286.
115. West, J., Fleming, K. M., Tata, L. J., Card, T. R. & Crooks, C. J. (2014). Incidence and prevalence of celiac disease and dermatitis herpetiformis in the UK over two decades: population-based study. Am J Gastroenterol. **109**, 757-768. https://doi.org/10.1038/ajg.2014.55.
116. Altobelli, E., Paduano, R., Petrocelli, R. & Di Orio, F. (2014). Burden of celiac disease in Europe: a review of its childhood and adulthood prevalence and incidence as of September 2014. Ann Ig. **26**, 485-498. https://doi.org/10.7416/ai.2014.2007.
117. Marild, K., Stephansson, O., Montgomery, S., Murray, J. A. & Ludvigsson, J. F. (2012). Pregnancy outcome and risk of celiac disease in offspring: a nationwide case-control study. Gastroenterology. **142**, 39-45 e33. https://doi.org/10.1053/j.gastro.2011.09.047.

118. Catassi, C. & Fasano, A. (2008). Celiac disease. Curr Opin Gastroenterol. **24**, 687-691. https://doi.org/10.1097/MOG.0b013e32830edc1e.
119. Sollid, L. M. (2000). Molecular basis of celiac disease. Annu Rev Immunol. **18**, 53-81. https://doi.org/10.1146/annurev.immunol.18.1.53.
120. Norris, J. M., Barriga, K., Hoffenberg, E. J., Taki, I., Miao, D., Haas, J. E., Emery, L. M., Sokol, R. J., Erlich, H. A., Eisenbarth, G. S. & Rewers, M. (2005). Risk of celiac disease autoimmunity and timing of gluten introduction in the diet of infants at increased risk of disease. JAMA. **293**, 2343-2351. https://doi.org/10.1001/jama.293.19.2343.
121. Stene, L. C., Honeyman, M. C., Hoffenberg, E. J., Haas, J. E., Sokol, R. J., Emery, L., Taki, I., Norris, J. M., Erlich, H. A., Eisenbarth, G. S. & Rewers, M. (2006). Rotavirus infection frequency and risk of celiac disease autoimmunity in early childhood: a longitudinal study. Am J Gastroenterol. **101**, 2333-2340. https://doi.org/10.1111/j.1572-0241.2006.00741.x.
122. Sollid, L. M. & Jabri, B. (2013). Triggers and drivers of autoimmunity: lessons from coeliac disease. Nat Rev Immunol. **13**, 294-302. https://doi.org/10.1038/nri3407.
123. Fasano, A. (2012). Leaky gut and autoimmune diseases. Clin Rev Allergy Immunol. **42**, 71-78. https://doi.org/10.1007/s12016-011-8291-x.
124. Molberg, O., McAdam, S. N., Korner, R., Quarsten, H., Kristiansen, C., Madsen, L., Fugger, L., Scott, H., Noren, O., Roepstorff, P., Lundin, K. E., Sjostrom, H. & Sollid, L. M. (1998). Tissue transglutaminase selectively modifies gliadin peptides that are recognized by gut-derived T cells in celiac disease. Nat Med. **4**, 713-717. https://doi.org/10.1038/nm0698-713.
125. Green, P. H. & Cellier, C. (2007). Celiac disease. N Engl J Med. **357**, 1731-1743. https://doi.org/10.1056/NEJMra071600.
126. Dieterich, W., Ehnis, T., Bauer, M., Donner, P., Volta, U., Riecken, E. O. & Schuppan, D. (1997). Identification of tissue transglutaminase as the autoantigen of celiac disease. Nat Med. **3**, 797-801. https://doi.org/DOI 10.1038/nm0797-797.
127. Jabri, B. & Sollid, L. M. (2009). Tissue-mediated control of immunopathology in coeliac disease. Nat Rev Immunol. **9**, 858-870. https://doi.org/10.1038/nri2670.
128. Sapone, A., de Magistris, L., Pietzak, M., Clemente, M. G., Tripathi, A., Cucca, F., Lampis, R., Kryszak, D., Carteni, M., Generoso, M., Iafusco, D., Prisco, F., Laghi, F., Riegler, G., Carratu, R., Counts, D. & Fasano, A. (2006). Zonulin upregulation is associated with increased gut permeability in subjects with type 1 diabetes and their relatives. Diabetes. **55**, 1443-1449. https://doi.org/10.2337/db05-1593.
129. Szajewska, H., Shamir, R., Chmielewska, A., Piescik-Lech, M., Auricchio, R., Ivarsson, A., Kolacek, S., Koletzko, S., Korponay-Szabo, I., Mearin, M. L., Ribes-Koninckx, C., Troncone, R. & Group, P. S. (2015). Systematic review with meta-analysis: early infant feeding and coeliac disease--update 2015. Aliment Pharmacol Ther. **41**, 1038-1054. https://doi.org/10.1111/apt.13163.
130. Szajewska, H., Shamir, R., Strozyk, A., Chmielewska, A., Zalewski, B. M., Auricchio, R., Koletzko, S., Korponay-Szabo, I. R., Mearin, M. L., Meijer, C., Ribes-Koninckx, C., Troncone, R. & Prevent, C. D. p. g. (2023). Systematic review: early feeding practices and the risk of coeliac disease. A 2022 update and revision. Aliment Pharmacol Ther. **57**, 8-22. https://doi.org/10.1111/apt.17290.

131. Marasco, G., Di Biase, A. R., Schiumerini, R., Eusebi, L. H., Iughetti, L., Ravaioli, F., Scaioli, E., Colecchia, A. & Festi, D. (2016). Gut Microbiota and Celiac Disease. Dig Dis Sci. **61**, 1461-1472. https://doi.org/10.1007/s10620-015-4020-2.
132. Scaramuzza, A. E., Mantegazza, C., Bosetti, A. & Zuccotti, G. V. (2013). Type 1 diabetes and celiac disease: The effects of gluten free diet on metabolic control. World J Diabetes. **4**, 130-134. https://doi.org/10.4239/wjd.v4.i4.130.
133. Cornell, H. J., Macrae, F. A., Melny, J., Pizzey, C. J., Cook, F., Mason, S., Bhathal, P. S. & Stelmasiak, T. (2005). Enzyme therapy for management of coeliac disease. Scand J Gastroenterol. **40**, 1304-1312. https://doi.org/10.1080/00365520510023855.
134. Konig, J., Holster, S., Bruins, M. J. & Brummer, R. J. (2017). Randomized clinical trial: Effective gluten degradation by Aspergillus niger-derived enzyme in a complex meal setting. Sci Rep. **7**, 13100. https://doi.org/10.1038/s41598-017-13587-7.
135. Wei, G., Helmerhorst, E. J., Darwish, G., Blumenkranz, G. & Schuppan, D. (2020). Gluten Degrading Enzymes for Treatment of Celiac Disease. Nutrients. **12**. https://doi.org/10.3390/nu12072095.
136. Janssen, G., Christis, C., Kooy-Winkelaar, Y., Edens, L., Smith, D., van Veelen, P. & Koning, F. (2015). Ineffective degradation of immunogenic gluten epitopes by currently available digestive enzyme supplements. PLoS One. **10**, e0128065. https://doi.org/10.1371/journal.pone.0128065.
137. BeyondCeliac.org (2024). DRUG DEVELOPMENT PIPELINE. https://www.beyondceliac.org/research/drugdevelopment/drug-development-pipeline/ (accessed 17.06.2024)
138. Schuppan, D., Maki, M., Lundin, K. E. A., Isola, J., Friesing-Sosnik, T., Taavela, J., Popp, A., Koskenpato, J., Langhorst, J., Hovde, O., Lahdeaho, M. L., Fusco, S., Schumann, M., Torok, H. P., Kupcinskas, J., Zopf, Y., Lohse, A. W., Scheinin, M., Kull, K., Biedermann, L., Byrnes, V., Stallmach, A., Jahnsen, J., Zeitz, J., Mohrbacher, R., Greinwald, R. & Group, C. E. C. T. (2021). A Randomized Trial of a Transglutaminase 2 Inhibitor for Celiac Disease. N Engl J Med. **385**, 35-45. https://doi.org/10.1056/NEJMoa2032441.
139. TOPAS-Therapeutics (2023). Topas Therapeutics Initiates Phase 2a Clinical Trial for TPM502 in Celiac Disease; Appoints Chief Business Officer and Chief Operating Officer.
140. Murray, J. A., Wassaf, D., Dunn, K., Arora, S., Winkle, P., Stacey, H., Cooper, S., Goldstein, K. E., Manchanda, R., Kontos, S. & Grebe, K. M. (2023). Safety and tolerability of KAN-101, a liver-targeted immune tolerance therapy, in patients with coeliac disease (ACeD): a phase 1 trial. Lancet Gastroenterol Hepatol. **8**, 735-747. https://doi.org/10.1016/S2468-1253(23)00107-3.
141. anokion (2024). ACeD-it Study - Phase 1b/2 Assessment of KAN-101 in Celiac Disease and Immune Tolerance. https://anokion.com/pipeline/aced-it-clinical-trial-study/ (accessed 07.07.2024)
142. anokion (2024). SynCeD Study - Phase 2A Study of KAN-101 Histologic Protection in Celiac Disease. https://anokion.com/pipeline/synced/#synced_study (accessed 07.07.2024)
143. Okura, Y., Ikawa-Teranishi, Y., Mizoroki, A., Takahashi, N., Tsushima, T., Irie, M., Harfuddin, Z., Miura-Okuda, M., Ito, S., Nakamura, G., Takesue, H., Ozono, Y., Nishihara, M., Yamada, K., Gan, S. W., Hayasaka, A., Ishii, S., Wakabayashi, T., Muraoka, M., Nagaya, N., Hino, H., Nemoto, T., Kuramochi,

T., Torizawa, T., Shimada, H., Kitazawa, T., Okazaki, M., Nezu, J., Sollid, L. M. & Igawa, T. (2023). Characterizations of a neutralizing antibody broadly reactive to multiple gluten peptide:HLA-DQ2.5 complexes in the context of celiac disease. Nat Commun. **14**, 8502. https://doi.org/10.1038/s41467-023-44083-4.

144. Hardy, M. Y., Henneken, L. M., Russell, A. K., Okura, Y., Mizoroki, A., Ozono, Y., Kobayashi, S., Murakami, Y. & Tye-Din, J. A. (2024). A bispecific antibody targeting HLA-DQ2.5-gluten peptides potently blocks gluten-specific T cells induced by gluten ingestion in patients with celiac disease. Clin Immunol. **264**, 110259. https://doi.org/10.1016/j.clim.2024.110259.
145. Lahdeaho, M. L., Scheinin, M., Vuotikka, P., Taavela, J., Popp, A., Laukkarinen, J., Koffert, J., Koivurova, O. P., Pesu, M., Kivela, L., Lovro, Z., Keisala, J., Isola, J., Parnes, J. R., Leon, F. & Maki, M. (2019). Safety and efficacy of AMG 714 in adults with coeliac disease exposed to gluten challenge: a phase 2a, randomised, double-blind, placebo-controlled study. Lancet Gastroenterol Hepatol. **4**, 948-959. https://doi.org/10.1016/S2468-1253(19)30264-X.
146. Cellier, C., Bouma, G., van Gils, T., Khater, S., Malamut, G., Crespo, L., Collin, P., Green, P. H. R., Crowe, S. E., Tsuji, W., Butz, E., Cerf-Bensussan, N., Macintyre, E., Parnes, J. R., Leon, F., Hermine, O., Mulder, C. J. & Investigators, R.-I. S. G. (2019). Safety and efficacy of AMG 714 in patients with type 2 refractory coeliac disease: a phase 2a, randomised, double-blind, placebo-controlled, parallel-group study. Lancet Gastroenterol Hepatol. **4**, 960-970. https://doi.org/10.1016/S2468-1253(19)30265-1.
147. West, J., Logan, R. F., Card, T. R., Smith, C. & Hubbard, R. (2004). Risk of vascular disease in adults with diagnosed coeliac disease: a population-based study. Aliment Pharmacol Ther. **20**, 73-79. https://doi.org/10.1111/j.1365-2036.2004.02008.x.
148. Ludvigsson, J. F., de Faire, U., Ekbom, A. & Montgomery, S. M. (2007). Vascular disease in a population-based cohort of individuals hospitalised with coeliac disease. Heart. **93**, 1111-1115. https://doi.org/10.1136/hrt.2006.097097.
149. Wei, L., Spiers, E., Reynolds, N., Walsh, S., Fahey, T. & MacDonald, T. M. (2008). The association between coeliac disease and cardiovascular disease. Aliment Pharmacol Ther. **27**, 514-519. https://doi.org/10.1111/j.1365-2036.2007.03594.x.
150. Emilsson, L., Smith, J. G., West, J., Melander, O. & Ludvigsson, J. F. (2011). Increased risk of atrial fibrillation in patients with coeliac disease: a nationwide cohort study. Eur Heart J. **32**, 2430-2437. https://doi.org/10.1093/eurheartj/ehr167.
151. Ludvigsson, J. F., James, S., Askling, J., Stenestrand, U. & Ingelsson, E. (2011). Nationwide Cohort Study of Risk of Ischemic Heart Disease in Patients With Celiac Disease. Circulation. **123**, 483-490. https://doi.org/10.1161/circulationaha.110.965624.
152. Ludvigsson, J. F., West, J., Card, T. & Appelros, P. (2012). Risk of stroke in 28,000 patients with celiac disease: a nationwide cohort study in Sweden. J Stroke Cerebrovasc Dis. **21**, 860-867. https://doi.org/10.1016/j.jstrokecerebrovasdis.2011.05.008.
153. Sari, C., Bayram, N. A., Dogan, F. E., Bastug, S., Bolat, A. D., Sari, S. O., Ersoy, O. & Bozkurt, E. (2012). The evaluation of endothelial functions in patients

with celiac disease. Echocardiography. **29**, 471-477. https://doi.org/10.1111/j.1540-8175.2011.01598.x.
154. De Marchi, S., Chiarioni, G., Prior, M. & Arosio, E. (2013). Young adults with coeliac disease may be at increased risk of early atherosclerosis. Aliment Pharmacol Ther. **38**, 162-169. https://doi.org/10.1111/apt.12360.
155. Emilsson, L., Lebwohl, B., Sundstrom, J. & Ludvigsson, J. F. (2015). Cardiovascular disease in patients with coeliac disease: A systematic review and meta-analysis. Dig Liver Dis. **47**, 847-852. https://doi.org/10.1016/j.dld.2015.06.004.
156. Heikkila, K., Koskinen, O. A., Agarwal, A., Tikkinen, K. A. O., Maki, M. & Kaukinen, K. (2015). Associations of coeliac disease with coronary heart disease and cerebrovascular disease: A systematic review and meta-analysis. Nutr Metab Cardiovasc Dis. **25**, 816-831. https://doi.org/10.1016/j.numecd.2015.05.004.
157. Ciaccio, E. J., Lewis, S. K., Biviano, A. B., Iyer, V., Garan, H. & Green, P. H. (2017). Cardiovascular involvement in celiac disease. World J Cardiol. **9**, 652-666. https://doi.org/10.4330/wjc.v9.i8.652.
158. Gajulapalli, R. D. & Pattanshetty, D. J. (2017). Risk of coronary artery disease in celiac disease population. Saudi J Gastroenterol. **23**, 253-258. https://doi.org/10.4103/sjg.SJG_616_16.
159. Potter, M. D. E., Brienesse, S. C., Walker, M. M., Boyle, A. & Talley, N. J. (2018). Effect of the gluten-free diet on cardiovascular risk factors in patients with coeliac disease: A systematic review. J Gastroenterol Hepatol. **33**, 781-791. https://doi.org/10.1111/jgh.14039.
160. Lebwohl, B., Green, P. H. R., Soderling, J., Roelstraete, B. & Ludvigsson, J. F. (2020). Association Between Celiac Disease and Mortality Risk in a Swedish Population. JAMA. **323**, 1277-1285. https://doi.org/10.1001/jama.2020.1943.
161. Naaraayan, A., Nimkar, A., Jesmajian, S., Gitler, B. & Acharya, P. (2021). Atherosclerotic Cardiovascular Disease Prevalence Among Patients With Celiac Disease in the United States: An Observational Study. Mayo Clin Proc. **96**, 666-676. https://doi.org/10.1016/j.mayocp.2020.04.051.
162. Fousekis, F. S., Beka, E. T., Mitselos, I. V., Milionis, H. & Christodoulou, D. K. (2021). Thromboembolic complications and cardiovascular events associated with celiac disease. Ir J Med Sci. **190**, 133-141. https://doi.org/10.1007/s11845-020-02315-2.
163. Huang, J. (2022). Assessment of the causal association between celiac disease and cardiovascular diseases. Front Cardiovasc Med. **9**, 1017209. https://doi.org/10.3389/fcvm.2022.1017209.
164. Haider, M. B., Naylor, P., Das, A., Haider, S. M. & Ehrinpreis, M. N. (2022). Celiac Disease Patients With Coronary Artery Disease: A Nationwide Population-Based Study. Cureus. **14**, e26151. https://doi.org/10.7759/cureus.26151.
165. Dore, M. P., Mereu, S., Saba, P. S., Portoghese, M. & Pes, G. M. (2023). Celiac Disease and Cardiovascular Risk: A Retrospective Case-Control Study. J Clin Med. **12**. https://doi.org/10.3390/jcm12062087.
166. Wang, Y., Chen, B., Ciaccio, E. J., Jneid, H., Virani, S. S., Lavie, C. J., Lebovits, J., Green, P. H. R. & Krittanawong, C. (2023). Celiac Disease and the Risk of Cardiovascular Diseases. Int J Mol Sci. **24**. https://doi.org/10.3390/ijms24129974.
167. Conroy, M., Allen, N., Lacey, B., Soilleux, E. & Littlejohns, T. (2023). Association between coeliac disease and cardiovascular disease: prospective analysis of

UK Biobank data. BMJ Med. **2**, e000371. https://doi.org/10.1136/bmjmed-2022-000371.
168. Milutinovic, S., Jancic, P., Adam, A., Radovanovic, M., Nordstrom, C. W., Ward, M., Petrovic, M., Jevtic, D., Delibasic, M., Kotseva, M., Nikolajevic, M. & Dumic, I. (2024). Cardiomyopathy in Celiac Disease: A Systematic Review. J Clin Med. **13**. https://doi.org/10.3390/jcm13041045.
169. Corrao, G., Corazza, G. R., Bagnardi, V., Brusco, G., Ciacci, C., Cottone, M., Sategna Guidetti, C., Usai, P., Cesari, P., Pelli, M. A., Loperfido, S., Volta, U., Calabro, A., Certo, M. & Club del Tenue Study, G. (2001). Mortality in patients with coeliac disease and their relatives: a cohort study. Lancet. **358**, 356-361. https://doi.org/10.1016/s0140-6736(01)05554-4.
170. West, J., Logan, R. F., Smith, C. J., Hubbard, R. B. & Card, T. R. (2004). Malignancy and mortality in people with coeliac disease: population based cohort study. BMJ. **329**, 716-719. https://doi.org/10.1136/bmj.38169.486701.7C.
171. Anderson, L. A., McMillan, S. A., Watson, R. G., Monaghan, P., Gavin, A. T., Fox, C. & Murray, L. J. (2007). Malignancy and mortality in a population-based cohort of patients with coeliac disease or "gluten sensitivity". World J Gastroenterol. **13**, 146-151. https://doi.org/10.3748/wjg.v13.i1.146.
172. Tierschutzgesetz (TierSchG)/ German Animal Welfare Act. https://www.gesetze-im-internet.de/tierschg/BJNR012770972.html
173. Galipeau, H. J., Rulli, N. E., Jury, J., Huang, X., Araya, R., Murray, J. A., David, C. S., Chirdo, F. G., McCoy, K. D. & Verdu, E. F. (2011). Sensitization to gliadin induces moderate enteropathy and insulitis in nonobese diabetic-DQ8 mice. J Immunol. **187**, 4338-4346. https://doi.org/10.4049/jimmunol.1100854.
174. Marietta, E., Black, K., Camilleri, M., Krause, P., Rogers, R. S., David, C., Pittelkow, M. R. & Murray, J. A. (2004). A new model for dermatitis herpetiformis that uses HLA-DQ8 transgenic NOD mice. Journal of Clinical Investigation. **114**, 1090-1097. https://doi.org/10.1172/jci200421055.
175. Sollid, L. M. (2002). Coeliac disease: dissecting a complex inflammatory disorder. Nat Rev Immunol. **2**, 647-655. https://doi.org/10.1038/nri885.
176. Thomas, K. E., Sapone, A., Fasano, A. & Vogel, S. N. (2006). Gliadin stimulation of murine macrophage inflammatory gene expression and intestinal permeability are MyD88-dependent: role of the innate immune response in Celiac disease. J Immunol. **176**, 2512-2521. https://doi.org/10.4049/jimmunol.176.4.2512.
177. Lammi, A., Arikoski, P., Vaarala, O., Kinnunen, T. & Ilonen, J. (2012). Increased peripheral blood CD4+ T cell responses to deamidated but not to native gliadin in children with coeliac disease. Clin Exp Immunol. **168**, 207-214. https://doi.org/10.1111/j.1365-2249.2012.04575.x.
178. Shewry, P. R. & Halford, N. G. (2002). Cereal seed storage proteins: structures, properties and role in grain utilization. J Exp Bot. **53**, 947-958. https://doi.org/10.1093/jexbot/53.370.947.
179. van de Wal, Y., Kooy, Y., van Veelen, P., Pena, S., Mearin, L., Papadopoulos, G. & Koning, F. (1998). Selective deamidation by tissue transglutaminase strongly enhances gliadin-specific T cell reactivity. J Immunol. **161**, 1585-1588.
180. Zhou, L., Kooy-Winkelaar, Y. M. C., Cordfunke, R. A., Dragan, I., Thompson, A., Drijfhout, J. W., van Veelen, P. A., Chen, H. & Koning, F. (2017). Abrogation of Immunogenic Properties of Gliadin Peptides through

Transamidation by Microbial Transglutaminase Is Acyl-Acceptor Dependent. J Agric Food Chem. **65**, 7542-7552. https://doi.org/10.1021/acs.jafc.7b02557.
181. Aldrich, S. (1994). Enzymatic Assay of TRANSGLUTAMINASE (EC 2.3.2.13). In SIGMA QUALITY CONTROL TEST PROCEDURE - (T5398) - Enzyme Assay Sigma Aldrich, https://www.sigmaaldrich.com/DE/en/product/sigma/t5398#product-documentation.
182. Folk, J. E. & Cole, P. W. (1966). Transglutaminase: mechanistic features of the active site as determined by kinetic and inhibitor studies. Biochim Biophys Acta. **122**, 244-264. https://doi.org/10.1016/0926-6593(66)90066-x.
183. Galipeau, H. J., McCarville, J. L., Huebener, S., Litwin, O., Meisel, M., Jabri, B., Sanz, Y., Murray, J. A., Jordana, M., Alaedini, A., Chirdo, F. G. & Verdu, E. F. (2015). Intestinal microbiota modulates gluten-induced immunopathology in humanized mice. Am J Pathol. **185**, 2969-2982. https://doi.org/10.1016/j.ajpath.2015.07.018.
184. Keppeler, K., Pesi, A., Lange, S., Helmstadter, J., Strohm, L., Ubbens, H., Kuntic, M., Kuntic, I., Mihalikova, D., Vujacic-Mirski, K., Rosenberger, A., Kuster, L., Frank, C., Oelze, M., Finger, S., Zakrzewska, A., Verdu, E., Wild, J., Karbach, S., Wenzel, P., Wild, P., Leistner, D., Munzel, T., Daiber, A., Schuppan, D. & Steven, S. (2024). Vascular dysfunction and arterial hypertension in experimental celiac disease are mediated by gut-derived inflammation and oxidative stress. Redox Biol. **70**, 103071. https://doi.org/10.1016/j.redox.2024.103071.
185. Feng, M., Whitesall, S., Zhang, Y., Beibel, M., D'Alecy, L. & DiPetrillo, K. (2008). Validation of volume-pressure recording tail-cuff blood pressure measurements. Am J Hypertens. **21**, 1288-1291. https://doi.org/10.1038/ajh.2008.301.
186. Wang, Y., Thatcher, S. E. & Cassis, L. A. (2017). Measuring Blood Pressure Using a Noninvasive Tail Cuff Method in Mice. Methods Mol Biol. **1614**, 69-73. https://doi.org/10.1007/978-1-4939-7030-8_6.
187. Wild, J., Ringen, J., Bieler, T., Knopp, T., Lagrange, J., Molitor, M., Sies, K., Kropp, A., Keller, K., Daiber, A., Munzel, T., Rauh, M., Waisman, A., Wenzel, P., Titze, J. & Karbach, S. (2022). Epicutaneous Application of Imiquimod to Model Psoriasis-Like Skin Disease Induces Water-Saving Aestivation Motifs and Vascular Inflammation. J Invest Dermatol. **142**, 3117-3120 e3112. https://doi.org/10.1016/j.jid.2022.04.023.
188. Finger, S., Knorr, M., Molitor, M., Schuler, R., Garlapati, V., Waisman, A., Brandt, M., Munzel, T., Bopp, T., Kossmann, S., Karbach, S. & Wenzel, P. (2019). A sequential interferon gamma directed chemotactic cellular immune response determines survival and cardiac function post-myocardial infarction. Cardiovasc Res. **115**, 1907-1917. https://doi.org/10.1093/cvr/cvz092.
189. Kroller-Schon, S., Daiber, A. & Schulz, E. (2018). Modulation of Vascular Function by AMPK: Assessment of NO Bioavailability and Surrogates of Oxidative Stress. Methods Mol Biol. **1732**, 495-506. https://doi.org/10.1007/978-1-4939-7598-3_31.
190. de Carvalho, H. F. & Taboga, S. R. (1996). Fluorescence and confocal laser scanning microscopy imaging of elastic fibers in hematoxylin-eosin stained sections. Histochem Cell Biol. **106**, 587-592. https://doi.org/10.1007/BF02473274.

191. Shu, J., Dolman, G. E., Duan, J., Qiu, G. & Ilyas, M. (2016). Statistical colour models: an automated digital image analysis method for quantification of histological biomarkers. Biomed Eng Online. **15**, 46. https://doi.org/10.1186/s12938-016-0161-6.
192. Kiouptsi, K., Pontarollo, G., Todorov, H., Braun, J., Jackel, S., Koeck, T., Bayer, F., Karwot, C., Karpi, A., Gerber, S., Jansen, Y., Wild, P., Ruf, W., Daiber, A., Van Der Vorst, E., Weber, C., Doring, Y. & Reinhardt, C. (2020). Germ-free housing conditions do not affect aortic root and aortic arch lesion size of late atherosclerotic low-density lipoprotein receptor-deficient mice. Gut Microbes. **11**, 1809-1823. https://doi.org/10.1080/19490976.2020.1767463.
193. Picot, J., Guerin, C. L., Le Van Kim, C. & Boulanger, C. M. (2012). Flow cytometry: retrospective, fundamentals and recent instrumentation. Cytotechnology. **64**, 109-130. https://doi.org/10.1007/s10616-011-9415-0.
194. Helmstadter, J., Frenis, K., Filippou, K., Grill, A., Dib, M., Kalinovic, S., Pawelke, F., Kus, K., Kroller-Schon, S., Oelze, M., Chlopicki, S., Schuppan, D., Wenzel, P., Ruf, W., Drucker, D. J., Munzel, T., Daiber, A. & Steven, S. (2020). Endothelial GLP-1 (Glucagon-Like Peptide-1) Receptor Mediates Cardiovascular Protection by Liraglutide In Mice With Experimental Arterial Hypertension. Arterioscler Thromb Vasc Biol. **40**, 145-158. https://doi.org/10.1161/atv.0000615456.97862.30.
195. Lopes, R. B., Valldecabres, A. & Silva-Del-Rio, N. (2019). Technical note: Glucose concentration in dairy cows measured using 6 handheld meters designed for human use. J Dairy Sci. **102**, 9401-9408. https://doi.org/10.3168/jds.2018-15688.
196. Beemer, O., Byers, S. & Bohn, A. (2013). Evaluation of four point-of-care glucose meters in alpacas. J Vet Intern Med. **27**, 990-995. https://doi.org/10.1111/jvim.12115.
197. Stahler, F., Munz, E. & Kattermann, R. (1975). [Enzymatic determination of total cholesterol in serum: accuracy and comparison with other methods (author's transl)]. Dtsch Med Wochenschr. **100**, 876-880, 885-877. https://doi.org/10.1055/s-0028-1106309.
198. Susilowati, R. & Setiawan, A. M. (2020). Cinnamomum burmannii (Nees & T. Nees) Blume and Eleutherine palmifolia (L.) Merr. extract combination ameliorate lipid profile and heart oxidative stress in hyperlipidemic mice. Vet World. **13**, 1404-1409. https://doi.org/10.14202/vetworld.2020.1404-1409.
199. O'Connell, K. E., Mikkola, A. M., Stepanek, A. M., Vernet, A., Hall, C. D., Sun, C. C., Yildirim, E., Staropoli, J. F., Lee, J. T. & Brown, D. E. (2015). Practical murine hematopathology: a comparative review and implications for research. Comp Med. **65**, 96-113.
200. Daiber, A., August, M., Baldus, S., Wendt, M., Oelze, M., Sydow, K., Kleschyov, A. L. & Munzel, T. (2004). Measurement of NAD(P)H oxidase-derived superoxide with the luminol analogue L-012. Free Radic Biol Med. **36**, 101-111. https://doi.org/10.1016/j.freeradbiomed.2003.10.012.
201. Steven, S., Frenis, K., Kalinovic, S., Kvandova, M., Oelze, M., Helmstadter, J., Hahad, O., Filippou, K., Kus, K., Trevisan, C., Schluter, K. D., Boengler, K., Chlopicki, S., Frauenknecht, K., Schulz, R., Sorensen, M., Daiber, A., Kroller-Schon, S. & Munzel, T. (2020). Exacerbation of adverse cardiovascular effects of aircraft noise in an animal model of arterial hypertension. Redox Biol. **34**, 101515. https://doi.org/10.1016/j.redox.2020.101515.
202. Kij, A., Mateuszuk, L., Sitek, B., Przyborowski, K., Zakrzewska, A., Wandzel, K., Walczak, M. & Chlopicki, S. (2016). Simultaneous quantification of PGI2

and TXA2 metabolites in plasma and urine in NO-deficient mice by a novel UHPLC/MS/MS method. J Pharm Biomed Anal. **129**, 148-154. https://doi.org/10.1016/j.jpba.2016.06.050.
203. Olink (2023). White paper - PEA: Exceptional specificity in a high multiplex format.
204. Engvall, E. & Perlmann, P. (1972). Enzyme-linked immunosorbent assay, Elisa. 3. Quantitation of specific antibodies by enzyme-labeled anti-immunoglobulin in antigen-coated tubes. J Immunol. **109**, 129-135.
205. Schuler, R., Brand, A., Klebow, S., Wild, J., Veras, F. P., Ullmann, E., Roohani, S., Kolbinger, F., Kossmann, S., Wohn, C., Daiber, A., Munzel, T., Wenzel, P., Waisman, A., Clausen, B. E. & Karbach, S. (2019). Antagonization of IL-17A Attenuates Skin Inflammation and Vascular Dysfunction in Mouse Models of Psoriasis. J Invest Dermatol. **139**, 638-647. https://doi.org/10.1016/j.jid.2018.09.021.
206. Chomczynski, P. & Sacchi, N. (1987). Single-step method of RNA isolation by acid guanidinium thiocyanate-phenol-chloroform extraction. Anal Biochem. **162**, 156-159. https://doi.org/10.1006/abio.1987.9999.
207. Bradford, M. M. (1976). A rapid and sensitive method for the quantitation of microgram quantities of protein utilizing the principle of protein-dye binding. Anal Biochem. **72**, 248-254. https://doi.org/10.1006/abio.1976.9999.
208. Knorr, M., Hausding, M., Kroller-Schuhmacher, S., Steven, S., Oelze, M., Heeren, T., Scholz, A., Gori, T., Wenzel, P., Schulz, E., Daiber, A. & Munzel, T. (2011). Nitroglycerin-induced endothelial dysfunction and tolerance involve adverse phosphorylation and S-Glutathionylation of endothelial nitric oxide synthase: beneficial effects of therapy with the AT1 receptor blocker telmisartan. Arterioscler Thromb Vasc Biol. **31**, 2223-2231. https://doi.org/10.1161/ATVBAHA.111.232058.
209. Encalada Ventura, M. A. (2020). Establishment and Validation of Mouse Models of Celiac Disease and the Pre-clinical Evaluation of a Novel Inhibitor of Tissue Transglutaminase ZED1227 to Treat Celiac Disease. Johannes Gutenberg-Universität Mainz.
210. Galipeau, H. (2015). EXPLORING NOVEL MECHANISMS AND THERAPIES FOR CELIAC DISEASE. In Medical Sciences (Division of Physiology/Pharmacology) McMaster University, MacSphere.
211. ter Steege, J., Buurman, W., Arends, J. W. & Forget, P. (1997). Presence of inducible nitric oxide synthase, nitrotyrosine, CD68, and CD14 in the small intestine in celiac disease. Lab Invest. **77**, 29-36.
212. Moss, S. F., Attia, L., Scholes, J. V., Walters, J. R. & Holt, P. R. (1996). Increased small intestinal apoptosis in coeliac disease. Gut. **39**, 811-817. https://doi.org/10.1136/gut.39.6.811.
213. Chen, D., Thayer, T. C., Wen, L. & Wong, F. S. (2020). Mouse Models of Autoimmune Diabetes: The Nonobese Diabetic (NOD) Mouse. Methods Mol Biol. **2128**, 87-92. https://doi.org/10.1007/978-1-0716-0385-7_6.
214. Taneja, V. & David, C. S. (2009). Spontaneous autoimmune myocarditis and cardiomyopathy in HLA-DQ8.NODAbo transgenic mice. J Autoimmun. **33**, 260-269. https://doi.org/10.1016/j.jaut.2009.09.005.
215. Agirman, G., Yu, K. B. & Hsiao, E. Y. (2021). Signaling inflammation across the gut-brain axis. Science. **374**, 1087-1092. https://doi.org/doi:10.1126/science.abi6087.
216. Kuntic, M., Kuntic, I., Krishnankutty, R., Gericke, A., Oelze, M., Junglas, T., Bayo Jimenez, M. T., Stamm, P., Nandudu, M., Hahad, O., Keppeler, K.,

Daub, S., Vujacic-Mirski, K., Rajlic, S., Strohm, L., Ubbens, H., Tang, Q., Jiang, S., Ruan, Y., Macleod, K. G., Steven, S., Berkemeier, T., Poschl, U., Lelieveld, J., Kleinert, H., von Kriegsheim, A., Daiber, A. & Munzel, T. (2023). Co-exposure to urban particulate matter and aircraft noise adversely impacts the cerebro-pulmonary-cardiovascular axis in mice. Redox Biol. **59**, 102580. https://doi.org/10.1016/j.redox.2022.102580.

217. Kuntic, M., Oelze, M., Steven, S., Kroller-Schon, S., Stamm, P., Kalinovic, S., Frenis, K., Vujacic-Mirski, K., Bayo Jimenez, M. T., Kvandova, M., Filippou, K., Al Zuabi, A., Bruckl, V., Hahad, O., Daub, S., Varveri, F., Gori, T., Huesmann, R., Hoffmann, T., Schmidt, F. P., Keaney, J. F., Daiber, A. & Munzel, T. (2019). Short-term e-cigarette vapour exposure causes vascular oxidative stress and dysfunction: evidence for a close connection to brain damage and a key role of the phagocytic NADPH oxidase (NOX-2). Eur Heart J. https://doi.org/10.1093/eurheartj/ehz772.
218. Nosalski, R. & Guzik, T. J. (2017). Perivascular adipose tissue inflammation in vascular disease. Br J Pharmacol. **174**, 3496-3513. https://doi.org/10.1111/bph.13705.
219. Kawai, T., Autieri, M. V. & Scalia, R. (2021). Adipose tissue inflammation and metabolic dysfunction in obesity. Am J Physiol Cell Physiol. **320**, C375-C391. https://doi.org/10.1152/ajpcell.00379.2020.
220. Marsh, M. N. (1992). Gluten, major histocompatibility complex, and the small intestine. A molecular and immunobiologic approach to the spectrum of gluten sensitivity ('celiac sprue'). Gastroenterology. **102**, 330-354.
221. Oberhuber, G. (2000). Histopathology of celiac disease. Biomed Pharmacother. **54**, 368-372. https://doi.org/10.1016/S0753-3322(01)80003-2.
222. FocusINCD (2022). Lesson 3 - Diagnosing Celiac Disease - 3.2 Biopsies and Histopathology. https://celiacfacts-onlinecourses.eu/mod/lesson/view.php?id=720&pageid=283 (accessed 22.06.2024)
223. Felber, J., Blaker, H., Fischbach, W., Koletzko, S., Laass, M., Lachmann, N., Lorenz, P., Lynen, P., Reese, I., Scherf, K., Schuppan, D., Schumann, M., Aust, D., Baas, S., Beisel, S., de Laffolie, J., Duba, E., Holtmeier, W., Lange, L., Loddenkemper, C., Moog, G., Rath, T., Roeb, E., Rubin, D., Stein, J., Torok, H. & Zopf, Y. (2022). Aktualisierte S2k-Leitlinie Zöliakie der Deutschen Gesellschaft für Gastroenterologie, Verdauungs- und Stoffwechselkrankheiten (DGVS). Z Gastroenterol. **60**, 790-856. https://doi.org/10.1055/a-1741-5946.
224. Godbout, J., Wulczynski, M., Galipeau, H. J., Constante, M., Ribeiro, T., Sloboda, D. & Verdu, E. (2022). A10 EARLY LIFE SENSITIZATION TO GLUTEN INDUCES SUSTAINED IMMUNOPATHOLOGY IN DR3-DQ2 MICE. Journal of the Canadian Association of Gastroenterology. **5**, 11-13. https://doi.org/10.1093/jcag/gwab049.009.
225. Clarizio, A. V., Galipeau, H. J., Jury, J., Rondeau, L., Godbout, J., Williams, L., Anderson, B. & Verdu, E. (2020). A19 NOVEL HLA-DQ2 TRANSGENIC MICE DEVELOP GLUTEN-IMMUNOPATHOLOGY FOLLOWING GLUTEN SENSITIZATION. Journal of the Canadian Association of Gastroenterology. **3**, 22-23. https://doi.org/10.1093/jcag/gwz047.018.
226. Mazzarella, G., Bergamo, P., Maurano, F., Luongo, D., Rotondi Aufiero, V., Bozzella, G., Palmieri, G., Troncone, R., Auricchio, S., David, C. & Rossi, M. (2014). Gliadin intake alters the small intestinal mucosa in indomethacin-

treated HLA-DQ8 transgenic mice. Am J Physiol Gastrointest Liver Physiol. **307**, G302-312. https://doi.org/10.1152/ajpgi.00002.2014.
227. Whelton, P. K., Carey, R. M., Aronow, W. S., Casey, D. E., Jr., Collins, K. J., Dennison Himmelfarb, C., DePalma, S. M., Gidding, S., Jamerson, K. A., Jones, D. W., MacLaughlin, E. J., Muntner, P., Ovbiagele, B., Smith, S. C., Jr., Spencer, C. C., Stafford, R. S., Taler, S. J., Thomas, R. J., Williams, K. A., Sr., Williamson, J. D. & Wright, J. T., Jr. (2018). 2017 ACC/AHA/AAPA/ABC/ACPM/AGS/APhA/ASH/ASPC/NMA/PCNA Guideline for the Prevention, Detection, Evaluation, and Management of High Blood Pressure in Adults: A Report of the American College of Cardiology/American Heart Association Task Force on Clinical Practice Guidelines. Hypertension. **71**, e13-e115. https://doi.org/10.1161/HYP.0000000000000065.
228. Stein, A. C., Liao, C., Paski, S., Polonsky, T., Semrad, C. E. & Kupfer, S. S. (2016). Obesity and Cardiovascular Risk in Adults With Celiac Disease. J Clin Gastroenterol. **50**, 545-550. https://doi.org/10.1097/MCG.0000000000000422.
229. Bayar, N., Cekin, A. H., Arslan, S., Cagirci, G., Kucukseymen, S., Cay, S., Harmandar, F. A. & Yesil, B. (2016). Assessment of Aortic Elasticity in Patients with Celiac Disease. Korean Circ J. **46**, 239-245. https://doi.org/10.4070/kcj.2016.46.2.239.
230. Riezzo, G., Ferreri, C., Orlando, A., Martulli, M., D'Attoma, B. & Russo, F. (2014). Lipidomic analysis of fatty acids in erythrocytes of coeliac patients before and after a gluten-free diet intervention: a comparison with healthy subjects. Br J Nutr. **112**, 1787-1796. https://doi.org/10.1017/S0007114514002815.
231. Tortora, R., Capone, P., De Stefano, G., Imperatore, N., Gerbino, N., Donetto, S., Monaco, V., Caporaso, N. & Rispo, A. (2015). Metabolic syndrome in patients with coeliac disease on a gluten-free diet. Aliment Pharmacol Ther. **41**, 352-359. https://doi.org/10.1111/apt.13062.
232. Ciacci, C., Cirillo, M., Giorgetti, G., Alfinito, F., Franchi, A., Mazzetti di Pietralata, M. & Mazzacca, G. (1999). Low plasma cholesterol: a correlate of nondiagnosed celiac disease in adults with hypochromic anemia. Am J Gastroenterol. **94**, 1888-1891. https://doi.org/10.1111/j.1572-0241.1999.01225.x.
233. Brar, P., Kwon, G. Y., Holleran, S., Bai, D., Tall, A. R., Ramakrishnan, R. & Green, P. H. (2006). Change in lipid profile in celiac disease: beneficial effect of gluten-free diet. Am J Med. **119**, 786-790. https://doi.org/10.1016/j.amjmed.2005.12.025.
234. Cakir, I. & Dogan, S. (2022). Association between systemic immune inflammation index and newly diagnosed adult celiac disease. Turkish Journal of Biochemistry. **47**, 59-64. https://doi.org/doi:10.1515/tjb-2021-0053.
235. Ye, Z., Hu, T., Wang, J., Xiao, R., Liao, X., Liu, M. & Sun, Z. (2022). Systemic immune-inflammation index as a potential biomarker of cardiovascular diseases: A systematic review and meta-analysis. Front Cardiovasc Med. **9**, 933913. https://doi.org/10.3389/fcvm.2022.933913.
236. Ma, J. & Li, K. (2023). Systemic immune-inflammation index is associated with coronary heart disease: a cross-sectional study of NHANES 2009-2018. Front Cardiovasc Med. **10**, 1199433. https://doi.org/10.3389/fcvm.2023.1199433.
237. Wolf, D. & Ley, K. (2019). Immunity and Inflammation in Atherosclerosis. Circ Res. **124**, 315-327. https://doi.org/10.1161/CIRCRESAHA.118.313591.

238. Pantic, N., Pantic, I., Jevtic, D., Mogulla, V., Oluic, S., Durdevic, M., Nordin, T., Jecmenica, M., Milovanovic, T., Gavrancic, T. & Dumic, I. (2022). Celiac Disease and Thrombotic Events: Systematic Review of Published Cases. Nutrients. **14**. https://doi.org/10.3390/nu14102162.
239. Bernardi, N., Sciatti, E., Pancaldi, E., Alghisi, F., Drera, A., Falco, R. & Vizzardi, E. (2022). Coeliac and cardiovascular disease: a possible relationship between two apparently separate conditions. Monaldi Arch Chest Dis. **93**. https://doi.org/10.4081/monaldi.2022.2366.
240. Elnour, S., Hashim, M. & Ibrahim, H. (2021). Dilated cardiomyopathy associated with celiac disease: A case report. Clin Case Rep. **9**, e04990. https://doi.org/10.1002/ccr3.4990.
241. Emilsson, L., Carlsson, R., James, S., Hambraeus, K. & Ludvigsson, J. F. (2015). Follow-up of ischaemic heart disease in patients with coeliac disease. Eur J Prev Cardiol. **22**, 83-90. https://doi.org/10.1177/2047487313502446.
242. Sapone, A., Lammers, K. M., Mazzarella, G., Mikhailenko, I., Carteni, M., Casolaro, V. & Fasano, A. (2010). Differential mucosal IL-17 expression in two gliadin-induced disorders: gluten sensitivity and the autoimmune enteropathy celiac disease. Int Arch Allergy Immunol. **152**, 75-80. https://doi.org/10.1159/000260087.
243. Monteleone, I., Sarra, M., Del Vecchio Blanco, G., Paoluzi, O. A., Franze, E., Fina, D., Fabrizi, A., MacDonald, T. T., Pallone, F. & Monteleone, G. (2010). Characterization of IL-17A-producing cells in celiac disease mucosa. J Immunol. **184**, 2211-2218. https://doi.org/10.4049/jimmunol.0901919.
244. Therrien, A., Kelly, C. P. & Silvester, J. A. (2020). Celiac Disease: Extraintestinal Manifestations and Associated Conditions. J Clin Gastroenterol. **54**, 8-21. https://doi.org/10.1097/MCG.0000000000001267.
245. von Stebut, E., Boehncke, W. H., Ghoreschi, K., Gori, T., Kaya, Z., Thaci, D. & Schaffler, A. (2019). IL-17A in Psoriasis and Beyond: Cardiovascular and Metabolic Implications. Front Immunol. **10**, 3096. https://doi.org/10.3389/fimmu.2019.03096.
246. Mills, K. H. G. (2023). IL-17 and IL-17-producing cells in protection versus pathology. Nat Rev Immunol. **23**, 38-54. https://doi.org/10.1038/s41577-022-00746-9.
247. Taleb, S., Tedgui, A. & Mallat, Z. (2015). IL-17 and Th17 Cells in Atherosclerosis. Arteriosclerosis, Thrombosis, and Vascular Biology. **35**, 258-264. https://doi.org/doi:10.1161/ATVBAHA.114.303567.
248. Rask-Madsen, C. & King, G. L. (2007). Mechanisms of Disease: endothelial dysfunction in insulin resistance and diabetes. Nat Clin Pract Endocrinol Metab. **3**, 46-56. https://doi.org/10.1038/ncpendmet0366.
249. Zou, M. H., Cohen, R. & Ullrich, V. (2004). Peroxynitrite and vascular endothelial dysfunction in diabetes mellitus. Endothelium. **11**, 89-97. https://doi.org/10.1080/10623320490482619.
250. Crow, J. P. & Beckman, J. S. (1995). Reactions between nitric oxide, superoxide, and peroxynitrite: footprints of peroxynitrite in vivo. Adv Pharmacol. **34**, 17-43. https://doi.org/10.1016/s1054-3589(08)61079-0.
251. Wenzel, P., Knorr, M., Kossmann, S., Stratmann, J., Hausding, M., Schuhmacher, S., Karbach, S. H., Schwenk, M., Yogev, N., Schulz, E., Oelze, M., Grabbe, S., Jonuleit, H., Becker, C., Daiber, A., Waisman, A. & Munzel, T. (2011). Lysozyme M-positive monocytes mediate angiotensin II-induced arterial hypertension and vascular dysfunction. Circulation. **124**, 1370-1381. https://doi.org/10.1161/CIRCULATIONAHA.111.034470.

252. Youn, J. C., Yu, H. T., Lim, B. J., Koh, M. J., Lee, J., Chang, D. Y., Choi, Y. S., Lee, S. H., Kang, S. M., Jang, Y., Yoo, O. J., Shin, E. C. & Park, S. (2013). Immunosenescent CD8+ T cells and C-X-C chemokine receptor type 3 chemokines are increased in human hypertension. Hypertension. **62**, 126-133. https://doi.org/10.1161/HYPERTENSIONAHA.113.00689.
253. Caillon, A., Mian, M. O. R., Fraulob-Aquino, J. C., Huo, K. G., Barhoumi, T., Ouerd, S., Sinnaeve, P. R., Paradis, P. & Schiffrin, E. L. (2017). gammadelta T Cells Mediate Angiotensin II-Induced Hypertension and Vascular Injury. Circulation. **135**, 2155-2162. https://doi.org/10.1161/CIRCULATIONAHA.116.027058.
254. Cave, A. C., Brewer, A. C., Narayanapanicker, A., Ray, R., Grieve, D. J., Walker, S. & Shah, A. M. (2006). NADPH oxidases in cardiovascular health and disease. Antioxid Redox Signal. **8**, 691-728. https://doi.org/10.1089/ars.2006.8.691.
255. Ryu, H. & Chung, Y. (2015). Regulation of IL-17 in atherosclerosis and related autoimmunity. Cytokine. **74**, 219-227. https://doi.org/10.1016/j.cyto.2015.03.009.
256. Wang, Y., Zang, J., Liu, C., Yan, Z. & Shi, D. (2022). Interleukin-17 Links Inflammatory Cross-Talks Between Comorbid Psoriasis and Atherosclerosis. Front Immunol. **13**, 835671. https://doi.org/10.3389/fimmu.2022.835671.
257. Nguyen, H., Chiasson, V. L., Chatterjee, P., Kopriva, S. E., Young, K. J. & Mitchell, B. M. (2012). Interleukin-17 causes Rho-kinase-mediated endothelial dysfunction and hypertension. Cardiovascular Research. **97**, 696-704. https://doi.org/10.1093/cvr/cvs422.
258. Tamehiro, N., Nishida, K., Yanobu-Takanashi, R., Goto, M., Okamura, T. & Suzuki, H. (2017). T-cell activation RhoGTPase-activating protein plays an important role in T(H)17-cell differentiation. Immunol Cell Biol. **95**, 729-735. https://doi.org/10.1038/icb.2017.27.
259. Myrsky, E., Caja, S., Simon-Vecsei, Z., Korponay-Szabo, I. R., Nadalutti, C., Collighan, R., Mongeot, A., Griffin, M., Maki, M., Kaukinen, K. & Lindfors, K. (2009). Celiac disease IgA modulates vascular permeability in vitro through the activity of transglutaminase 2 and RhoA. Cell Mol Life Sci. **66**, 3375-3385. https://doi.org/10.1007/s00018-009-0116-1.
260. Aboulaghras, S., Piancatelli, D., Taghzouti, K., Balahbib, A., Alshahrani, M. M., Al Awadh, A. A., Goh, K. W., Ming, L. C., Bouyahya, A. & Oumhani, K. (2023). Meta-Analysis and Systematic Review of HLA DQ2/DQ8 in Adults with Celiac Disease. Int J Mol Sci. **24**. https://doi.org/10.3390/ijms24021188.
261. Abadie, V., Kim, S. M., Lejeune, T., Palanski, B. A., Ernest, J. D., Tastet, O., Voisine, J., Discepolo, V., Marietta, E. V., Hawash, M. B. F., Ciszewski, C., Bouziat, R., Panigrahi, K., Horwath, I., Zurenski, M. A., Lawrence, I., Dumaine, A., Yotova, V., Grenier, J. C., Murray, J. A., Khosla, C., Barreiro, L. B. & Jabri, B. (2020). IL-15, gluten and HLA-DQ8 drive tissue destruction in coeliac disease. Nature. **578**, 600-604. https://doi.org/10.1038/s41586-020-2003-8.
262. Batt, R. M., Carter, M. W. & McLean, L. (1984). Morphological and biochemical studies of a naturally occurring enteropathy in the Irish setter dog: a comparison with coeliac disease in man. Res Vet Sci. **37**, 339-346.
263. Bethune, M. T., Ribka, E., Khosla, C. & Sestak, K. (2008). Transepithelial transport and enzymatic detoxification of gluten in gluten-sensitive rhesus macaques. PLoS One. **3**, e1857. https://doi.org/10.1371/journal.pone.0001857.

264. Chen, D., Ueda, R., Harding, F., Patil, N., Mao, Y., Kurahara, C., Platenburg, G. & Huang, M. (2003). Characterization of HLA DR3/DQ2 transgenic mice: a potential humanized animal model for autoimmune disease studies. Eur J Immunol. **33**, 172-182. https://doi.org/10.1002/immu.200390020.
265. Harris, R. L., Streett, J. W., Morrow, D. & Lord, P. F. (1984). Villus atrophy and malabsorption in a rhesus monkey. Lab Anim Sci. **34**, 610-613.
266. Polvi, A., Garden, O. A., Houlston, R. S., Maki, M., Batt, R. M. & Partanen, J. (1998). Genetic susceptibility to gluten sensitive enteropathy in Irish setter dogs is not linked to the major histocompatibility complex. Tissue Antigens. **52**, 543-549. https://doi.org/10.1111/j.1399-0039.1998.tb03085.x.
267. Guo, L., Liu, M. F., Huang, J. N., Li, J. M., Jiang, J. & Wang, J. A. (2020). Role of interleukin-15 in cardiovascular diseases. J Cell Mol Med. **24**, 7094-7101. https://doi.org/10.1111/jcmm.15296.
268. Colquitt, R. B., Colquhoun, D. A. & Thiele, R. H. (2011). In silico modelling of physiologic systems. Best Pract Res Clin Anaesthesiol. **25**, 499-510. https://doi.org/10.1016/j.bpa.2011.08.006.
269. Jean-Quartier, C., Jeanquartier, F., Jurisica, I. & Holzinger, A. (2018). In silico cancer research towards 3R. BMC Cancer. **18**, 408. https://doi.org/10.1186/s12885-018-4302-0.
270. S. Lange , K. K., A. Pesi, M. Neerukonda, H. Ubbens, L. Strohm, I. Kuntic, M. Kuntic, A. Rosenberger, E. Verdu, D. Schuppan, P. Lurz, A. Daiber, D. Leistner, S. Steven (2024). Gender differences in a murine celiac disease model - effects on the cardiovascular system. Clinical Research in Cardiology. **113**, 1285-1285. https://doi.org/10.1007/s00392-024-02406-5.

VIII. Appendix

- Image J Macros:

```
macro "DoTheBrownSeparation [a]" {
    selectWindow("Stain Color Detection");
    run("8-bit");
    setThreshold(60, 175)
    run("Create Selection");
    run("Measure");
    selectWindow("Stain Color Detection");
    run("Close");
}
```

```
macro "DoTheTissueArea [s]" {
   run("Set Scale...", "distance=0 known=0 pixel=1 unit=pixel global");
   run("8-bit");
   setThreshold(2, 220);
   run("Create Selection");
   run("Measure");
   run("Close");
}
```

```
macro "ClearOutside [c]" {
   setBackgroundColor(255, 255, 255);
   run("Clear Outside");
}
```

- Complete Olink Plasma Proteomics Results

Table 5-1: Proteomics overview: Complete Olink Results Table

Target	Uniprot ID	NPX (Gliadin) - NPX (Zein)	-log10 (p-val.)	Target	Uniprot ID	NPX (Gliadin) - NPX (Zein)	-log10 (p-val.)
Il17a	**Q62386**	**0.8733**	**1.5262**	Matn2	O08746	0.0690	0.1491
Il17f	Q7TNI7	0.5277	0.6969	Tnfsf12	O54907	0.0680	0.3528
Rgma	Q6PCX7	0.5213	0.6999	Kitlg	P20826	0.0521	0.0852
Hgf	Q08048	0.5150	0.6321	Il23r	Q8K4B4	0.0480	0.1780
Pdgfb	P31240	0.4991	0.3588	Tnf	P06804	0.0461	0.1177
Crim1	Q9JLL0	0.4561	0.6073	Adam23	Q9R1V7	0.0406	0.1212
Cxcl9	P18340	0.4538	0.9825	Csf2	P01587	0.0374	0.1251
Il5	P04401	0.4416	0.6229	Ghrl	Q9EQX0	0.0283	0.0271
Il10	P18893	0.4329	1.5896	Clmp	Q8R373	0.0193	0.0712
Gcg	P55095	0.3863	0.6574	Ntf3	P20181	0.0109	0.0380
Il6	P08505	0.3663	0.5517	Sez6l2	Q4V9Z5	0.0040	0.0164

Target	Uniprot ID	NPX (Gliadin) - NPX (Zein)	-log10 (p-val.)
Riox2	Q8CD15	0.3503	0.4959
Parp1	P11103	0.3487	0.6779
Fas	P25446	0.3072	1.9285
Dll1	Q61483	0.2864	1.2700
Qdpr	Q8BVI4	0.2696	0.5340
Gfra1	P97785	0.2641	0.8866
Tgfb1	P04202	0.2623	0.7347
Yes1	Q04736	0.2498	0.8503
Nadk	P58058	0.2462	0.4169
Eda2r	Q8BX35	0.2444	0.7550
Tnni3	P48787	0.2382	0.1137
Itgb1bp2	Q9R000	0.2301	0.5897
Ccl2	P10148	0.2242	0.4699
Tnfrsf12a	Q9CR75	0.2132	0.3604
Dlk1	Q09163	0.2040	1.6158
Wisp1	O54775	0.2035	0.7405
Foxo1	Q9R1E0	0.1988	0.8808
Ccl20	O89093	0.1865	0.2811
Cant1	Q8VCF1	0.1788	0.9172
Fst	P47931	0.1767	0.3928
Ccl5	P30882	0.1577	1.4943
Epo	P07321	0.1517	0.2259
Cyr61	P18406	0.1292	0.1970
Gdnf	P48540	0.1224	0.7966
Acvrl1	Q61288	0.1217	0.3478
Fstl3	Q9EQC7	0.1179	0.6678
Tgfbr3	O88393	0.1131	0.4154
Lgmn	O89017	0.1111	0.3356
Clstn2	Q9ER65	0.1079	0.3296
Igsf3	Q6ZQA6	0.1013	0.6365
Prdx5	P99029	0.0862	0.1361
Wfikkn2	Q7TQN3	0.0832	0.4259
Ddah1	Q9CWS0	0.0827	0.3700
Eno2	P17183	0.0748	0.3476
Epcam	Q99JW5	0.0708	0.4826

Target	Uniprot ID	NPX (Gliadin) - NPX (Zein)	-log10 (p-val.)
Dctn2	Q99KJ8	-0.0053	0.0115
Il1b	P10749	-0.0061	0.0129
Mia	Q61865	-0.0078	0.0264
Pak4	Q8BTW9	-0.0105	0.0284
Tnr	Q8BYI9	-0.0199	0.0736
Erbb4	Q61527	-0.0226	0.0682
Flrt2	Q8BLU0	-0.0247	0.1214
Ahr	P30561	-0.0285	0.0638
Cpe	Q00493	-0.0337	0.1441
Plin1	Q8CGN5	-0.0361	0.0200
Tgfa	P48030	-0.0457	0.1156
Tpp1	O89023	-0.0799	0.1969
Cntn4	Q69Z26	-0.0800	0.3370
Ppp1r2	Q9DCL8	-0.0866	0.1423
Cxcl1	P12850	-0.0897	0.1623
Map2k6	P70236	-0.1191	0.1425
Vegfd	P97946	-0.1193	0.6460
Cntn1	P12960	-0.1272	1.0682
Apbb1ip	Q8R5A3	-0.1330	0.3425
Itgb6	Q9Z0T9	-0.1402	0.1528
Il1a	P01582	-0.1478	0.1449
Tnfrsf11b	O08712	-0.1856	0.5339
Pla2g4a	P47713	-0.1889	0.2487
Axin1	O35625	-0.2155	0.5366
Notch3	Q61982	-0.2247	2.3071
Cdh6	P97326	-0.2401	0.5839
Plxna4	Q80UG2	-0.2632	0.3344
Vsig2	Q9Z109	-0.2804	0.3585
Ccl3	P10855	-0.3065	0.8867
S100a4	P07091	-0.3075	0.9666
Lpl	P11152	-0.3324	1.4025
Ca13	Q9D6N1	-0.4006	0.6502
Fli1	P26323	-0.4589	1.1541
Casp3	P70677	-0.6486	2.0199
Snap29	Q9ERB0	-0.6742	0.7790

IX. Curriculum vitae

xx

X. List of Scientific Contributions

- Original Publications:

The title of the publications related to this thesis is marked in bold.

Keppeler K, Pesi A, Lange S, Helmstädter J, Strohm L, Ubbens H, Kuntić M, Kuntić I, Mihaliková D, Vujačić-Mirski K, Rosenberger A, Küster L, Frank C, Oelze M, Finger S, Zakrzewska A, Verdu E, Wild J, Karbach S, Wenzel P, Wild P, Leistner D, Münzel T, Daiber A, Schuppan D, Steven S. **Vascular dysfunction and arterial hypertension in experimental celiac disease are mediated by gut-derived inflammation and oxidative stress.** Redox Biol. 2024 Apr;70:103071. doi:10.1016/j.redox.2024.103071. Epub 2024 Feb 8. PMID: 38354629; PMC10876911.

Kuntic M, Kuntic I, Krishnankutty R, Gericke A, Oelze M, Junglas T, Bayo Jimenez MT, Stamm P, Nandudu M, Hahad O, **Keppeler K**, Daub S, Vujacic-Mirski K, Rajlic S, Strohm L, Ubbens H, Tang Q, Jiang S, Ruan Y, Macleod KG, Steven S, Berkemeier T, Pöschl U, Lelieveld J, Kleinert H, von Kriegsheim A, Daiber A, Münzel T. Co-exposure to urban particulate matter and aircraft noise adversely impacts the cerebro-pulmonary-cardiovascular axis in mice. Redox Biol. 2023 Feb;59:102580. doi: 10.1016/j.redox.2022.102580. Epub 2022 Dec 18. PMID: 36566737; PMC9804249.

Frenis K, Kalinovic S, Ernst BP, Kvandova M, Al Zuabi A, Kuntic M, Oelze M, Stamm P, Bayo Jimenez MT, Kij A, **Keppeler K**, Klein V, Strohm L, Ubbens H, Daub S, Hahad O, Kröller-Schön S, Schmeisser MJ, Chlopicki S, Eckrich J, Strieth S, Daiber A, Steven S, Münzel T. Long-Term Effects of Aircraft Noise Exposure on Vascular Oxidative Stress, Endothelial Function and Blood Pressure: No Evidence for Adaptation or Tolerance Development. Front Mol Biosci. 2022 Jan 31;8:814921. doi: 10.3389/fmolb.2021.814921. PMID: 35174211; PMC8841864.

Helmstädter J, **Keppeler K**, Aust F, Küster L, Frenis K, Filippou K, Vujacic-Mirski K, Tsohataridis S, Kalinovic S, Kröller-Schön S, Oelze M, Bosmann M, Münzel T, Daiber A, Steven S. GLP-1 Analog Liraglutide Improves Vascular Function in Polymicrobial Sepsis by Reduction of Oxidative Stress and Inflammation. Antioxidants (Basel). 2021 Jul 23;10(8):1175. doi:10.3390/antiox10081175. PMID: 34439423; PMC8388926.

Helmstädter J, **Keppeler K**, Küster L, Münzel T, Daiber A, Steven S. Glucagon-like peptide-1 (GLP-1) receptor agonists and their cardiovascular benefits-The role of the GLP-1 receptor. Br J Pharmacol. 2022 Feb;179(4):659-676. doi:10.1111/bph.15462. Epub 2021 May 6. PMID: 33764504; PMC8820186.

- Presentations:

Keppeler K, Pesi A, Lange S, Helmstädter J, Strohm L, Ubbens H, Frank C, Mihalikova D, Kuntic I, Kuntic M, Bayo Jimenez M. T, Vujacic-Mirski K, Finger S, Oelze M, Wenzel P, Leistner D, Zakrzewska A, Kij A, Chlopicki S, Münzel T, Daiber A, Verdu E, Schuppan D, Steven S. Endotheliale Dysfunktion bei experimenteller Zöliakie wird durch darmbedingte Gefäßentzündung und oxidativen Stress vermittelt. Zeitschrift für Gastroenterologie 2023; 61(08): 370 – 371. doi: 10.1055/s-0043-1771663.

Keppeler K. Gut-Driven Vascular Dysfunction, Inflammation and Oxidative Stress in an Animal Model of Celiac Disease. 9th Science Day by the TransMed Graduate School of the Johannes Gutenberg University Mainz, 2023.

Keppeler K, Helmstädter J, Kuester L, Strohm L, Ubbens H, Bayo Jimenez M. T, Mihalikova D, Kuntic I, Kuntic M, Vujacic-Mirski K, Finger S, Oelze M, Wenzel P, Münzel T, Daiber A, Schuppan D, Steven, S. Endothelial Dysfunction in Experimental Celiac Disease Is Mediated by Gut-Derived Vascular Inflammation And Oxidative Stress. Vascular Discovery: From Genes to Medicine 2022 by the American Heart Association.

Keppeler, K. Celiac disease - a cardiovascular risk factor? Studies of vascular function in a mouse model of celiac disease. 7th Science Day by the TransMed Graduate School of the Johannes Gutenberg University Mainz, 2021.

XI. Acknowledgement

xx

XII. Declaration

Eidesstattliche Erklärung

Hiermit versichere ich gemäß §12, Abs. 2 der Promotionsverordnung vom 01.04.2018, dass ich die als Dissertation vorgelegte Arbeit selbst angefertigt und alle benutzten Hilfsmittel in der Arbeit angegeben habe. Weiterhin habe oder hatte ich die als Dissertation vorgelegte Arbeit nicht als Prüfungsarbeit für eine staatliche oder andere wissenschaftliche Prüfung eingereicht. Ich hatte weder die als Dissertation vorgelegte Arbeit noch Teile davon bei einer anderen Fakultät bzw. einem anderen Fachbereich als Dissertation eingereicht.

_____

Mainz, Juni 2025 Karin Keppeler